**The Dissertation Committee for Peter Louis Voyvodic Certifies that this is the approved version of the following dissertation:**

# The Role of Syndecan-1 in Flow-Mediated Endothelial Mechanotransduction

**Committee:**

Aaron B. Baker, Supervisor

Michael S. Sacks

Jeanne C. Stachowiak

Ernst-Ludwig Florin

David W. Terreson

# The Role of Syndecan-1 in Flow-Mediated Endothelial Mechanotransduction

**by**

**Peter Louis Voyvodic, B.S.; B.S.; M.S.E.**

**Dissertation**

Presented to the Faculty of the Graduate School of

The University of Texas at Austin

in Partial Fulfillment

of the Requirements

for the Degree of

**Doctor of Philosophy**

**The University of Texas at Austin**

**December 2015**

# Dedication

For my Mother and Father

## Acknowledgements

My journey to this point would not have been possible without the innumerable contributions from so many people in my life. I would like to take this opportunity to thank as many of them as possible. I apologize if I overlook anyone, but know that your contributions and advice have not gone unnoticed.

Early in my academic career I had the opportunity of enrolling in Challenge Middle School in its inaugural year. Between the flexible academic curriculum, fourth-eighth grade structure, and terrific teaching staff, I was allowed to challenge myself by taking higher level courses that would not have been available to me elsewhere. I would like to specifically thank Mr. Morrow, who was integral in my early fascination with and exposure to advanced mathematics.

In high school I enrolled in numerous math and science classes, but no teacher had as dramatic an impact on my life as Mrs. Bartholomew. In both CP and AP Chemistry classes, her empathetic devotion to her students was inspiring and has left a lasting impression on my life. I would also like to thank Andy Artz for asking if I wanted to spend a Saturday morning taking a scholarship test for some school called Boston University.

In the spring of 2002, I began looking for a summer research position. The late Dr. George Eisenbarth was kind enough to allow a high school kid with no prior experience to get a first taste of research in his lab. In addition to numerous laboratory techniques I still use on a regular basis, I was exposed to research culture for the first time and developed a taste for it. I would also like to thank Dr. Eisenbarth for helping me find my first permanent research position after graduating from college. You are truly missed.

An undergraduate education is an exciting and transformative time and I was lucky enough to have several strong mentors to help me in research aspects. Dean (later Provost) David Campbell was kind enough to allow me to work with him the summer before my freshman year, teaching me about nonlinear systems and chaos theory. Years later these resonated with me as I heard my Controls Systems professor speak about his research: modifying *E. coli* to produce a genetic toggle switch. Awestruck, I approached Professor Jim Collins after class and he was extremely generous in offering me an opportunity to conduct my senior thesis project in his lab. I would like to thank his whole lab, specifically Michael Kohanski, for their valuable advice throughout my senior year.

I would not be in my current Ph.D. program without the help and guidance of Drs. Joe and Lydia Bryan. As my mentors while I was a laboratory technician, they provided a nurturing environment for me to grow as a researcher and scientist. I learned from them not only in the laboratory, but from the stories of their careers in science during Thanksgiving dinners at their house on Vashon Island. I would also like to thank David, Hiroshi, and Yumiko for helping my find my footing and being all-around terrific laboratory companions. Finally, I would like to thank Lindsay for her willingness to be the first ever student I mentored and helping to teach me as much as I was able to teach her.

My time here in Austin has been filled with so many wonderful people that I feel like the list could occupy half of this dissertation document; however, I would like to thank a few people in particular. I would like to thank my professors who helped teach me valuable skills during their courses that I was able to use in my research. I would like to thank all of my fellow graduate students who helped me feel comfortable in a new city, specifically Kevin, Jardin, Robin, Alex, Stephanie, and Colin. I'd like to thank my fellow members of Lone Star Rickshaw and 3SC for fueling my sense of adventure. And finally

I'd like to thank my unbelievable labmates. Moy, you and I have been here from the beginning and I know I couldn't have done it without you. Jason and Anthony, I have every bit of confidence that you will be more than successful as the soon-to-be senior lab members. And to Adrianne and Vicky, I thank you for all your help.

As much I enjoyed the opportunity to learn from so many terrific mentors, I was equally honored to have the privilege to be a mentor to several undergraduate students. To Daniel, Robert, Evan, Ashwin, Darshil, and Cody, thank you for putting up with my semi-chaotic system of instruction and for teaching me how to mentor others. I hope to take those skills into my future research positions.

I would like to thank Dr. Baker for taking me on as his first graduate student. I was given hands-on mentorship and daily advice about my experimental struggles in ways that are available to few. I would also like to thank the rest of my committee; Dr. Stachowiak, Dr. Sacks, Dr. Florin, and Dr. Terreson, you have all been extremely helpful in helping me craft this research project and I thank you for your guidance.

Last, but far from least, I would like to thank my family. Without all of you, I surely would not be writing this document today. I'd like to thank my grandfather, Dr. Louis Voyvodic, for inspiring a young kid interested in science by showing him around the supercollider ring of Fermi Lab. The impression you left on my scientific career is immeasurable. Elise and Krista, you have taught me so much and I am so proud of everything you do and for your place in my life. And finally, to my parents: I could not have asked for greater mother and father. Every day I appreciate more everything that you do and have done for me and you are solely responsible for all of the positive aspects for my personality today.

# The Role of Syndecan-1 in Flow-Mediated Endothelial Mechanotransduction

Peter Louis Voyvodic, Ph.D.

The University of Texas at Austin, 2015

Supervisor: Aaron B. Baker

Cardiovascular disease kills over 750,000 people in the United States and an estimated 17.3 million people worldwide each year. Atherosclerosis, the formation of lipid-rich plaques in the walls of blood vessels, is the primary driver of complications in cardiovascular disease. These plaques partially or totally occlude downstream blood flow, resulting in ischemia and in peripheral limbs can require amputation. Alternatively, they can develop a vulnerable 'fibrous cap' phenotype that is susceptible to rupture, leading to a massive thrombotic cascade that can cause stroke or myocardial infarction. Current treatments predominately focus on either physically opening the blood vessels (e.g. balloon catheters and stenting) or creating bypass grafts. These treatments, however, frequently need to be repeated, particularly if patients do not change their dietary and exercise protocols. Therefore, a new approach to treating atherosclerosis that targets the mechanisms that drive vessels towards a pathogenic phenotype could be extremely helpful for preventing disease.

Endothelial cells line blood vessels and are the principle cells responsible for interactions between blood flow and the surrounding tissue. In addition to providing a barrier, they are capable of sensing the mechanical forces induced by the blood flow. This sensing mechanism is responsible for driving their phenotype between an

‘atheroprotective’ or ‘atheroprone’ state; specifically, steady laminar shear stress results in ‘healthy’ endothelial cells while low or oscillatory shear stresses induces an inflammatory phenotype. While research has been conducted to look at the effects of shear stress on endothelial cells, the initial sensing mechanism that drives these downstream pathways remains unclear. Here we investigate the heparan sulfate proteoglycan syndecan-1 as a potential upstream regulator of these changes. Using custom-built shear stress application devices, we show that endothelial cells lacking syndecan-1 have a reduced response to shear stress and a general increase in inflammatory state. *In vivo* studies in a knockout mouse model extend these results; syndecan-1 knockout mice have more pronounced inflammatory responses and an increase in leukocyte-binding proteins in low shear conditions. These findings illustrate syndecan-1 as a potential target for future therapeutics aimed at driving potentially vulnerable vasculature away from a pathogenic phenotype.

# Table of Contents

# List of Figures

# Chapter 1: Introduction

## 1.1 Motivation

Cardiovascular disease is the number one cause of death worldwide with 17.3 mortalities annually[1]. This is projected to rise as increasing adoption of a Western diet leads to rapidly increasing global risk factors for cardiovascular disease; the estimated annual worldwide death toll will be more than 23.6 million by 2030. Obesity has doubled since 1980 and is estimated to cause 3-4 million deaths annually[2]. While some risk factors, such as smoking, have decreased in recent years, these declines have not nearly alleviated the need to find better treatments in the near future.

Cardiovascular death and complications are primarily the result of atherosclerosis, which involves the formation of lipid-rich plaques in the walls of blood vessels. Atherosclerosis can cause a wide range of pathological ailments. Peripheral vascular disease limits blood flow to the extremities and can cause ulcers and subsequent amputations[3,4]. Coronary artery disease causes occlusion of blood flow to the heart, resulting in heart attacks. While occlusion itself has dangerous consequences, plaques can further develop into so called 'vulnerable plaques' in which the border between lipid-rich plaque and lumen is only separated by a thin fibrous cap. When large forces are applied, these thin caps can rupture, evicting the contents of the plaque into the lumen resulting in a massive thrombotic response. This thrombus then travels downstream where it can cause instant occlusion of the coronary arteries or parts of the brain, resulting in a heart attack or stroke, respectively.

Treatment for atherosclerosis can be pharmacological or interventionist in nature. Physicians may prescribe medications such as statins, fibrates, or aspirin to reduce risk factors such as LDL cholesterol, triglycerides, and blood clots, but these do not directly

target atherosclerotic plaques and frequently cannot counterbalance other many risk factors[5-8]. Surgical interventions are divided into bypass grafts and angioplasty. Bypass grafting involves harvesting vasculature from elsewhere in the body, typically either diverting the left internal mammary artery or harvesting a saphenous vein from the leg, and attaching it as a bypass for the occluded vessel. This results in blood flow through a new, unoccluded vessel; however, the procedure requires long hospitalization periods since surgery must be performed using a cardiopulmonary bypass. Furthermore, if the patient continues their current diet/lifestyle the new graft is susceptible to developing its own atherosclerotic plaques. In some studies, up to 50% of the patients that undergo bypass surgery have another major cardiac event within ten years[9,10]. Balloon angioplasty is another common treatment for atherosclerosis. It involves running a catheter though the vasculature to the occlusion site and then expanding a balloon to push away the plaque tissue. While installation of a stent can help keep the vessel open, these procedures frequently suffer from restenosis occluding the vessel over time. While current treatments can help alleviate immediate conditions, they all suffer from a lack of long term success; therefore, a new class of therapeutics is needed that targets the pathways that drive vascular tissue toward dysfunction in order to prevent plaque formation in the first place.

Endothelial cells have long been known to be able to sense the shear stress from blood flow[11]. Specifically, high levels of laminar shear stress drive endothelial cells towards a healthy, robust phenotype, while low or oscillatory shear levels induce the endothelial cells down pro-inflammatory, pro-atherosclerotic pathways[12-14]. While a great deal of interesting research has been conducted on the endothelial response to shear, little is still known about the initial mechanisms that drive these changes. Recent research has looked at the glycocalyx, which is a thick layer of glycans and proteoglycans that covers the lumenal surface of the cell, as a prime target for containing these initial sensory mechanisms[15-17]. Pahakis *et al*. showed that by digesting the glycosaminoglycan chains

from the glycocalyx with heparinase they could reduce the shear-induced increase of eNOS[18]. We are interested in how syndecan-1, a single-transmembrane protein in the glycocalyx with extracellular attachment sites for heparan sulfate and chondroitin sulfate, is involved in the endothelial shear mechanotransduction response. Indeed, shortly after beginning our studies, Koo *et al*. showed that syndecan-1 was unique among glycocalyx core proteins to increase levels in laminar 'atheroprotective' flow and decrease levels in oscillatory 'atheroprone' flow[19]. We examined the effects of syndecan-1 directly using a syndecan-1 knockout model both *in vitro* and *in vivo*. We showed that the absence of syndecan-1 results in a reduced mechanotransductive response to shear and an overall proinflammatory state. Our *in vitro* findings were corroborated by an increased VCAM-1 presence in syndecan-1 knockout aortae and in neointimal formation in response to a partial carotid ligation surgery in our knockout mice. These studies, which are the first comprehensive analysis of syndecan-1's role as a mechanotransducer in endothelial cells, support the hypothesis that it is directly involved in driving endothelial cell phenotype and may be a potentially novel pathway for future cardiovascular therapeutics.

### 1.2 Dissertation Roadmap

The motivation for this dissertation study and a formative outline are listed in Chapter 1. A brief background and description of prior work that led to this research are described in Chapter 2. In Chapter 3, the design, optimization, and construction of novel devices for application of shear stress to in vitro cell cultures is described. Chapter 4 highlights how these devices were used to investigate the role of syndecan-1 in endothelial mechanotransduction by application of shear stress to wild-type (WT) and syndecan-1 knockout (S1KO) endothelial cells in culture. These effects are examined in an *in vivo* setting in Chapter 5, which looks at the role of syndecan-1 in both native and induced shear environments. Chapter 6 illustrates conclusions from this dissertation study and provides directions for future research endeavors on this subject.

# Chapter 2: Background

## 2.1 ATHEROSCLEROSIS

Cardiovascular disease is currently the number one cause of mortality worldwide and is responsible for 17.3 million deaths annually. In the United States, nearly 40% of people over age 40 and nearly 70% of people over age 60 have some form of cardiovascular disease[1]. With the increasing prevalence of a Western diet and reduced physical activity worldwide, the exponential rise of cardiovascular disease globally is quickly reaching epidemic levels. By 2030, cardiovascular disease is estimated to be responsible for 23.6 million annual deaths globally. Even for those for whom mortality is not an immediate consequence, the reduction in quality of life can be profound. Peripheral vascular disease can result in amputations and gangrene due to ischemia and those who survive myocardial infarction and stroke frequently have a long list of downstream complications including risk of future events and decreased mental and physical performance[20-22]. Additionally, the direct and indirect costs of cardiovascular disease and stroke cost more than $320 billion each year from health expenditures and lost productivity[1]. Therefore, the early diagnosis and treatment of cardiovascular disease is of paramount concern to overall global health.

Atherosclerosis is the primary cause of cardiovascular complications. It is the result of a long-term, chronic development of plaque formation in the blood vessels. Briefly, chronically inflamed tissue develops a 'fatty streak' that causes frequent and persistent extravasation of leukocytes[23]. Over time, a combination of smooth muscle cell stenosis and inflammatory perfusion result in wall thickening that begins to occlude blood flow. This occlusion results in ischemia downstream of the plaque. In peripheral vascular disease, this results in a lack of blood flow to the extremities that frequently necessitates surgical intervention and eventual amputation[24]. Coronary artery disease

occlusion restricts blood flow to the heart and results in myocardial infarction. Additionally, atherosclerosis progression frequently results in the formation of a thin-fibrous cap separating the plaque from the lumen. These 'vulnerable plaques' are prone to rupture, which results in a massive thrombotic response that travels downstream and can be lodged and block blood flow[25]. This frequently results in heart attack or stroke and has a high incidence of mortality.

Current treatments for cardiovascular disease traditionally fall into two fields: grafting and angioplasty. For coronary grafting, a blood vessel is harvested or diverted from elsewhere in the body, usually a mammary artery or saphenous vein, and sutured to bypass the occlusion. This method restores normal blood flow; however, the long-term success is limited. Nearly 50% of patients who receive grafts have another cardiac event due to plaque occlusion within ten years[9,10]. Open heart surgery itself also results in long post-surgical hospital stays due to the highly invasive nature and recovery from time on a cardiopulmonary bypass. Another alternative is balloon angioplasty, in which a catheter is led into the occluded vessel and inflated to physically push the occlusion outwards radially. Installation of stents, wire metal meshes, has helped in recent years to hold the vessel open; however, the endothelial denudation the procedure causes often results in excessive smooth muscle cell proliferation and reclosing of the vessel due to restenosis[26]. While newer drug-eluting stents can help mitigate this response by releasing anti-proliferative small molecules, such as rapamycin, this seems to only delay the progression and may increase the risk of thrombosis[27].

Most therapies for cardiovascular disease are either surgical or are very broad targeting. Changes in diet and exercise are traditionally prescribed, but patient adherence is frequently poor. Common pharmaceuticals include statins, fibrates, and aspirin, which can help to lower risk factors, but these are frequently not sufficient to overcome disease[5-8]. Therefore, it would be extremely useful to fully understand the mechanisms that lead to vascular pathology in order to develop a new generation of cardiovascular therapeutics.

## 2.2. ENDOTHELIAL SHEAR-MEDIATED MECHANOTRANSDUCTION

The current practice of clinical cardiovascular medicine lacks therapies that specifically combat the powerful effects of disturbed hemodynamics that underlie widespread diseases such as hypertension and atherosclerosis. Arterial mechanotransduction has been the subject of intense experimental and theoretical study over the past decades[23,28]. The search for potential mechanotransducers, molecules that serve as force sensors and activators of mechanical responses, has revealed a variety of complex and fascinating mechanisms through which hemodynamic forces can alter arterial biology[29-33]. In the artery, endothelial cells (ECs) line the lumen of the vessel and are exposed directly to shear forces from blood flow. Atherosclerotic plaques have long been known to preferentially localize to particular regions of the vasculature[34]. A fluid dynamical analysis of these atherosclerotic regions reveals that they coincide with the areas where the fluid flow is disturbed. In contrast to regions of healthy vasculature where blood flow imparts a regular, laminar shear stress on the endothelial cells lining the vessel, these susceptible regions impart a low, oscillatory shear stress on the vessel wall. It appears that the initial sensory mechanisms that drive vascular tissue down either a healthy or disease-driven pathway is in part mechanically mediated.

Since the initial discovery of endothelial shear-mediated mechanotransduction, there have been a multitude of studies investigating the pathways involved. Initial studies showed that exposing *in vitro* endothelial cells to fluid shear stress results in cell alignment with flow[35]. Other studies have found that laminar shear stress results in increased production of vasodilatory factors such as endothelial nitric oxide synthase (eNOS) and decreased production of many inflammatory cytokines[36,37]. Several key players in this process have been identified. Krüppel-like factor 2 (KLF2) was shown to drive many of these responses[38,39]. Integrins have long been thought to play a role in

endothelial mechanotransduction[40]. Additionally, Tzima *et al*. showed that platelet endothelial cell adhesion molecule-1 (PECAM-1), vascular endothelial cadherin (VE-Cadherin), and vascular endothelial growth factor receptor-2 (VEGFR-2) form a complex between cell-cell junctions that drives many of the responses previously seen[41]. Both of these mechanisms, however, require transmittance of force from the lumenal surface either directly via the cell membrane or cytoskeleton or via currently unknown biochemical pathways.

Studies of endothelial mechanotransduction have also been conducted *in vivo*. Typically they fall into two categories: differing regions of native shear stress and those of induced shear stress. Native shear stress studies utilize a fluid mechanical analysis of fluid flow through the vasculature to identify regions that have differing wall shear stresses. These regions are frequently found on the inside walls of high angle curvature and after vessel bifurcations. Gelfand *et al*. showed that in the aorta, the lesser arch has higher nuclear localization levels of β-catenin[42]. Induced shear stress experiments use surgical techniques to alter the native shear stress characteristics and study how the vasculature remodels and responds to the change in shear stress. One method is the carotid cuff, in which a piece polyetherketone tubing is perivascularly applied to the carotid artery of a mouse and then tied off, restricting downstream blood flow[43]. This produces an increase in vascular cell adhesion molecule-1 (VCAM-1) and a decrease in eNOS production[43,44]. One shortcoming of the carotid cuff is any observed inflammatory response cannot be solely attributed to change in shear stress patterns because the cuff itself can cause some irritation. To overcome this, Nam *et al*. developed a partial carotid ligation model in which the external carotid, internal carotid, and occipital arteries are all ligated, allowing downstream flow only through the smaller superior thyroid artery[45]. This creates a robust region of low shear stress that also exhibits oscillatory flow characteristics common in atherosclerosis-prone regions of the vasculature. Using a plaque-susceptible ApoE knockout mouse model, they demonstrated profound plaque

formation and vessel remodeling in response to this change in shear stress. All of these studies, however, are focused downstream of the initial endothelial mechanotransduction sensing mechanism, and thus a different approach must be taken to investigate this principle response.

### 2.3. GLYCOCALYX

Recently the endothelial glycocalyx has become of potential target of interest for this initial endothelial mechanotransduction response. The glycocalyx is a relatively thick structure of glycans and proteoglycans that extends out from the luminal side of the endothelial cell. Proteoglycans contain one or more glycosaminoglycan (GAG) chains attached to a single core protein that is either transmembrane or bound via a glycosylphosphatidylinositol (GPI)-linker. These GAG chains typically have 90-95% carbohydrate content, interact with numerous growth factors and other signaling molecules, and are much larger than their core protein[46]. One class of proteoglycans, the heparan sulfate proteoglycans (HSPGs), has become an increasingly interesting target in recent years. These complex molecules consist of a protein core modified with heparan sulfate glycosaminoglycan chains and can interact directly with the forces produced by blood flow. These surface molecules extend beyond the surface of the endothelial cell by nearly three times the cell thickness[47]. On the molecular scale, this dwarfs the extension of other surface receptors and is clearly the first point of contact for blood flow applied to the cells. Consequently, these poorly understood molecules are likely among the first molecules to be affected by applied forces from blood flow. Due to their location on the cell surface and their interaction with cytoskeletal and adhesion-associated molecules, cell surface proteoglycans are ideally located to be one of the primary sensing components for stretch- and flow-induced cellular responses within arteries and to mediate endothelial interactions with circulating cells.

Previous studies have focused on using enzymatic digestion techniques to examine the endothelial response to shear stress with or without the various glycosaminoglycan chains. Using cultured cells, Florian *et al*. studied the production of nitric oxide (NO) in endothelial cells under shear stress[48]. They treated cells with an enzyme to digest heparan sulfate chains (heparinase) and then exposed the cells to various shear stress regimes. Heparan sulfate digestion led to a three-fold decrease in the NO production after exposure to steady shear stress as well as a four-fold decrease in the NO production following treatment with oscillatory shear stress. In addition, digestion with heparinase did not inhibit bradykinin-induced increases in NO production. Other studies on endothelial cells in culture also demonstrated that digestion with neuraminidase and hyaluronidase attenuated shear-induced NO release while digestion with chondroitinase did not[49]. Additionally, shear-induced increases in prostacyclin-2 (PGI2) were not affected by removal of heparan sulfate, sialic acid, chondroitin sulfate or hyaluronan[18]. *In vivo* studies have also supported the involvement of proteoglycans in controlling shear stress-induced arterial vasodilation. Increases in blood flow cause arteries to dilate in an endothelium-dependent manner[50,51]. Several studies have supported the role of elements of the glycocalyx in the control of the shear-induced vasodilatory response of arteries. Hecker *et al*. examined the vasoconstriction of rabbit femoral arteries in *ex vivo* organ culture and found that incubation with neuraminidase, an enzyme that digests sialic acid moieties, reduced shear stress-induced NO release[52]. In contrast, neuraminidase digestion did not have an effect on acetylcholine-induced NO release. A recent study examined the effect of long-term shear stress on relative gene and protein production of different glycocalyx components; syndecan-1 was unique in that it had an increased production in the presence of laminar shear stress but decreased production during oscillatory, 'atheroprone' shear stress[19]. Therefore, syndecan-1 is a very interesting target for a proteoglycan that may govern the endothelial mechanotransduction response seen in other glycocalyx studies.

## 2.4. SYNDECAN-1

Syndecan-1 is a member of the syndecan family of heparan sulfate proteoglycans. It is a 310 amino acid single transmembrane protein with serine residues attachment sites for three heparan sulfate and two chondroitin sulfate glycosaminoglycan chains[53]. It can be converted into a soluble form via proteolytic cleavage of its ectodomain; indeed, higher levels of soluble syndecan-1 in serum are found in several forms of inflammation and cancer[54,55]. Syndecan-1 is involved in synthesizing numerous biochemical pathways including functioning as a cofactor for growth factors[56], activating $\alpha_v\beta_3$ and $\alpha_v\beta_5$ integrins[57], and linking to the actin cytoskeleton via the cytoplasmic tail[58].

Some studies have shown syndecan-1 to be a potentially interesting regulator of endothelial mechanotransduction shear response. Götte *et al*. showed that syndecan-1 knockout mice demonstrated an increase in leukocyte adhesion in the blood vessels in the retina[59]. Additionally, these mice have been shown to have a reduced glycocalyx thickness[60]. While these studies illustrate syndecan-1 as in interesting target, there has not yet been a detailed function analysis of the role of syndecan-1 in endothelial shear-mediated mechanotransduction. Therefore, it is the purpose of this study to investigate the role both *in vitro* and *in vivo* using novel mechanical devices and surgical manipulation techniques.

## 2.5. MOUSE MODELS

This study uses two different mouse models: C57BL/6J (wild-type [WT]) and syndecan-1 knockout (S1KO) mice from a C57BL/6J background. The WT mice are the most widely studied mouse model and have been prolifically used to create genetically-modified mouse strains. They have also been used in a wide variety of research areas including cardiovascular biology. The S1KO mice were a generous gift from Dr. Ram

Sasisekharan (Massachusetts Institute of Technology) and were created from, and recently backcrossed to, a C57BL/6J line. This combination of a robustly-studied base strain and global genetic knockout provides a powerful toolset to investigate the role of syndecan-1 in endothelial mechanotransduction.

# Chapter 3: Shear Stress Application Devices[1]

## 3.1 INTRODUCTION

The past decades of cardiovascular research have revealed a variety of shear stress-mediated processes that are powerful regulators of vascular homeostasis and disease progression[61]. These mechanical force-mediated mechanisms are integral in controlling a diverse set of pathophysiological processes including thrombosis, atherosclerosis and the response to arterial injury[62]. Fluid shear forces have direct effects on the endothelium and mediate circulating cell interactions[63]. In addition, shear forces can also have a direct mechanical effect on the vessel wall and can mediate the interactions of blood proteins and circulating cells with the luminal surface[64]. As shear forces have been found to be integral in regulating many aspects of vascular biology, a number of systems have been created to examine the effects of shear forces on cultured cells in a controlled manner[65-71].

Existing devices have utilized two broad categories of driving mechanisms for creating flow over cultured cells[72]. The first is the parallel-plate or channel configuration[65-67]. These systems consist of a culture chamber coated to allow cell culture on one or more of the surfaces. Fluid flow through the chamber is typically driven by either a syringe or peristaltic pump with an elevated reservoir to control pressure and create steady flow. Microfluidic platforms using this principle have also been adapted to serve to provide shear stress to cells in culture[73-75]. An alternative type of flow system involves the use of a low-angle cone that is rotated at a constant velocity over the cells[69-

[1] Some work contained in this chapter was previous published in the following journal article: Voyvodic, P. L., Min, D. & Baker, A. B. A multichannel dampened flow system for studies on shear stress-mediated mechanotransduction. *Lab on a chip* **12**, 3322-3330, doi:10.1039/c2lc40526a (2012). The individual contributions by the authors are as follows: Peter L Voyvodic- Principle author and conductor of the research; Daniel Min- Undergraduate research assistant to PL Voyvodic; Aaron B Baker- Supervisor to PL Voyvodic.

[71]. This has the advantage of being able to create defined fluid stresses and has been used to create both steady flow and complex, time-varying flow profiles[71].

### 3.2 MULTI-THROUGHPUT SHEAR STRESS DEVICE

We sought to create a flow system that is capable of creating steady flow in cells cultured in multichannel flow plates. This is a critical parameter for studies that aim to examine the interactiolns of multiple pathways or to understand systems-level behavior in mechanotransduction. Limitations of many of the current systems for creating fluid flow on cultured cells include the low throughput of the system and the length of experiments that can be performed. Understanding the chronic, long-term response to changes in fluid shear stress is critical to understanding the mechanisms that mediate chronic vascular diseases. Consequently, long term experiments on cellular adaptation to shear stresses are clearly of interest. In addition, shear stresses also mediate the interactions of the various cell types that are suspended in the blood flow. Thus, *in vitro* assays of cells in suspension interacting with adherent cell types are critical in studying the mechanisms of important pathophysiological processes including immune cell recruitment[76], cancer cell metastasis[77], and thrombosis[78].

Our aim was to create a system that could overcome the limitations of previous designs by allowing higher and expandable throughput with steady flow and a closed-loop configuration to allow cells to be cultured indefinitely under flow in isolation from other flow channels. The system presented here consists of a multichannel peristaltic pump connected with a novel pulse dampening system to allow steady flow in a closed loop. We performed a detailed optimization of this pulse dampener to minimize volume and flow variation from pumping. Finally, we compared the cellular response to undamped, partially-damped, and fully-damped flow in terms of shear stress induced changes in endothelial cell alignment/cytoskeletal arrangement and production of eNOS.

### 3.2.1 Materials and Methods

#### *3.2.1.1. Flow Loop Components and Pulsatility Measurements.*

A multichannel peristaltic pump (MCP Standard, Ismatec) with a 24 channel pump head was used to create flow in the system. The pumping heads were calibrated for average flow rates using pumped volume measurements to an accuracy of less than ±0.5%. The recorded flow velocities were measured using an in-line ultrasonic flowsensor (Model ME3PXN; Transonic USA) connected to a flowmeter (TS410 Transit Time Flowmeter; Transonic USA) with an accuracy of ±4%. The output signal from the flow was processed using Powerlab 4/30 and LabChart Pro software (ADInstruments). Post-processing was performed with Matlab (Mathworks). Shear stress in the flow chambers at the cell culture surface was calculated based on the mean flow rate from the flowsensor using the following relation for laminar flow in a rectangular channel:

$$\tau = \eta \frac{\phi}{q}\left\{\sum_{n=0}^{\infty}\frac{(-1)^n}{(2n+1)^2}\left(\frac{2}{\pi}\right)^3 \tanh\left[(2n+1)\frac{\pi h}{2b}\right]\right\}$$

$$q = \frac{4}{3}hb^3 - 8b^4\left(\frac{2}{\pi}\right)^5 \sum_{n=0}^{\infty}\frac{1}{(2n+1)^5}\tanh\left[\frac{(2n+1)\pi h}{2b}\right]$$

where $2h$ is the height of the channel, $2b$ is the width of the channel, $\eta$ is viscosity, and $\phi$ is the flow rate through the channel[79].

#### *3.2.1.2. Cell Culture and Immunocytochemical Staining.*

Human umbilical vein endothelial cells (HUVECs) were used between passages 4 and 6. These cells were grown in MCDB-131 media with growth supplements (Lonza) with a total of 7.5% fetal bovine serum (FBS; Invitrogen). HUVECs were seeded into the flow chambers ($\mu$-Slide VI$^{0.4}$; ibidi, LLC) at $7\text{x}10^5$ cells/mL and grown to confluence. During the application of flow, the entire system was placed in an incubator and kept at

37°C and 5% $CO_2$. The cells were then washed with PBS and fixed in 4% paraformaldehyde for 20 min. The cells were then permeabilized in 0.1% Triton X-100 and blocked with 5% FBS for 1 hour. Next, the cells were exposed to a 1:50 dilution of primary antibodies for paxillin and eNOS (Santa Cruz Biotechnology) in 1% bovine serum albumin (BSA) overnight at 4°C. The cells were then washed three times in PBS/1% BSA and treated with a 1:1000 dilution of fluorescently-labeled secondary antibodies for 1 hour at room temperature. The actin cytoskeleton was also labeled by treating the cells for 1 hour in a 1:500 solution of Alexa 594-labeled phalloidin (Invitrogen). Finally the cells were mounted in a 4',6-diamidino-2-phenylindole (DAPI)-containing mounting medium and imaged using an epifluorescent microscope (Carl Zeiss). Morphometric analysis of the cells was performed using Metamorph software (Molecular Devices).

#### *3.2.1.3. Statistical Analysis.*

All results are shown as mean ± standard error of the mean. Comparisons between only two groups were performed using a 2-tailed Student's t-test. Differences were considered significant at $p<0.05$. Multiple comparisons between groups were analyzed by 2-way ANOVA followed by a Tukey post-hoc test. A 2-tailed probability value $<0.05$ was considered statistically significant.

### 3.2.2. Results

#### *3.2.2.1. Characterization of baseline pulsation in the multichannel peristaltic pump.*

Peristaltic pumping works through the rhythmic constriction of flexible tubing to create a local pressure gradient that drives flow. This mode of pumping is advantageous in that it does not require flow-driving elements (impeller or similar components) to interact with the flow directly. We first characterized the temporal profiles of flow in the closed flow loop with a peristaltic pump. Baseline measurements of the fluid velocity are

shown in **Figure 3.1**. These demonstrate that the pump produced significant pulsation in a closed-loop system with the peristaltic pump. The magnitude of the variation (from minimum trough to maximum peak) was quantified and expressed as relative to the mean velocity (**Figure 3.1**). At all pumping speeds tested, the variation in velocity was greater than 100% of the mean flow.

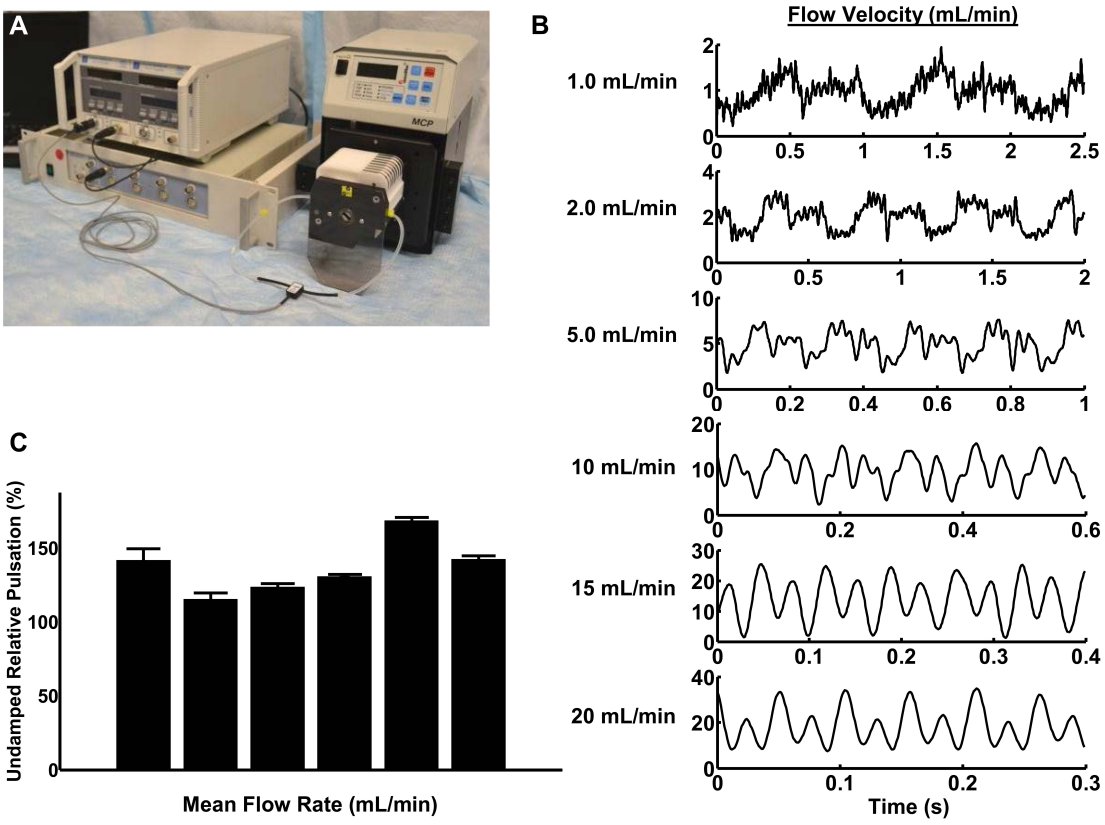


**Figure 3.1. Baseline characterization of flow loop velocity profiles at different mean flow rates.** (A) Experimental set-up including an in-line ultrasonic flow probe with an analog-to-digital converter and software recording program was used to measure flow within the loop. (B) The magnitude and form of the flow from the peristaltic pump varied with the mean flow rate. (C) Pulsation of the pump varied with mean flow velocity. Quantitative measurement of relative pulsation was calculated as a ratio of minimum to maximum flow to the overall mean flow rate.

### *3.2.2.2. Two dampening chambers are required to effectively limit flow pulsation in a closed flow loop.*

We designed a prototype system for a pulsation dampener that consisted of a simple chamber having inflow and outflow ports (**Figure 3.2**). We first incorporated this single pulse dampener into our system between the outflow of the peristaltic pump and the inlet of the parallel-plate flow channel. The pulsation dampening chamber was partially filled with culture media while it was open to the surrounding atmosphere. The lid was then closed to trap a volume of air within the system. This mode of initiating the system eliminated trapped bubbles and allowed us to adjust the ratio between air and culture media. The tubing in the non-pumping region of the system was gas permeable to allow for gas exchange.

We found that a single pulse dampener in the outflow of the pump had little effect on the mean variation in flow (**Figure 3.3**). The single dampener essentially shifted the

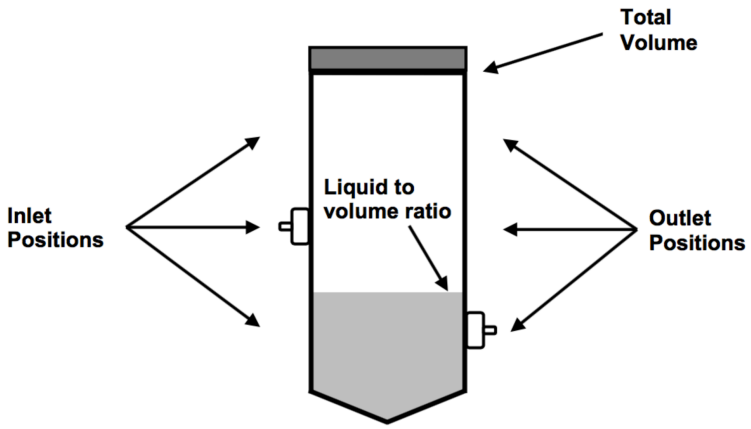


**Figure 3.2. Prototype pulse dampener design with optimized parameters.** The pulse dampener consists of an enclosed, fixed-volume chamber with an inlet and outlet. Inside, there is a variable liquid level with the rest of the volume taken up by trapped air. During the course of optimizing our system for pulsatility reduction, we focused on three parameters: 1) the total chamber volume, 2) the liquid to total volume ratio, and 3) the position of the inlet and outlet.

flow pulsation to a lower magnitude, lowering the maximum flow but maintaining the same mean flow variation. This effect is likely due to the closed-loop configuration of the system we were using. In a closed system, the input and output pressure for the peristaltic pump is a complex function of the type and mechanism of pumping[80]. We added a second pulse dampener at the output side of the parallel-plate flow chamber and the input side of the pump. The addition of the second pulse dampener dramatically decreased the mean flow variation. The effectiveness of the dual pulse dampener system increased with increasing mean velocity, correlating also with increased frequency of pulsation (**Figure 3.3**).

***3.2.2.3. Effect of total volume on pulse dampening effectiveness.***

After demonstrating the need for a two pulse dampener system to reduce flow pulsation, we sought to further optimize other design parameters to maximize reduction of pulsation while minimizing the fluidic volume needed per flow loop. While a larger volume of fluid protects the cells from rapid changes in temperature, pH, and the buildup of metabolic products, a compromise is needed between these factors and the economic burden of high volumes of media. To test the effects of altering the total overall volume of the pulse dampener on damping the flow pulsations, we chose a fixed intermediate liquid volume to total volume ratio of 0.4 within the various chambers. Our experimental tests of chambers of differing total volume demonstrated a relation between mean velocity of pumping, chamber size, and the mean flow variation (**Figure 3.4**). Larger chambers reduced the amount of pulsatility but with diminishing returns as the chamber size increased. From the sizes tested we selected the total volume size of 15 mL as this captured the majority of the dampening effect while minimizing the media volume and maintaining an overall size that was compatible with culture incubators.

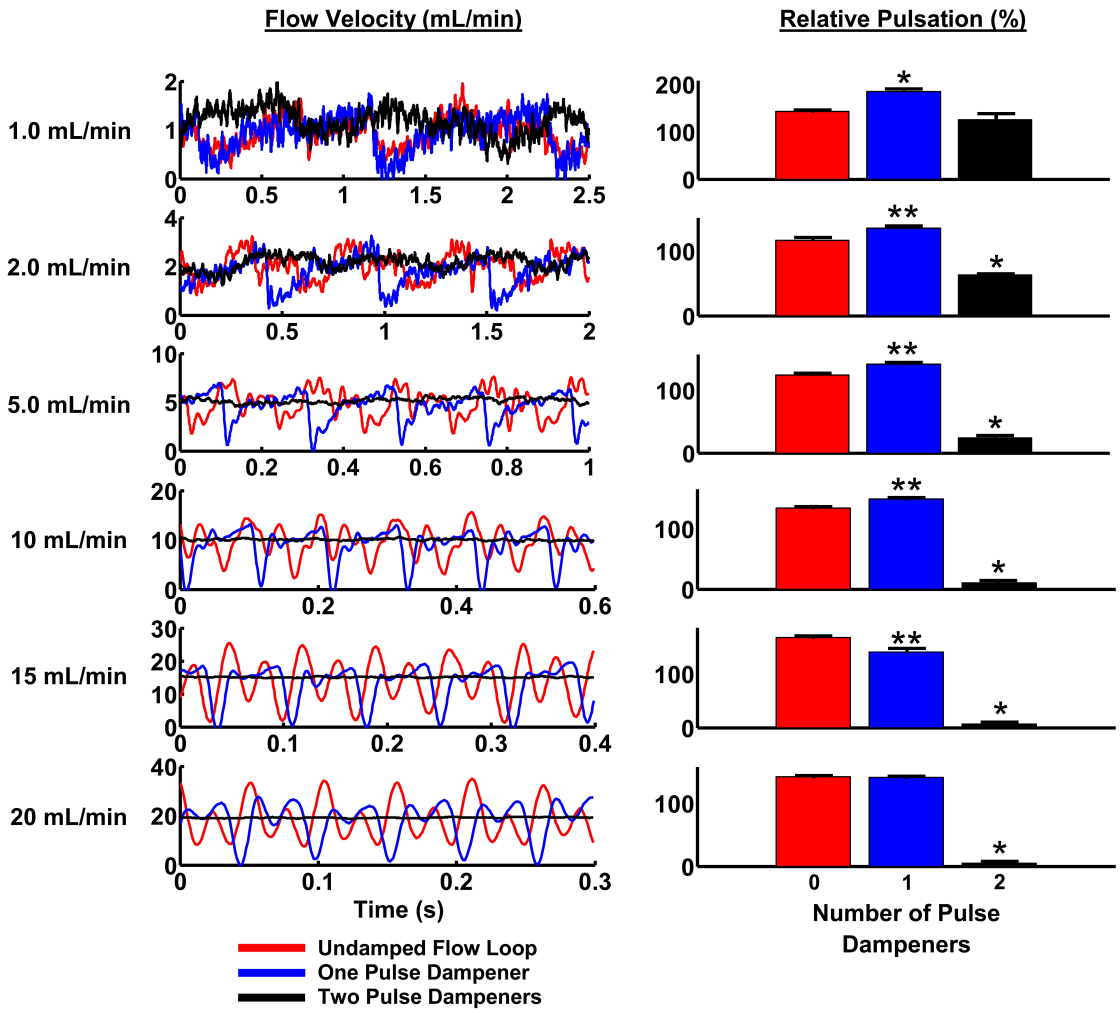


**Figure 3.3. Two pulse dampening units are needed to reduce pulsatility from a peristaltic pump in a closed flow loop.** Flow waveforms were recorded for the undamped system, with a single pulse dampener upstream of the flow probe, and with two pulse dampeners (one on each the inlet and outlet sides of the peristaltic pump). For these recordings, the inlet and outlet of the dampening chambers were placed at the middle and lower positions, respectively, and the liquid to volume ratio was set to 0.40. *Significantly different from the other two conditions ($p<0.05$). **The single-damped system is significantly different than the undamped system ($p<0.05$).

### *3.2.2.4. Effect of liquid volume ratio on pulse dampening of flow system.*

We next investigated the effects of altering the liquid to total volume ratio within the pulse dampener chamber. The gas component in the dampener provides compliance through its compressibility while the liquid component provides compliance through changes in fluid height. We found that maximizing the air in the chamber (a liquid to

total volume ratio of 0.25) led to close to a 100% decrease in pulsation in comparison to a ratio of 0.85 (**Figure 3.5**).

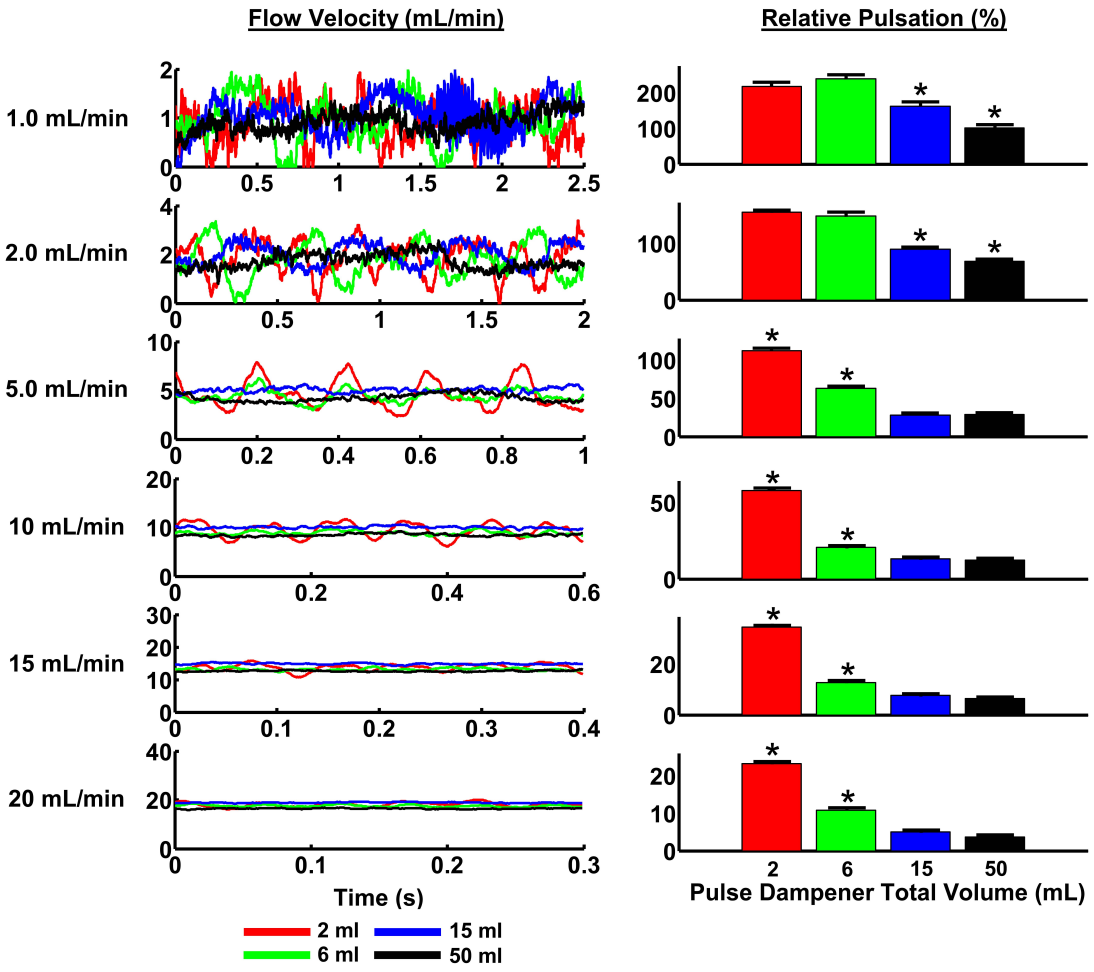


**Figure 3.4. Increased pulse dampener volume reduces pulsation in a peristaltic, closed-loop system.** Flow waveforms were recorded using pulse dampeners of varying total volumes. The inlets and outlets were placed at the middle and lower positions, respectively, and the liquid to total volume ratio was set to 0.40. Relative pulsation was calculated as the peak-to-peak measurement divided by the mean flow rate. *Significantly different values from the other three conditions ($p < 0.05$).

### *3.2.2.5. Inlet-to-outlet height had a limited effect on pulse dampening effectiveness.*

The transition between small diameter tubing and a larger chamber induces a small region of complex flow that introduces resistance. In addition, this transition creates a reflected wave similar to those formed in arterial systems at bifurcations[81]. Flow

within the chamber is complex and may contain circulation currents that depend on flow velocity. Flow circulation itself can be used as a means of pulse dampening and flow circulation pulse dampeners have been designed to work on large scale, industrial hydraulic systems[82]. To examine whether these effects altered the effectiveness of the pulse dampening system, we explored the effect of altering the ratio between the inlet and outlet height on the pulse dampener effectiveness. The rationale was that the positioning of the inlet and outlet may lead to changes in flow within the dampener. We found that at most of the mean flow velocities, the location of the inlet and outlet had only a weak effect on the damping that occurred. However, in the high flow case (20 mL/min), having the flow in a high-inlet/mid-outlet configuration caused a small decrease in damping capacity (**Figure 3.6**). This presumably was a consequence of the internal flow created within the chamber (having a greater effect as flow velocities increased). Due to its high damping capacity and compatibility with other optimized parameters, the mid-inlet/low-outlet configuration was chosen.

#### *3.2.2.6. Alterations in fluid viscosity over the physiological range for blood had a minimal effect on pulse dampener effectiveness.*

While standard culture media is a common and simple way to create fluid shear over cells in culture, many groups have also explored using fluids that have a viscosity similar to blood[83,84]. In addition, studies on thrombosis have used blood in a flow system to examine the mechanisms of thrombosis[85]. We examined the ability of the flow system to dampen flow pulsation while varying the viscosity of the flowing liquid to match that of culture media, blood and twice the value of blood viscosity. Over this range of viscosities there was little change in the overall pulse dampening (**Figure 3.7**).

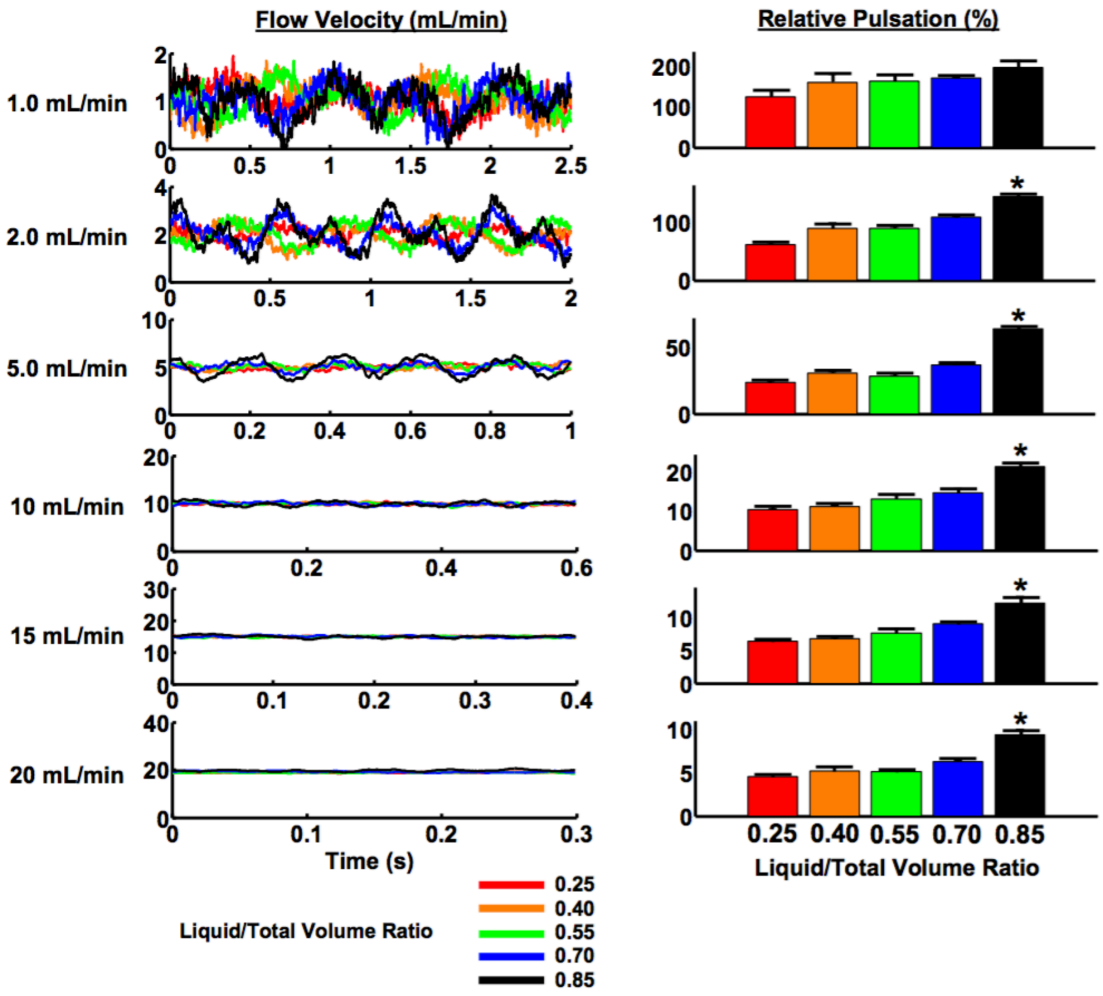


**Figure 3.5. Effect of liquid ratio within the pulse dampener on variations in fluid flow.** Liquid ratio reduces dampening capacity at high values. Flow waveforms were recorded using pulse dampeners filled to five different liquid fractional volumes: 0.25, 0.40, 0.55, 0.70, and 0.85. The inlet and outlet were in the middle and lower positions, respectively, and the total chamber volume was 15 mL. Relative pulsation was calculated as the ratio of peak-to-peak measurement divided by the mean flow rate. *At liquid volume ratio = 0.85, the system shows significantly higher values than the other four conditions ($p<0.05$).

### *3.2.2.7. Final design and validation of high-throughput pulse dampener.*

After optimizing the prototype system, we created a final version of the device that has two polycarbonate dampeners with six 15mL chambers each mounted on a support plate. (**Figure 3.8**). Two ports have been machined into each chamber to allow the mounting of a tubing connector for interfacing the pulse dampeners with the flow

loop. These two multichamber blocks are made air tight with a steel plate that compresses a silicone seal. These multichamber blocks are attached to an underlying mounting plate with an indentation for mounting a multichamber flow slide. The system was designed to be modular, allowing each six-well flow plate to be used in isolation as experimental demands change. In addition, the support plate immobilizes the flow plate and simplifies

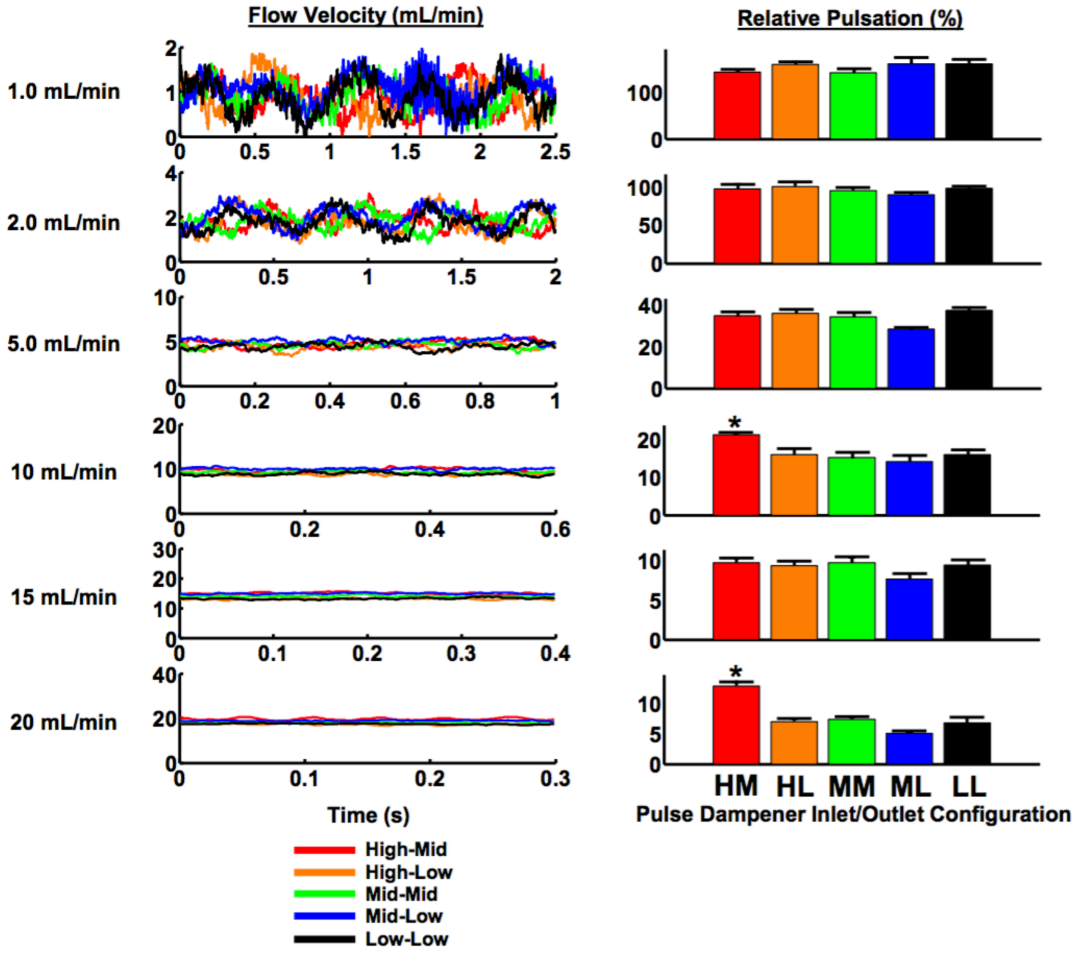


**Figure 3.6. Inlet/outlet configuration has a minimal effect on system pulsatility.** Only at the high-mid configuration does inlet/outlet configuration produce a significant effect and only then at high flow rates. Flow waveforms were recorded using the following inlet-outlet configuration: high-mid, high-low, mid-mid, mid-low, and low-low. Recordings were performed at liquid volume ratios of 0.24 and 0.55 and the total chamber volume was 15 mL. Relative pulsation was calculated as the ratio of peak-to-peak measurement to total flow rate. *At high-mid configuration, the system shows significantly higher values than the other four conditions ($p<0.05$).

the logistics of performing higher-throughput experiments with flow. Overall this system provides flow profiles for each isolated flow loop that were identical to those of the optimized prototype system.

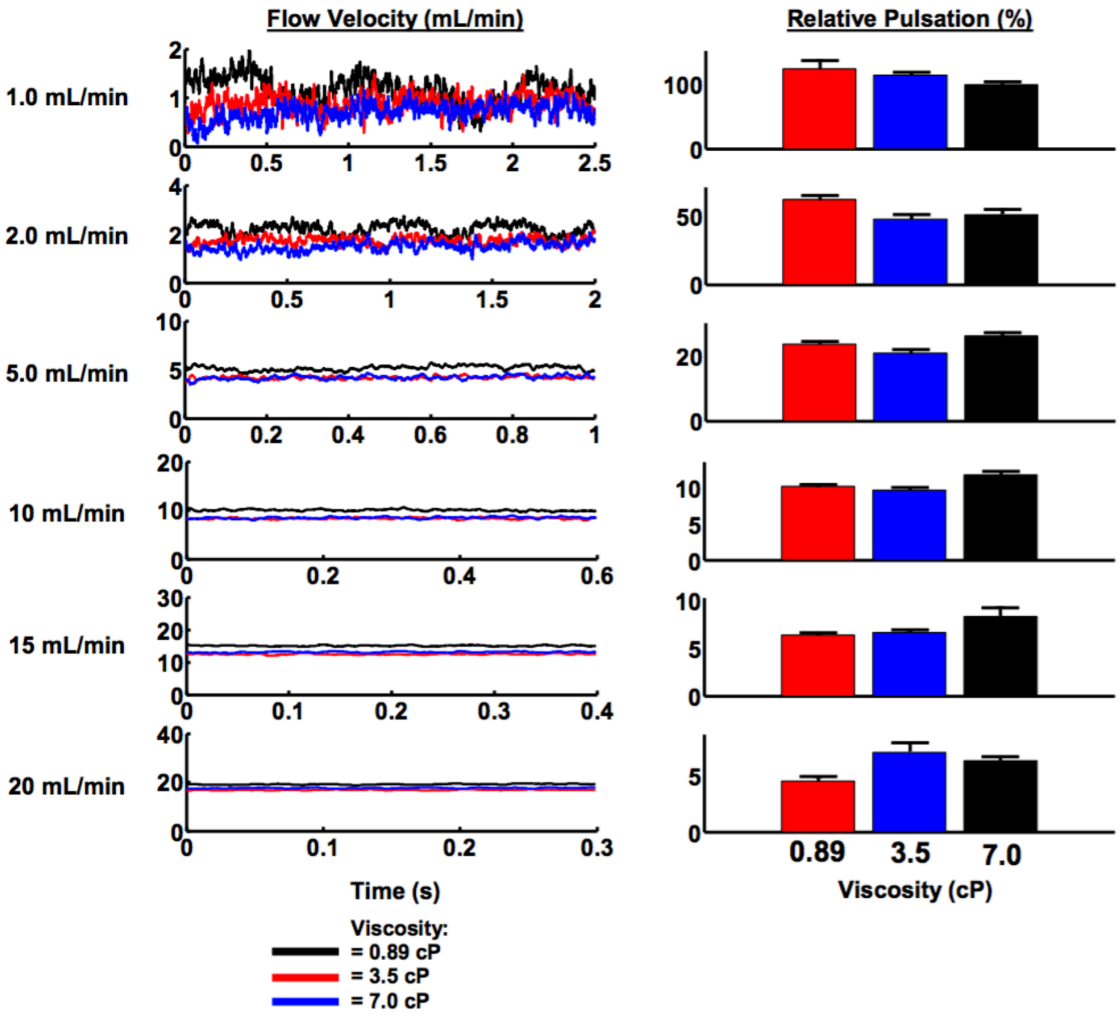


**Figure 3.7. Optimized pulse dampener design is effective at increased viscosities.** Using higher viscosity media has little effect on the effectiveness of the pulse dampener system. Flow waveforms were recorded using pulse dampeners at three different viscosities: 0.89, 3.5, and 7.0 cP. The inlet and outlet were in the middle and lower positions, respectively, and the total chamber volume was 15 mL. Relative pulsation was calculated as the ratio of peak-to-peak measurement to total mean flow rate.

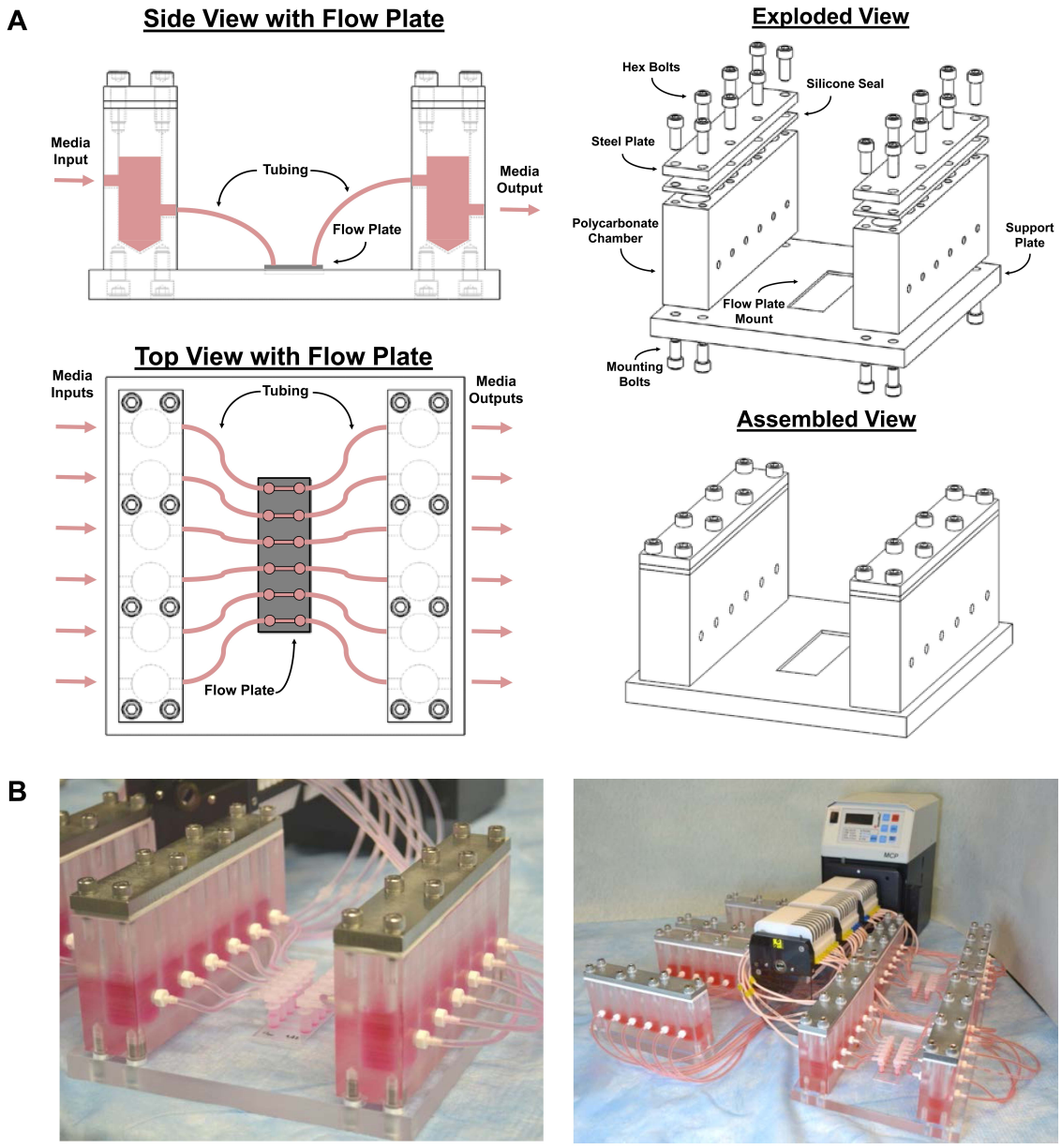


**Figure 3.8. Design of low-volume pulse dampener for multichannel flow.** (A) The dampener consists of two compliance chambers containing culture media and air. A flow plate with six parallel-plate flow chambers was placed between the pairs of compliance chambers and connected with tubing and elbow connectors. (B) Photographs of the assembled pulse dampener with up to 24 parallel channels.

### *3.2.2.8. Comparison of pulsating flow versus steady flow in controlling endothelial cell response to shear stress.*

To examine the biocompatibility and utility of our multichannel flow system we

examined the viability and responsiveness of cultured endothelial cells to shear flow. We applied 20 dynes/cm$^2$ of shear stress to HUVECs for 12 hours in the flow system without pulse dampeners (undamped), with a single pulse dampener or with full system with two dampeners. Cells exposed to the undamped flow loop were found to detach and had 80% less surface coverage of cells in comparison to those in the system with a single or dual pulse dampening unit (**Figure 3.9A and 3.9B**).

Shear stress induced alterations in cellular elongation and cytoskeletal organization is a well-characterized response in endothelial cells. We examined the effect of treating cells with 20 dynes/cm$^2$ of mean shear stress using the undamped, single-damped and double-damped systems. Both the undamped and single-damped system applied pulsatile flow while the double-damped system applied steady flow. Elongation by flow was seen in 80% of cells exposed to steady flow in the double-damped system while only 40-50% of cells elongated that were exposed to pulsatile flow after 12 hours (**Figure 3.9C**). To examine the long-term compatibility of the system we applied steady flow using the pulse dampened system for 38 hours and found no signs of cell loss (**Figure 3.9D)**. These cells had increased alignment and elongation in comparison to cells at the shorter time points (**Figure 3.9E-G**).

We next examined the ability of the shear stress in the system to stimulate two well-characterized endothelial cell responses to shear stress including cytoskeletal remodeling and an enhancement in the production of expression of eNOS and production of NO[85]. After 12 hours of exposure to steady flow endothelial cells in the system had enhanced formation of actin stress fibers and overall actin intensity (**Figure 3.10A and 3.10B**). Focal adhesion formation was also enhanced under steady flow as evidenced by paxillin staining with most, but most prominently in the undamped system (**Figure 3.10C**). Cells treated with 20 dynes/cm$^2$ mean shear stress in the double-damped system also had enhancement in eNOS expression of around 2.5 fold over the static control after

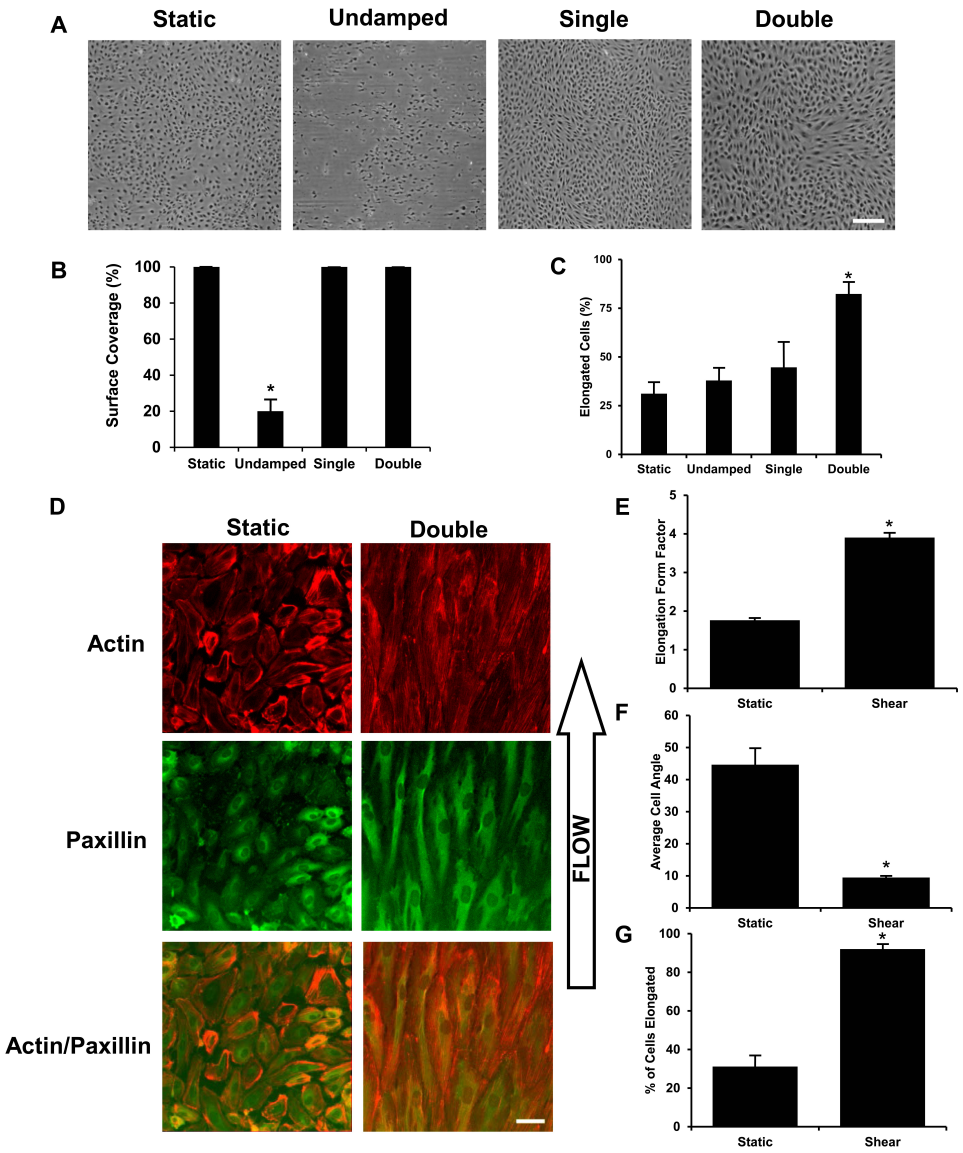


**Figure 3.9. Cell coverage and elongation in response to steady and pulsatile shear stress.** Mean flow of 16.3 mL/min (20 dynes/cm$^2$) was applied to endothelial for 12 hours using the undamped, single-damped, and double-damped systems. (A) Phase contrast images of the cells after each of the flow conditions: static, undamped, single-damped, and double damped. Scale bar = 200$\mu$m. (B) Cell coverage is the percent area covered by the cells in the monolayer. The undamped system shows a significant loss in cell coverage during flow. (C) Cell elongation was defined as a major-to-minor axis greater than two. (D) Mean flow of 16.3 mL/min (20 dynes/cm$^2$) was applied to endothelial for 38 hours using the double-damped system. Scale bar = 50 $\mu$m. (E) Cell elongation was defined as the major-to-minor axis ratio. (F) Cell angle was relative to direction of flow and was calculated for cells with an elongation form factor > 2. (G) Cell elongation was defined as a major-to-minor axis greater than two. *Statistically different from all other groups ($p < 0.05$).

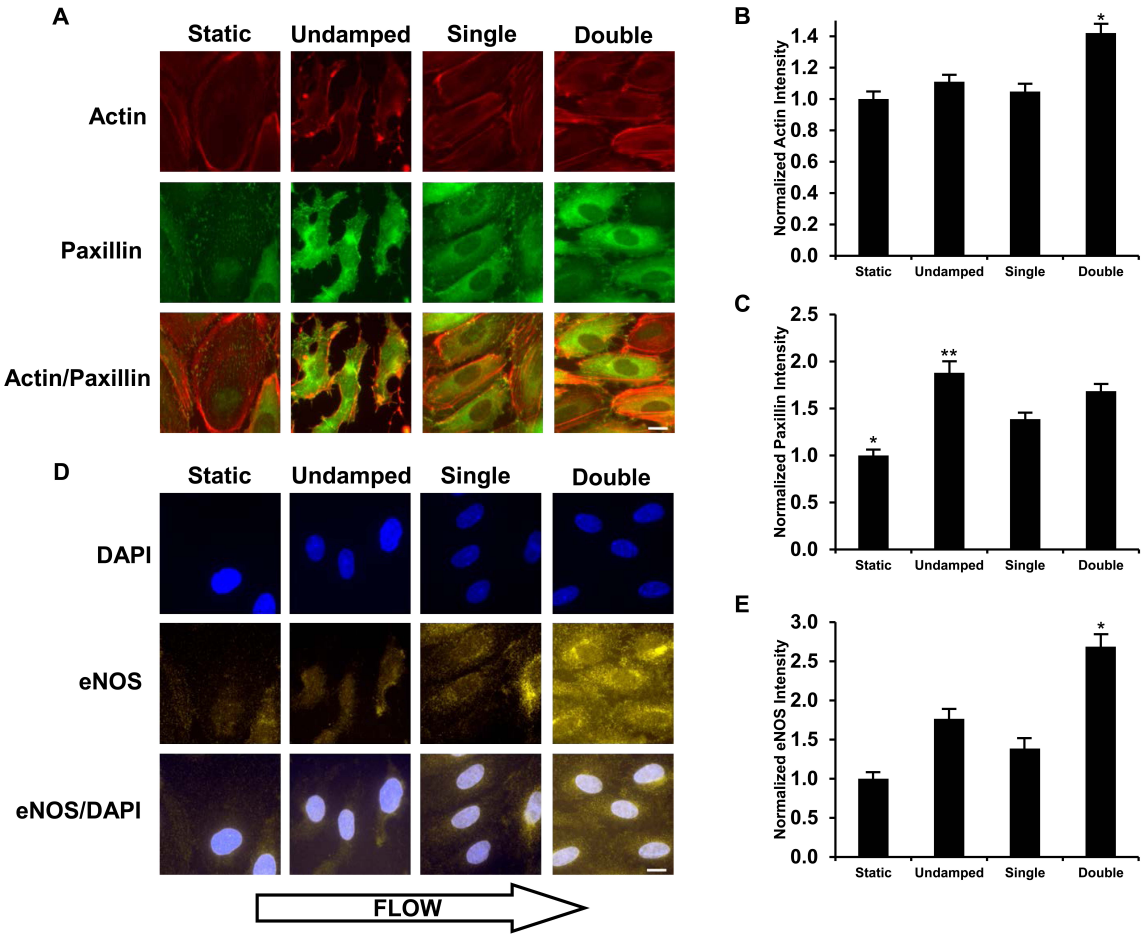


**Figure 3.10. Biological validation of the double-damped flow system versus undamped and single-damped flow systems.** (A) Fluorescence images were stained for actin and paxillin in each of the flow conditions: static, undamped, single-damped, and double-damped. Cells were treated with 20 dynes/cm2 shear stress for 12 hours. (B) Average actin intensity per cell was normalized to static culture levels. The double-damped system shows a significant increase in actin levels compared to the static, undamped, and single-damped conditions. (C) Average paxillin intensity per cell was normalized to static culture levels. *Significantly lower values than the other three conditions ($p<0.05$). **Significantly higher than the single-damped system ($p<0.05$). (D) Fluorescence images were labeled with DAPI and an antibody against eNOS in each of the flow conditions: static, undamped, single-damped, and double-damped flow. (E) Steady flow increases eNOS to a greater extent than pulsatile flow. Average eNOS intensity per cell was normalized to static culture levels. *The double-damped system shows a significant increase in eNOS levels over the other conditions ($p < 0.05$). Scale bar = 25 $\mu$m.

12 hours of flow and at least 50% greater than that of the undamped and single-damped systems (**Figure 3.10D and 3.10E**).

### 3.2.3. Discussion:

Systems for studying vascular mechanotransduction in cultured cells have shown the importance of mechanical environment in controlling many aspects of vascular biology[62]. We sought to develop a simple, high-throughput device to allow the application of fluid shear stress to cultured cells that was accessible to many laboratories. Several main approaches have been used in the past to create flow over cells in culture. These include parallel-plate flow chambers[65-67], flow tubes[86], and cone-and-plate devices[69,70]. We chose to pursue the parallel-plate flow chamber configuration as it creates flow in a format highly amenable to live cell imaging, immunofluorescent staining, and other common assays used in studying mechanotransduction. Parallel-plate flow chambers compatible with our system are available commercially and are also easily custom manufactured. Recently a number of microfluidic platforms have been developed to provide devices to study cultured cells under flow conditions[73-75]. The system developed in this work presents a very accessible means to apply steady flow in a multiwell format. This capability allows it to interface with existing commercially available flow chambers and would allow the application of long term multichannel flow to microfluidic chips.

In our system, we found that at least one pulse damper was essential for maintaining cell viability and attachment in the closed flow loop. The likely reason for this finding is the reduction in maximum flow rate from the undamped system versus the system with a single pulse dampener. The addition of a single pulse dampener at a mean flow rate of 15 mL/min reduces the maximum flow rate of the system from 25 mL/min to around 18 mL/min. This corresponds to shift from 31 dynes/cm$^2$ to 22 dynes/cm$^2$ in

maximum shear stress. Thus, cell detachment with this high shear rate is the likely the cause of cell loss in the undamped system at physiological flows of 18 mL/min.

We optimized our system to effectively remove pulsation in the flow loop at physiologic arterial flow rates. The compliance added into a flow system by adding a volume of trapped compressible gas acts as a low-pass filter, passing lower frequencies with greater magnitude than high frequencies[87]. In a peristaltic pump, the flow rate is increased by accelerating the rotation of the rollers and, thus, the frequency of the rhythmic occlusion of the tubing. Consequently, as we move to higher flow rates the frequency of pulsation increases. A major consequence of this pump behavior and the use of a capacitance as a pulse dampener is that as the mean flow rate decreases and frequency of pumping decreases, the pulse damping system becomes less effective. Therefore, for slower flow rates/pulsatility a larger compliance is needed to fully dampen the unsteady nature of the flow as observed in our studies. While we concentrated on exploring a two-dampener system, one could potentially use additional dampeners in series; however, we feel that this would not have a substantial advantage over increasing the gas volume in the compliance chamber.

We tested the biocompatibility of our system by examining several shear-mediated behaviors in endothelial cells. Previous studies have shown that shear stress can activate the eNOS pathway in endothelial cells[88-92]. This activity is an essential property of the healthy endothelium and is lost when endothelial cells become dysfunctional in disease[93]. In our study, we compared the effects of pulsatile flow versus steady flow in activating eNOS under the identical mean flow conditions. Our results demonstrated that steady flow induces a more robust increase in the eNOS expression in comparison to the high-frequency pulsatile flow produced by the system with a single dampener. These findings are consistent with those of other groups that compared eNOS mRNA expression and found reduced production of nitric oxide and eNOS mRNA with flow simulating human arterial pulsatile flow versus continuous flow[88]. In our study we used a

pulsation cycle that was about 10-15 fold faster than human arterial pulsation. While this is beyond the physiological heart rate of humans, the rate of pulsation from the pump corresponds to a heart rate of 600-900 beats per minute, a rate similar to the average or elevated heart rate of mice. In addition to validating the biocompatibility of our system, these findings also suggest that the endothelium is capable of sensing high frequency pulsations and can markedly alter the endothelial cell production of eNOS.

## 3.3 LARGE FORMAT DEVICE

Our twenty-four channel, multi-throughput shear system contains many novel characteristics over existing systems. It uses a minimal media volume, particularly important in experiments that require the addition of expensive growth factors, and can run many experiments in parallel that previously needed to be conducted serially. However, it does still have limitations. The ibidi six-channel plates the system was designed to work with have a minimal cell growth area. This is ideal for live or fixed cell imaging, but creates a poor signal-to-noise ratio for cell lysis techniques; real-time polymerase chain reaction (PCR) is possible, but noisy, and Western blot assays have produced inconsistent results. Additionally, many assays that analyze cell excretions into the surrounding media, such as chemokine and nitrite/nitrate assays, are a challenge. Therefore, we wanted to design a system that was analogous to the multi-throughput technology of our optimized system, but allowed for the growth of a larger number of cells for many of these techniques.

To facilitate the larger cell growth area, we took a step back and looked at the initial parallel-plate flow systems. These systems, which use an extracellular matrix-coated glass slide as the substrate, allow for more than an order of magnitude increase in surface area. A rectangular gasket is then applied between the slide and the top plate that has the inlet and outlet for media flow. While traditionally done in a single channel setup, this system is highly compatible with the peristaltic pump/pulse dampener setup for our optimized system. Therefore, we designed a new baseplate and parallel-plate apparatus setup to allow for a twenty-four channel system that accommodates cells grown on standard microscopy slides.

### 3.3.1. Materials and Methods

#### *3.3.1.1. Device Design and Fabrication*

Design of the initial gasket and top plate were modeled after the Rectangular Flow Chamber Kit from GlycoTech Corporation. However, in lieu of a vacuum-based system, which is more complex for a multichannel setup, a top bar was designed to hold each 'sandwich' in place. Parts were designed using SolidWorks (Dassault Systèmes) and converted to proprietary software for fabrication by eMachineShop. A multichannel peristaltic pump (MCP Standard; Ismatec) with a 24 channel pump head was used to create flow in the system. Shear stress in the flow chambers at the cell culture surface was calculated using the following relation for laminar flow in a rectangular channel:

$$\tau = \eta \frac{\phi}{q}\left\{\sum_{n=0}^{\infty}\frac{(-1)^n}{(2n+1)^2}\left(\frac{2}{\pi}\right)^3 \tanh\left[(2n+1)\frac{\pi h}{2b}\right]\right\}$$

$$q = \frac{4}{3}hb^3 - 8b^4\left(\frac{2}{\pi}\right)^5 \sum_{n=0}^{\infty}\frac{1}{(2n+1)^5}\tanh\left[\frac{(2n+1)\pi h}{2b}\right]$$

where $2h$ is the height of the channel, $2b$ is the width of the channel, $\eta$ is viscosity, and $\phi$ is the flow rate through the channel[79].

#### *3.3.1.2. In Vitro Testing*

HUVECs were used between passages 4 and 6. These cells were grown in MCDB-131 media with growth supplements (Lonza) with a total of 7.5% FBS (Invitrogen). Standard 1"x3" glass microscopy slides were autoclaved and coated with collagen at 37°C for 1 hour before cells were seeded and grown to confluence. During the application of flow, the entire system was placed in an incubator and kept at 37°C and 5% $CO_2$.

For immunostaining, the cells were then washed with PBS and fixed in 4% paraformaldehyde for 20 min. The cells were then permeabilized in 0.1% Triton X-100

and blocked with 5% FBS for 1 hour. Next, the cells were exposed to a 1:50 dilution of primary antibodies for paxillin and eNOS (Santa Cruz Biotechnology) in 1% bovine serum albumin (BSA) overnight at 4°C. The cells were then washed three times in PBS/1% BSA and treated with a 1:1000 dilution of fluorescently-labeled secondary antibodies for 1 hour at room temperature. Finally, the cells were mounted in a hardset DAPI-containing mounting medium, coverslipped, and imaged using an epifluorescent microscope (Carl Zeiss).

### 3.3.2. Results

#### *3.3.2.1. Large Format Parallel-Plate Design*

In order to modify our original optimized system to accommodate cell-coated microscopy slides, we needed to a) redesign the baseplate to allow for the large surface area of the slides, b) design a parallel-plate 'sandwich' system, and c) create a system to secure each setup in place during experimentation. The new baseplate still includes attachments for the pulse dampeners but has six 1"x3" grooves for the slides. We based our parallel-plate 'sandwich' design on the Rectangular Flow Chamber Kit from GlycoTech Corporation. Each unit consists of a 0.01" silicone gasket with a rectangular hole that is placed on the cell-coated glass microscopy slide. Then, a polycarbonate top piece is applied which contains tapped holes and triangular grooves that function as the inlet and outlet for media flow. While the system from GlycoTech uses a vacuum-based system to hold the 'sandwich' together, this becomes a much more complicated endeavor in a multi-throughput system. Therefore, we simplified for the system by designing a top bar that screws into the baseplate and holds the six 'sandwiches' together. This design can be seen in **Figure 3.11A and Figure 3.11B**.

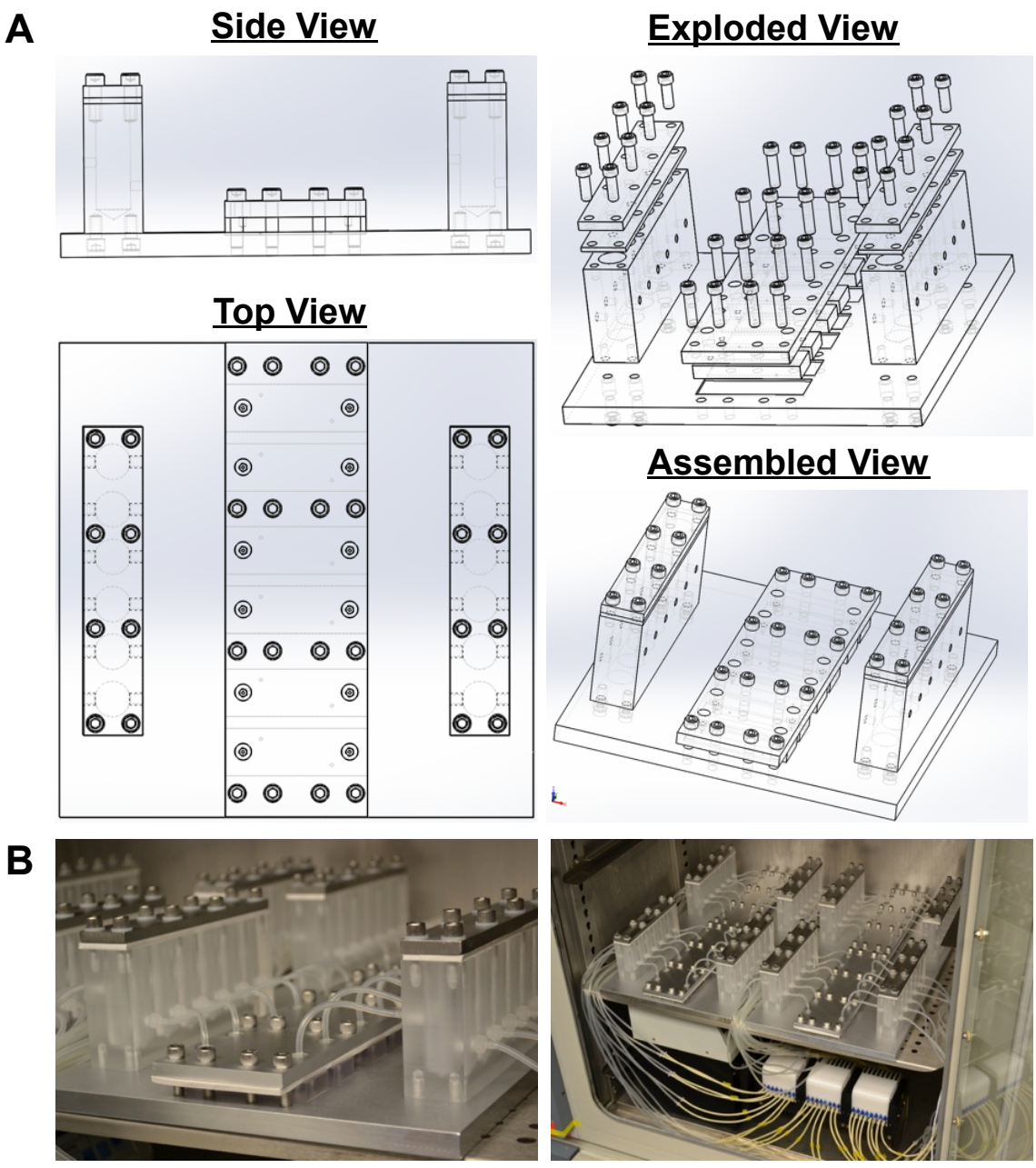


**Figure 3.11. Large format parallel-plate flow design.** (A) The design uses the pulse dampeners from our original device attached to a larger baseplate with recesses for 1"x3" microscopy slides. Silicone gaskets and top inlet/outlet pieces are held down onto the slides by the securing top bar and sixteen bolts. Side, Top, Exploded, and Assembled Views from SolidWorks are shown. (B) The final modular system set up for twenty-four independent experiments.

### *3.3.2.2. In Vitro Device Validation*

In order to test that the cells in the system were able to respond to shear stress in a manner consistent with previous studies, we cultured HUVECs on collagen-coated glass microscopy slides and applied a shear of 12 dynes/cm$^2$ for 24 hours using our system. To test the feasibility of the system for immunostaining, the cells were fixed in 4% paraformaldehyde and stained fluorescently labeled for actin and eNOS. As shown in **Figure 3.12A**, our system maintains the ability of cells to align to flow and increase eNOS production. We later used our system to conduct shear stress experiments for Western blotting, such as in **Figure 4.3B**.

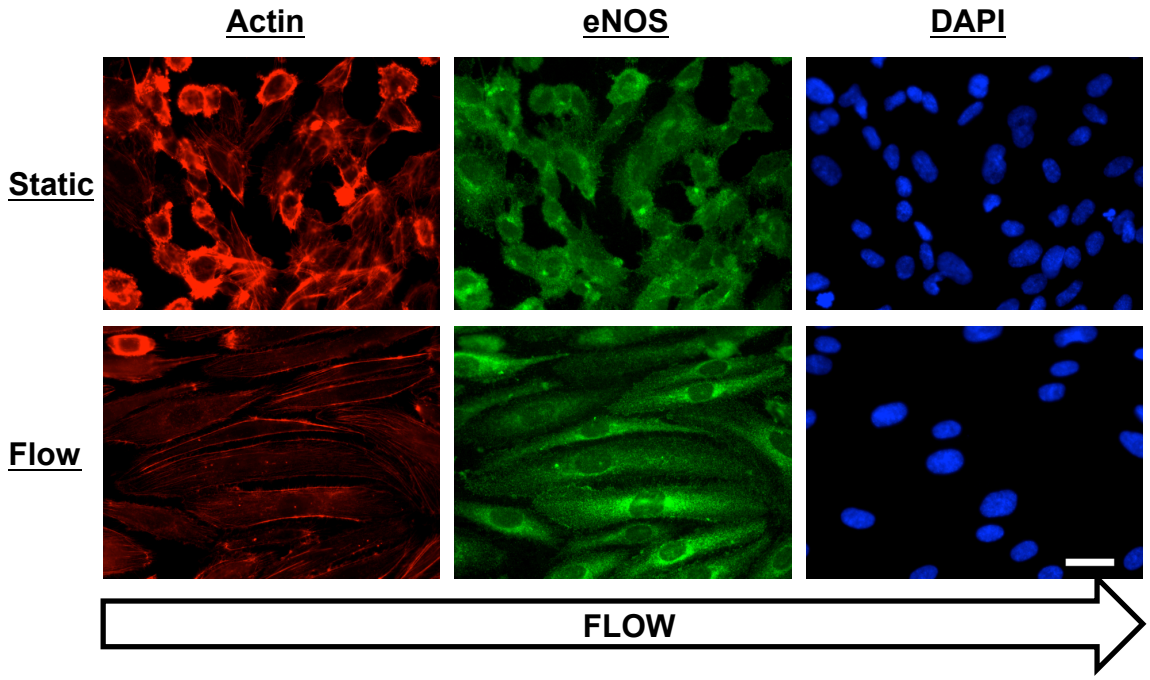


**Figure 3.12. Immunostaining with Large Format Parallel-Plate Device.** HUVECs were exposed to 24 hours of 12 dynes/cm$^2$ shear stress, fixed, and immunostained for eNOS expression and the actin cytoskeleton. Exposure to shear stress induces cell alignment with flow and increased levels of eNOS expression. Scale bar = 50 $\mu$m.

### 3.3.3. Discussion

While our initial optimized multichannel flow system improved on many of the issues with existing systems, we wanted to create an analogous modification that would allow us to address some of its own issues. Mainly, the low number of cells in the ibidi six-channel flow plates precludes many downstream analysis applications such as Western blotting and chemokine assays. Therefore, we looked back to some of the initial systems that used cells cultured on microscopy slides, which have an order of magnitude higher surface area, and sought to merge those systems with the low media requirements and multichannel capabilities of our system. We were able to create a system that is robust and compatible with our peristaltic pump/pulse dampener system and capable of both immunostaining and cell lysis-based (e.g. Western blot) downstream techniques. The new toolset allows us a new set of analysis applications with which to study endothelial shear mechanotransduction responses.

### 3.4 CONE-AND-PLATE DEVICE

Our multichannel parallel-plate flow system and larger format modification allow us to conduct a large range of analytical techniques to investigate the endothelial shear mechanotransduction response, including immunostaining, real-time PCR, Western blotting, and chemokine assays. One large limitation, however, is the lack of temporally dynamic waveforms that we can apply as the shear response. While this is technically feasible with a parallel-plate system, a far easier alternative is the other canonical *in vitro* shear stress tool: the cone-and-plate system. Briefly, a low-angle cone is rotated just above the cultured cells at a given rotational velocity. The further away the cells are from the center of the plate, the further the distance between the cone and the cells; however, the tangential velocity of the cone also increases. Thus the equation to calculate the shear stress from the cone can be simplified to:

$$\tau = \frac{\mu\omega}{\theta}$$

where $\tau$ = shear stress, $\mu$ = fluid viscosity, $\omega$ = rotational speed, and $\theta$ = angle of the cone[94]. The principle benefit of this system is that the shear stress is directly related to the rotational speed and so a dynamic rotational speed profile translates into a dynamic shear stress profile.

Dynamic shear stress profiles have come under increased interest in recent years. While static culture is frequently used as a control during *in vitro* shear experiments, this is clearly not the case in atheroprone regions of the vasculature. Indeed, cultured cells have shown some very different responses to a low amplitude, low frequency oscillatory shear profile versus static conditions[95]. Additionally, the ability to apply dynamic waveforms allows for complex, physiologically accurate waveforms; Dai *et al*. used flow profiles measured from human patient's carotid arteries via ultrasound to generate a shear stress waveform that recapitulates that found in the carotid artery (**Figure 3.13**)[96]. These complex dynamics both yield interesting new findings in the complexities of dynamic

mechanotransduction, but also may allow fast therapeutic design due to the use of specifically physiologically relevant waveforms.

For the design and construction of our cone-and-plate system, we aimed to take the important characteristics of existing systems and improve upon them in a similar fashion to our other machines. Our main design criteria were to create a system that: (1) was modular to allow for simultaneous units to run in parallel, (2) was driven by a motor capable of running most physiologically relevant waveforms, (3) applied shear stress to enough cells in culture to allow for downstream analysis techniques such as Western blotting, and (4) allowed for long experiment duration (at least 24 hours).

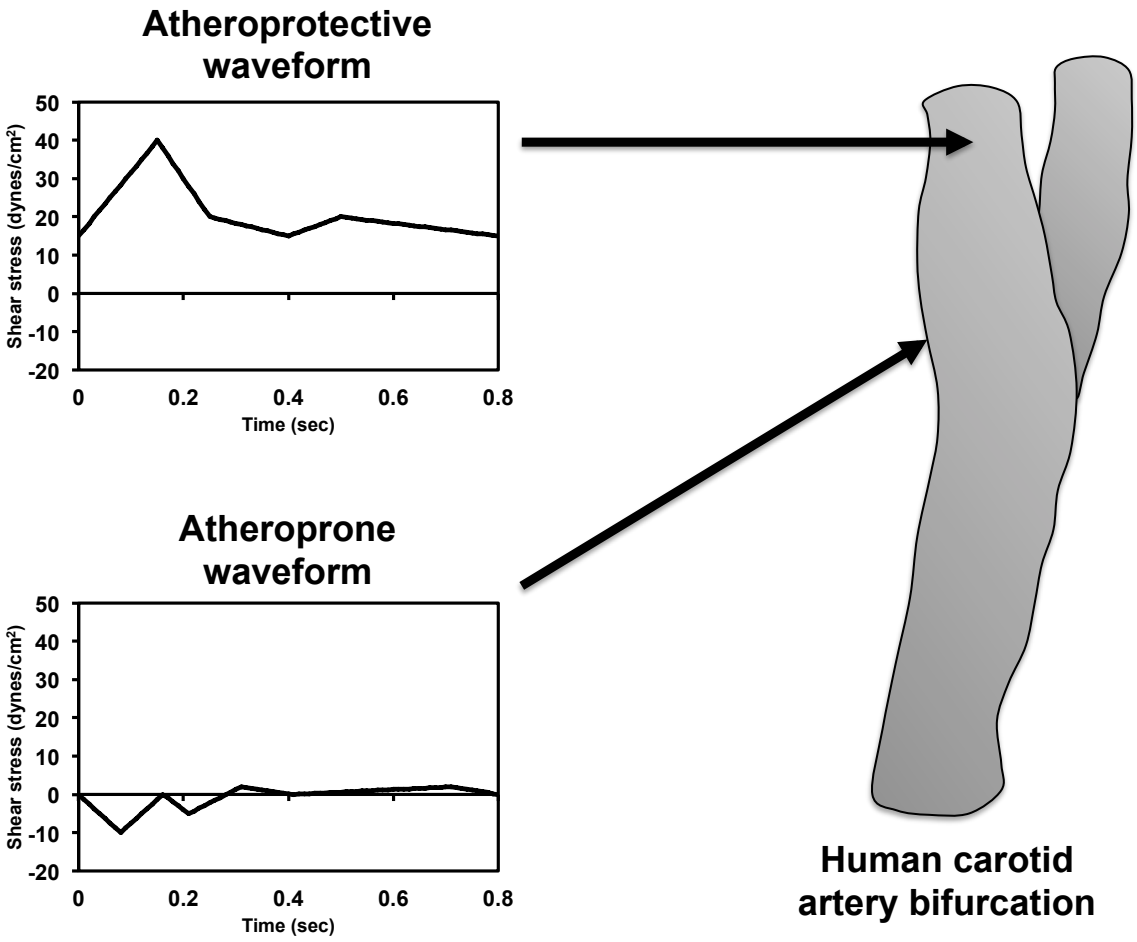


**Figure 3.13. Carotid artery flow profile.** Graphs of carotid artery local shear stress levels based on ultrasound data from Dai *et al*[96].

### 3.4.1. Materials and Methods

#### *3.4.1.1. Device Design and Fabrication*

Parts were initially designed in SolidWorks (Dassault Systèmes) and later translated into the custom software for eMachineShop for fabrication. With the exception of the cone, which was made from 316 stainless steel, all parts were manufactured from aluminum. The flange was purchased from SealMaster and the motor and controls were purchased from Quicksilver Controls.

#### *3.4.1.2. In Vitro Testing*

Human umbilical vein endothelial cells (HUVECs) were used between passages 4 and 6. These cells were grown in MCDB-131 media with growth supplements (Lonza) with a total of 7.5% FBS (Invitrogen). Cells were seeded onto standard 10 cm cell culture dishes (Corning) and grown to confluence. During the application of flow, the cone-and-plate device was placed in an incubator and kept at 37°C and 5% $CO_2$. The cells were then washed with PBS and lysed with 20mM Tris, 150mM NaCl buffer (pH 8.0) containing 1% Triton X-100, 0.1% SDS, 2mM sodium orthovanadate, 2mM PMSF, 50mM NaF, and 1 complete protease inhibitor pellet (Roche) per 50mL lysis buffer. For Western blotting, a 1:500 dilution of primary antibodies (VCAM-1, ERK1/2, and GAPDH from Cell Signaling) was used for overnight incubation at 4°C and a 1:3500 dilution of secondary antibodies (Santa Cruz Biotech) was used at room temperature for 2 hours as previously described [97].

### 3.4.2. Results

#### *3.4.2.1. Device Design*

The initial design consideration we had was the dimension of the cone. The three major design characteristics were the material, the angle, and the width. We chose to use 316 stainless steel due to the high level of biocompatibility, durability to reduce scratches and blemishes that would affect shear profile, and ease of sterilization. For the angle, we

elected to use a 2° angle cone due to the uniform shear profile it creates, based on previous computational calculations by our lab[98]. Finally, the width of the cone relative to the cell culture dish affects the volume of media that can be used during an experiment. We wanted to ensure that the media volume during experimental runs would not fully dry out due to evaporation and wicking. After calculating the maximum media volume possible for a range of different cone widths we finalized on 2.9" due to its maximum media volume of 13.8 mL. Additionally, this design leaves a clearance of 0.25" between the cone and the culture dish wall to allow for a media exchange system if necessary for longer runs.

The other major design consideration we had was the power requirement of the motor. In order to ensure optimal performance, we needed to make sure the motor we chose was able to produce enough power to overcome the frictional and inertial forces present in our most aggressive waveforms. We calculated the fluid drag force from the media and inertial force from accelerating the cone to a maximal shear stress level of 45 dynes/cm$^2$, which yielded a motor that required 0.123 Nm of torque. Based on these physical, as well as financial, considerations, we opted for the QCI-34L-1 motor from Quicksilver Controls.

The final design was done in SolidWorks and then converted into proprietary software for machining by eMachineShop (**Figure 3.14A**). For visual confirmation and conception of the design in the incubator, we used the virtual reality feature of the eDrawings app (SolidWorks) for Apple iPad to assess the scale and if we would be able to fit four modules in our incubator (**Figure 3.14B**).

#### *3.4.2.2. Fabrication, Assembly, and Calibration*

Once the parts were machined, we assembled the cone-and-plate devices. Most of the assembly consists of bolts and tapped holes, but the major part that needed to be calibrated was the cone height. (**Figure 3.15A**) To ensure proper shear stress, the point of

the cone needs to be just above the cell height. While once the cone is locked in place it will remain in the same spot during each experiment, we needed to devise a way to assess when the cone was just above the bottom of the cell culture plate. To accomplish this we created a rudimentary circuit using the top piece, aluminum foil, and a multimeter.

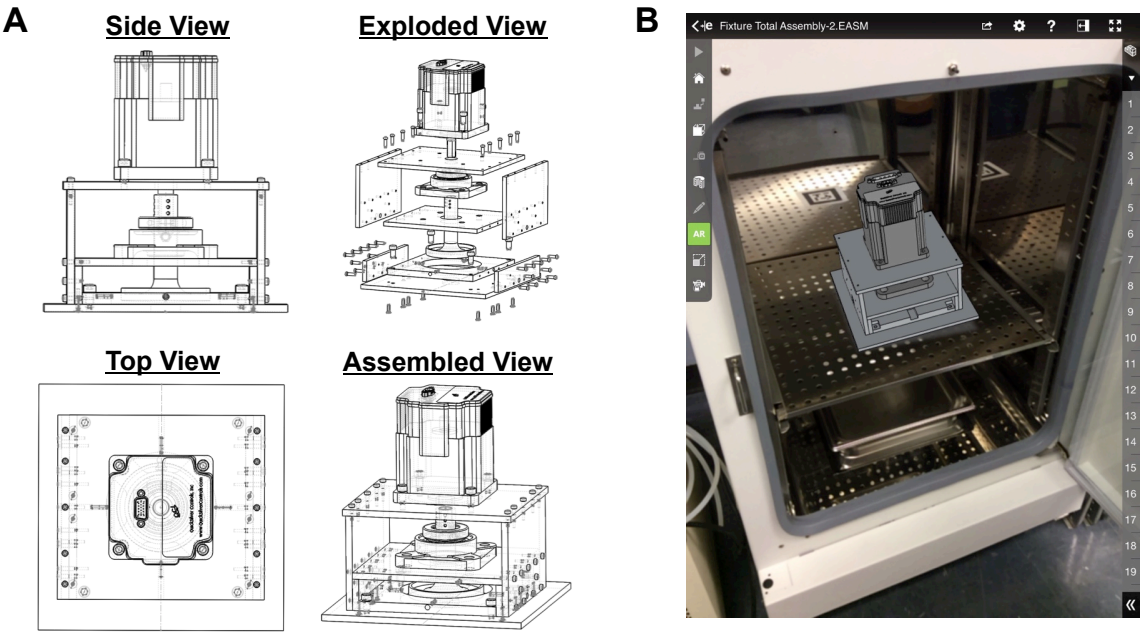


**Figure 3.14. Design of cone-and-plate device.** (A) Side, top, exploded, and assembled views in SolidWorks. (B) Picture of device in incubator using the virtual reality feature on eDrawings app (SolidWorks) for Apple iPad.

(**Figure 3.15B**). Briefly, the aluminum foil was flattened on the bottom of a cell culture plate and connected to the multimeter via a wire. Another wire connected the top piece to the multimeter. When the machine was assembled, the cone was gently lowered until it touched the aluminum foil, closing the circuit and creating a measureable resistance on the multimeter. The cone was then mechanically tapped up slightly and tested again until the point where the circuit was just broken. Then the cone was secured in place and the procedure was repeated with the remaining modules. (**Figure 3.15C**).

### *3.4.2.3. Initial In Vitro Testing*

In order to validate the system, we wanted to run a simple experiment to validate that we could achieve one of our principle goals with the system: to use Western blotting techniques to analyze the effects of different dynamic shear profiles on cultured endothelial cells. We applied two different shear profiles, laminar shear at 12 dynes/cm$^2$ and oscillatory shear at ± 0.5 dynes/cm$^2$, for four hours in addition to our static control. Cells were then lysed, normalized by BCA assay, and Western blotted for VCAM-1 and ERK1/2. GAPDH was used as a housekeeping marker to validate uniform well loading (**Figure 3.16**). The laminar shear condition had lower levels of both ERK1/2 and VCAM than the oscillatory and static conditions, and the GAPDH validated that we were able to effectively load uniform levels of protein in each well.

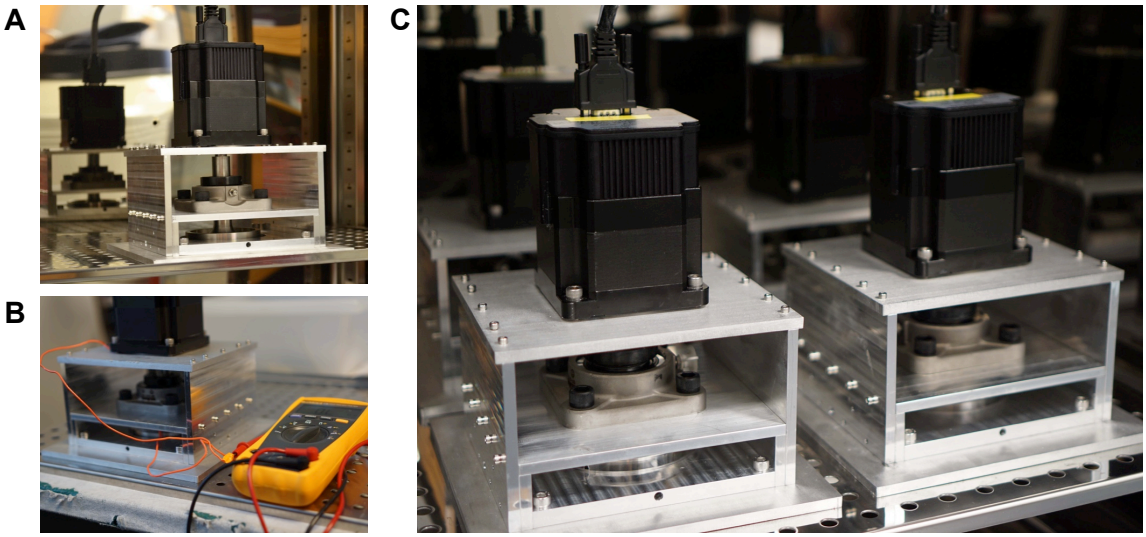


**Figure 3.15. Completed cone-and-plate devices.** (A) Picture of device in incubator. (B) Picture of closed-loop resistance measurement calibration setup. (C) Picture of four cone-and-plate devices.

## 3.4.3. Discussion

To supplemental our existing toolbox of shear stress application devices, we wanted to design a device that allowed us to apply dynamic shear stress waveforms to

cultured cells. In order to most simply achieve this goal, we deviated from our parallel-plate shear stress devices in favor of a cone-and-plate model. The benefit of this system is that it allows us to dynamically alter the shear stress with the speed of cone rotation. Additionally, we had several design characteristics that we wanted to include: (1) a modular system, (2) the ability to run multiple waveforms, (3) applying shear to enough cells for downstream techniques such as Western blotting, and (4) to enable the system to perform for long shear runs. We have created four devices that can be run in parallel, but the system is only limited by the available space in a cell culture incubator. We ensured that the motors were able to produce the necessary power to create almost any physiological shear waveform. Using an *in vitro* pilot run we ensured that the system could successfully perform downstream Western blots. And finally we designed the cone to enable enough media for long experiments. Additionally, we have created space between the cone and cell culture sidewall to allow us to use our peristaltic pump as a media exchange system for experiments that are longer than the existing media allows.

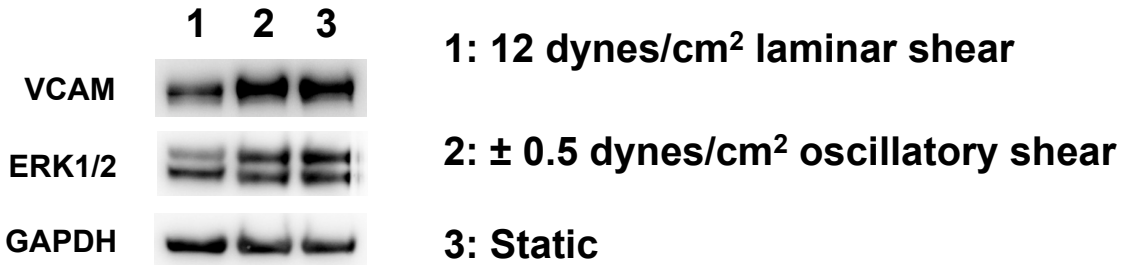


**Figure 3.16. Western Blot of Initial Test Run.** Four hours of 12 dynes/cm$^2$ laminar shear stress lowers expression of VCAM-1 and ERK1/2 from static culture levels, while ± 0.5 dynes/cm$^2$ oscillatory shear does not.

## 3.5 CONCLUSIONS

Endothelial shear stress mechanotransduction *in vitro* experiments require mechanical devices that can use media to apply shear stress over endothelial cells. Our goal was to design machines that used the basic framework of long-established shear application methods and improve them to allow us to carry out experiments in parallel. With our first device, we created a multithroughput system that allows us to carry out twenty-four simultaneous experiments in parallel while reducing the necessary media requirements for each by more than an order of magnitude over most conventional parallel-plate systems. The modified second version allows for shear over a larger number of cells to facilitate Western blotting and chemokine assays. Finally, our cone-and-plate devices can produce dynamic waveforms to investigate the temporal effects of physiological shear waveforms. Overall these devices give us a powerful toolset to allow us to examine the role of syndecan-1 in the shear-mediated endothelial mechanotransduction response.

# Chapter 4: In Vitro Effects of Syndecan-1[2]

## 4.1 INTRODUCTION

Arterial mechanotransduction has been the subject of intense experimental and theoretical study over the past decades[23,28]. The search for potential mechanotransducers, molecules that serve as force sensors and activators of mechanical responses, has revealed a variety of intricate mechanisms through which hemodynamic forces can alter arterial biology[30-32,99,100]. A key finding in these studies is that certain arterial flow profiles induce an atheroprotective phenotype in endothelial cells leading to broad alterations in endothelial function relating to inflammation, vasodilation, and thrombosis whereas other profiles induce a more inflammatory, atheroprone phenotype[23]. Multiple signaling and transcriptional regulators, such as the Krüppel-like factor (KLF) family of transcription factors, have been found to strongly modulate this response[101-104]. Several key mechanosensitive elements have been identified in endothelial cells, including platelet endothelial cell adhesion molecule (PECAM-1), cadherins, and the actin cytoskeleton[105], but the full scope and complexity of the mechanosensing mechanisms remains unclear.

The endothelial glycocalyx is a structure of glycans and proteoglycans present on the luminal surface of arteries. Recent cryo-electron microscopy images have shown that it can extend up to 11 μm into the lumen, inevitably making it the endothelial structure first exposed to changes in fluid shear stress[106]. In addition, modeling studies have postulated that the entirety of fluid shear force is dissipated in the glycocalyx before

[2] Some work contained in this chapter was previous published in the following journal article: Voyvodic, P. L., *et al*. Loss of syndecan-1 induces a pro-inflammatory phenotype in endothelial cells with a dysregulated response to atheroprotective flow. *Journal of Biological Chemistry* **289** (14), 9547-9559, doi: 10.1074/jbc.M113.541573 (2014). The individual contributions by the authors are as follows: Peter L Voyvodic- Principle author and conductor of the research; Daniel Min- Undergraduate research assistant to PL Voyvodic; Robert Liu- Undergraduate research assistant to PL Voyvodic; Evan Williams- Undergraduate research assistant to PL Voyvodic; Vipul Chitalia- Helped design lentiviral mutants to used to produce pSyn1 line; Andrew K Dunn- No contribution in Chapter 4; Aaron B Baker- Supervisor to PL Voyvodic.

reaching the cell membrane[107]. Removal of heparan sulfate glycoaminoglycans from the cell surface using enzymatic digestion reduces endothelial production of vasodilatory factors in response to shear stress[48]. However, it is unknown which proteoglycans are important in these processes and their scope of mechanistic involvement in mechanosensing of shear stress.

The syndecan family of transmembrane cell surface proteoglycans are an appealing group of candidate molecules for mechanosensing owing to their location at the cell surface and interactions with integrins and cytoskeletal elements[108]. The syndecans are single-pass transmembrane proteins known to be capable of transmitting extracellular signals into intracellular signaling pathways[109]. These molecules are a component of the glycocalyx and are likely exposed to extracellular forces from flow and adherence to the extracellular matrix. In addition, the cytoplasmic domain of syndecans interact with cytoskeletal and focal adhesion complex proteins as well as multiple intracellular signaling pathways[110]. The syndecans act synergistically with integrins through their extracellular domain and serve as regulators of cell adhesion[111-113]. Thus, syndecans and other cell surface proteoglycans are uniquely positioned to interact with externally applied mechanical forces and transmit these signals to multiple pathways within the cell.

We hypothesized that syndecan-1 is a critical element in shear stress-mediated signaling and phenotypic regulation in endothelial cells. Using endothelial cells isolated from sdc-1 knockout mice, we demonstrate that sdc-1 is required for the activation of Akt and RhoA and for the formation of a phosphorylation gradient in paxillin in the initial stages of the endothelial response to shear stress. In addition, sdc-1 knockout profoundly alters the shear stress induced expression of transcription factors, vasodilatory mediators, and inflammatory soluble factors and receptors. Based on these findings, we propose that sdc-1 is an important atheroprotective molecule that governs both the inflammatory state of the endothelial cells and the induction of atheroprotective phenotypes by shear stress. Thus, this work expands our limited understanding of the role of cell surface

proteoglycans in vascular mechanobiology and may provide insight into the mechanisms of shear stress-mediated regulation of atherogenesis.

## 4.2. Materials and Methods

### 4.2.1. Cell Culture.

Endothelial cells were isolated from the lungs of wild-type (WT) and syndecan-1 knockout (S1KO) mice as previously described[114]. Briefly, the lungs were macerated and digested with collagenase followed by sorting with CD31 Dynabeads (Invitrogen). After cells were expanded, they underwent a second round of CD31 Dynabead sorting to ensure cell purity. Endothelial phenotype was confirmed using cellular uptake of fluorescently labeled Ac-LDL and through the expression of Tie-2 mRNA. Cells were later examined for size differences due to loss of sdc-1 (**Figure 4.1**). Area was calculated using Metamorph software (Molecular Devices) of over forty cells for both wild type and sdc-1 knockout cells. Volume was measured using a Z-series Coulter Counter (Beckman Coulter). We also measured gene expression to evaluate compensatory increases in other heparan sulfate proteoglycan core proteins and synthetic enzymes (**Figure 4.2**). The cells were cultured in MCDB-131 media with 5% fetal bovine serum (FBS) and antibiotics (Invitrogen). Experiments using human synstatin (GenScript) were performed at 3 μM synstatin on HUVECs grown in MCDB-131 media with growth supplements (Lonza) with a total of 7.5% FBS (Invitrogen).

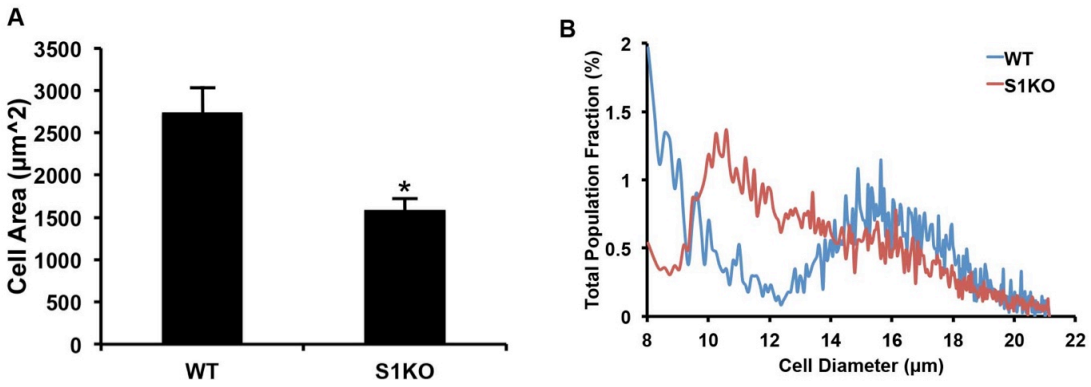


**Figure 4.1. Loss of sdc-1 results in reduced cell size and adhesion area.** (A) S1KO endothelial cells adhered to a smaller surface area than the WT cells ($n > 40$). *$p < 0.05$ for S1KO versus WT group. (B) The volume of S1KO cells is reduced compared to the WT model.

### 4.2.2. Cloning of lentiviral constructs for expressing wild type and mutant forms of syndecan-1 and expression in endothelial cells.

To allow robust expression in primary vascular cell lines we cloned the sdc-1 gene into an enhanced lentiviral expression system[115] (kind gift of Dr. Gustavo Mostoslavsky, Boston University) and validated the expression of sdc-1 in endothelial cells (pSyn1). This lentiviral system is highly efficient in infecting vascular cells and led to over 99% efficiency of cells as measured by constitutive expression of GFP through an internal ribosome entry site (IRES) promoter incorporated into the vector. The construct was confirmed by DNA sequencing and nuclease digestion. The lentiviral vector was then transfected with packaging vectors into a HEK-293T packaging line to allow viral production and transduced into cells as previously described[115].

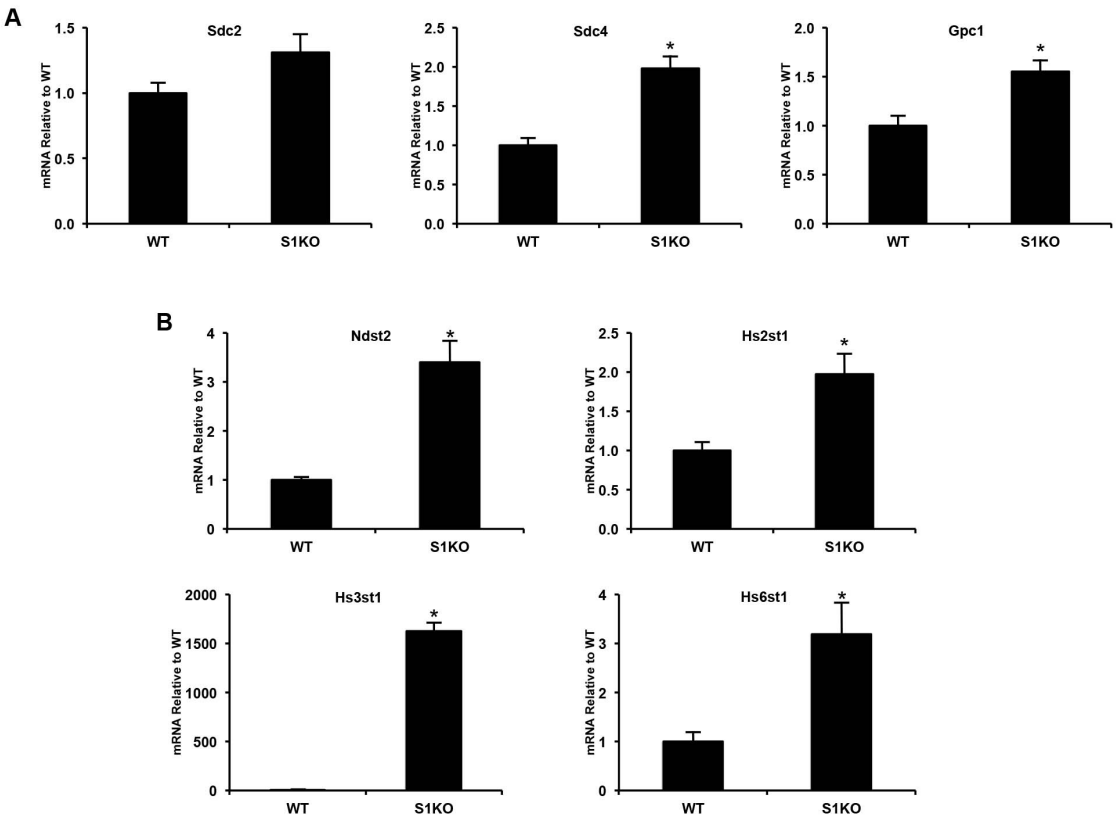


**Figure 4.2. Loss of sdc-1 alters the expression of other glycocalyx components and heparan sulfate sulfotransferases.** WT and S1KO endothelial cells were lysed under static conditions and examined for gene expression (n = 6). (A) S1KO endothelial cells express higher levels of other glycocalyx components, particularly sdc-4 and gpc-1. *$p < 0.05$ for S1KO versus WT group. (B) Expression of sulfotransferases was dramatically increased in the S1KO model. *$p < 0.05$ for S1KO versus WT group. Abbreviations used are as follows: Sdc2, syndecan-2; Sdc4, syndecan-4; Gpc1, glypican-1; Ndst2, N-deacetylase/N-sulfotransferase (heparan glucosaminyl) 2; Hs2st1, heparan sulfate 2-O-sulfotransferase 1; Hs3st1, heparan sulfate glucosamine 3-O-sulfotransferase 1; Hs6st1, heparan sulfate 6-O-sulfotransferase 1.

### 4.2.3. In-Vitro Flow Studies.

For Western lysis flow experiments, cells were seeded onto glass slides coated with fibronectin; for all other flow experiments, cells were seeded into multichannel flow chambers (μ-Slide $VI^{0.4}$; ibidi, LLC). Flow was applied using our multichannel flow device that provides steady flow in up to 24 flow channels simultaneously as previously described[116]. The entire system was kept in an incubator at 37 °C with a 5% $CO_2$ atmosphere throughout the experiment.

### 4.2.4. Immunocytochemical Staining.

Following treatments, the cells were washed with PBS and fixed in 4% paraformaldehyde for 20 minutes. The cells were quenched with 0.2M glycine and then permeabilized with 0.2% Triton X-100 and blocked with 5% FBS in PBS/1% bovine serum albumin (BSA) for 1 hour. Next, the cells were labeled with a 1:100 dilution of primary antibodies in PBS/1%BSA overnight at 4°C. They were then washed three times in PBS/1%BSA and labeled with a 1:1000 dilution of fluorescently labeled secondary antibody for 1 hour at room temperature. For experiments studying the actin cytoskeleton, the cells were also labeled with a 1:500 dilution of Alexa 594-labelled phalloidin (Invitrogen) for 1 hour at room temperature. Finally, the cells were washed five times in PBS/1%BSA, mounted in a DAPI-containing mounting medium (Vector Labs) and imaged using an epifluorescent microscope (Carl Zeiss). Morphometric and intensity analysis of the cells was performed using Metamorph software (Molecular Devices) and Photoshop software (Adobe). The following antibodies were used for immunostaining: phospho-Akt (Ser473) and Akt from Cell Signaling; phospho-paxillin (Tyr118) from Invitrogen; paxillin from BD Biosciences; and secondary antibodies from Santa Cruz Biotechnology. Activation of integrin $\alpha_v\beta_3$ was detected with the WOW-1 antibody using a 1:5 dilution (kind gift of Dr. Shattil Sanford, UCSD).

### 4.2.5. Cell Lysis and Immunoblotting.

Following treatments, the cells were lysed with 20mM Tris, 150mM NaCl buffer (pH 8.0) containing 1% Triton X-100, 0.1% SDS, 2mM sodium orthovanadate, 2mM PMSF, 50mM NaF, and 1 complete protease inhibitor pellet (Roche) per 50mL lysis buffer. For Western blotting, a 1:500 dilution of primary antibodies (phospho-Akt (Ser473) and Akt from Cell Signaling) was used for overnight incubation at 4°C and a 1:3500 dilution of secondary antibodies (Santa Cruz Biotech) was used at room temperature for 2 hours as previously described [97].

### 4.2.6. Focal Adhesion Quantification.

Fluorescent images were acquired for endothelial cells immunostained for paxillin and phosphorylated paxillin. The images were background subtracted and the phospho-paxillin image was divided by the total paxillin image using Photoshop (Adobe). The greyscale image was then indexed and assigned to a linear psuedocolor lookup table with a value of 0 assigned to black to differentiate the cell from the background. Linescans of the greyscale ratio image were generated using Metamorph software.

### 4.2.7. Colocalization Analysis.

Following flow, images were acquired from stainings for actin and a high-affinity form of integrin $\alpha_v\beta_3$ using the WOW-1 antibody. Pearson correlation coefficients were calculated for 10 cells in each condition using ImageJ open source software and plug-ins developed by the Bob and John Wright Cell Imaging Facility of the University of Ontario Canada (www.uhnresearch.ca/facilities/wcif/fdownload.html).

### 4.2.8. Measurement of RhoA activity using FRET.

The plasmid for the RhoA-FRET Biosensor construct was used as previously described (pBabe-Puro-RhoA Biosensor; Addgene)[117]. The plasmid was transfected into packaging HEK293T cells using Lipofectamine 2000 (Invitrogen) to produce retroviruses. Viruses were collected after 48 hours, centrifuged to remove cell debris, filtered with a 0.45 μm filter, and added at a 50% final concentration to WT or S1KO endothelial cells. Media was replaced after 24 hours and the cells were given 48 hours to recover before undergoing resistance selection with 1 μg/mL puromycin for 10 days followed by selection with 10 μg/mL puromycin for an additional 10 days. During selection and routine cell culture, the media contained 10 μg/mL doxycycline to suppress RhoA construct transcription through a TetCMV repressor. At 48 hours prior to the experiment, the cells were given media without doxycycline to allow for RhoA construct transcription. The cells were seeded in flow chambers (μ-Slide $VI^{0.4}$, ibidi) and grown to

confluence. Using a syringe pump (Kent Scientific), media was flowed over the cells until the given time points, at which point the channel was immediately read using a plate reader (Varioskan; Thermo-Scientific). To prevent alterations in RhoA activation due to starting and stopping flow, separate flow channels were used for each time point. The FRET ratio was calculated by dividing the FRET signal (Excitation: 436 ± 12nm; Emission: 535 ±12nm) by the donor signal (Excitation: 436 ± 12nm; Emission: 470 ± 12nm) and then normalizing to the acceptor signal (Excitation: 500 ± 12nm; Emission: 535 ± 12nm) to account for changes in copy number.

### 4.2.9. Measurement of Gene Expression by Real Time PCR.

Messenger RNA was harvested from the cells following flow using an RNAeasy kit (Qiagen) and the relative mRNA copy numbers were quantified using real time PCR as described previously[118,119]. Copy numbers were normalized to GAPDH gene expression.

### 4.2.10. Assay for Monocyte Adhesion.

Confluent monolayers of WT, S1KO and pSyn1 endothelial cells were grown in slide mounted flow chambers (ibidi) and then stimulated with the addition of 10 ng/mL TNF-α for 4 hours. The flow chambers were positioned on a inverted microscope and CellTracker dye (Invitrogen) labeled THP-1 cells ($5 \times 10^5$ cells/mL) were perfused through the chamber with a syringe pump (Kent Scientific) for 5 min at a controlled flow rate to generate a shear stress of 0.5 dynes/cm$^2$. The entire period of perfusion was recorded as a digital video and analyzed to determine the number of rolling THP-1 cells over monolayers in three 90-second intervals. After 5 min the flow was changed to MCDB-131 media to wash out unadhered cells and the plates were imaged in 8 separate locations. The number of cells adhered per field of view was by quantified using Metamorph software.

### 4.2.11. Statistical Analysis.

All results are shown as mean ± SEM. Comparisons between groups were analyzed using a 2-way ANOVA followed by a Tukey post-hoc test. Comparisons between only two groups were analyzed using a Student's t-test. A 2-tailed probability value $<0.05$ was considered statistically significant.

## 4.4. RESULTS

### 4.4.1. Loss of syndecan-1 in endothelial cells inhibits the activation of Akt in response to shear stress.

Shear stress rapidly activates the Akt pathway in endothelial cells leading to alterations in oxidative stress[120], suppression of apoptotic signaling pathways[121], and production of nitric oxide (NO)[122]. We applied shear stress to endothelial cells using a custom, *in vitro* system allowing the application of steady flow of culture media through 24 microchannels simultaneously[116]. Using this system, wild-type (WT) and sdc-1 knockout (S1KO) endothelial cells were exposed to 12 dynes/cm$^2$ of steady shear stress for 15 minutes. This level of steady shear stress induces an atheroprotective phenotype in endothelial cells that has been well-characterized[23]. After 5 to 15 minutes of exposure to flow, wild-type endothelial cells had a robust increase in Akt phosphorylation with an approximately two-fold increase in Akt phosphorylation following flow as measured by immunostaining (**Figure 4.3A**) and western blotting (**Figure 4.3B**). In contrast, there was minimal activation in sdc-1 knockout endothelial cells by flow.

### 4.4.2. Syndecan-1 knockout abrogates the formation of a phosphorylation gradient in paxillin following flow.

Endothelial cells are known to modulate their cytoskeletal arrangement and alignment in response to shear stress through the formation of a gradient in paxillin phosphorylation across the cell[123]. We grew endothelial cells in flow chambers and

exposed them to 12 dynes/cm$^2$ of shear stress for 15 minutes. We immunostained for paxillin and phospho-paxillin and performed a ratiometric analysis for paxillin phosphorylation from these images. There was a robust formation of a paxillin phosphorylation gradient in the WT cells with higher phosphorylation on the downstream edge of the cell after flow exposure (**Figure 4.4A and 4.4B**). In contrast, there was no discernable polarity to paxillin phosphorylation for sdc-1 knockout cells in all cases.

### 4.4.3. Loss of syndecan-1 results in reduced co-localization of activated $\alpha_v\beta_3$ integrins with the actin cytoskeleton under static and atheroprotective flow conditions.

Activation of focal adhesions is an important shear-mediated mechanotransduction pathway and involves accompanying activation of integrins and their association with the actin cytoskeleton[23]. Integrin $\alpha_v\beta_3$ is activated by shear stress in endothelial cells adhered to fibronectin or fibrinogen[124] and controls the release of endothelial elastase and FGF-2 in response to flow[125]. We exposed confluent endothelial cells to 12 dynes/cm$^2$ for 5 minutes and imaged activated integrin $\alpha_v\beta_3$ using the WOW-1 antibody that recognizes the high affinity form of $\alpha_v\beta_3$[126]. Wild type endothelial cells had

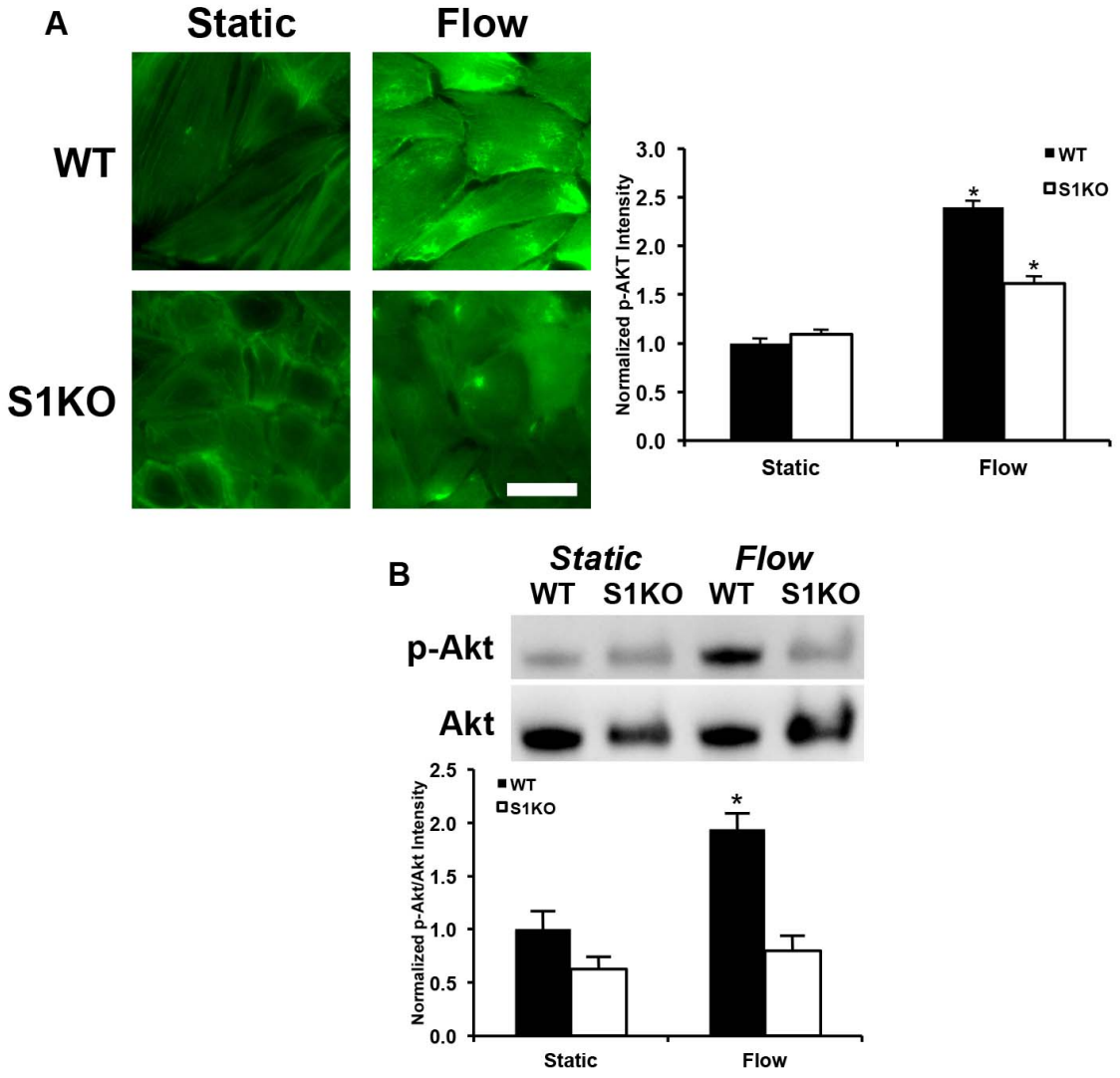


**Figure 4.3. Loss of sdc-1 alters shear stress-induced activation of Akt pathway signaling.** (A) WT and S1KO endothelial cells were exposed to flow at 12 dynes/cm$^2$ for 5 minutes. Immunohistochemical staining demonstrated an increase in Akt phosphorylation (Ser473) in WT cells after flow. In contrast this increase was not observed in the S1KO cells. Scale bar = 50mm. Chart displays semi-quantitative analysis of pAkt staining intensity (n = 40). *Statistically significant difference versus all other groups ($p < 0.05$). (B) Western blotting analysis of lysed cells following 15 minutes of flow at 12 dynes/cm$^2$ revealed a reduced relative phosphorylation of Akt in S1KO cells (n = 8). *Statistically significant difference versus all ($p < 0.05$).

co-localization between the activated $\alpha_v\beta_3$ integrins and the actin stress fibers, particularly at the periphery of the cell both under static and flow conditions (**Figure**

**4.4C and 4.4D**). This co-localization was markedly reduced in sdc-1 knockout cells under both of these conditions.

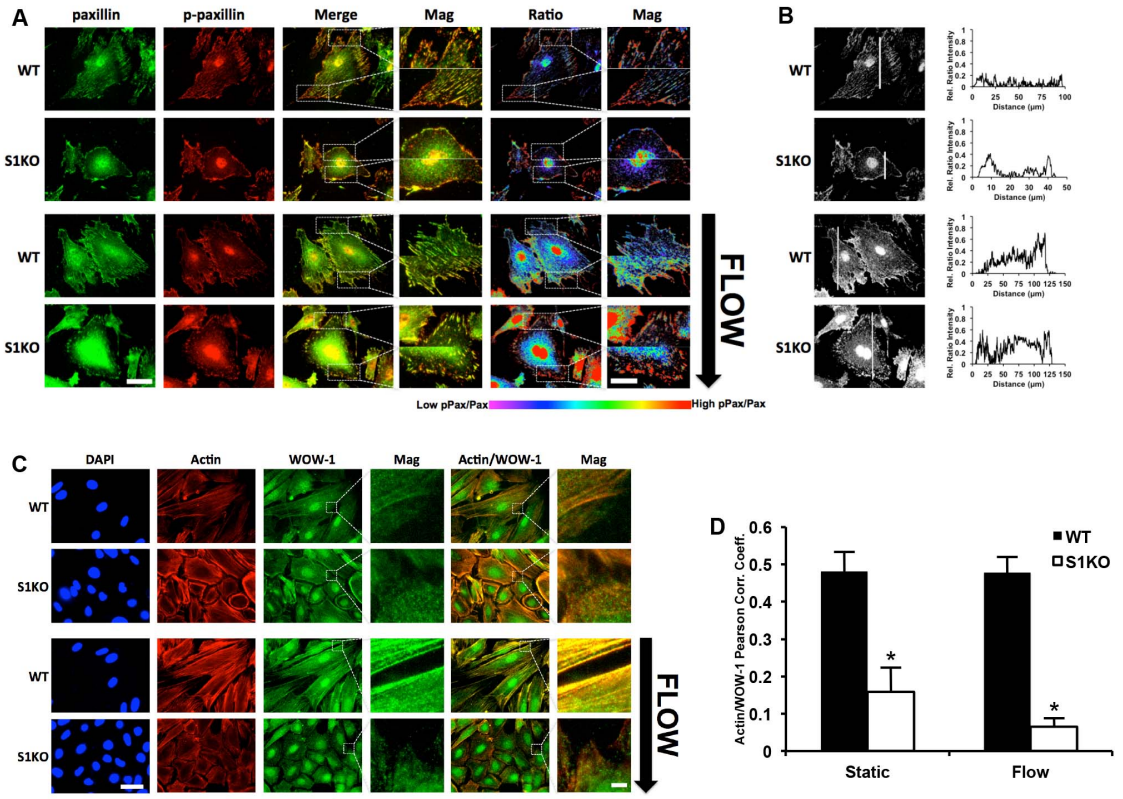


**Figure 4.4. Loss of sdc-1 alters shear stress-induced formation of intracellular spatial gradients in paxillin phosphorylation and reduces active integrin $\alpha_v\beta_3$ association with actin.** (A) WT and S1KO endothelial cells were exposed to flow at 12 dynes/cm$^2$ for 15 minutes. Immunostaining for phospho-paxillin and total paxillin under static and flow conditions shows that WT cells developed a gradient in paxillin phosphorylation across the cell whereas S1KO cells did not. Scale bar = 50μm (Mag = 25 μm). (B) Line scans of p-paxillin/total paxillin ratio under static and flow illustrate the gradient in paxillin phosphorylation. (C) Actin stress fiber formation and elongation of the cells resulted from 5 minutes of flow exposure in WT cells. In these cells, activated $\alpha_v\beta_3$ (WOW-1 staining) was co-localized with actin stress fibers, particularly at the periphery of the cell. Knockout of sdc-1 reduced this association under both static and flow conditions. Scale bar = 50 μm (Mag = 5 μm). (D) Co-localization analysis for WOW-1 and actin staining following exposure to flow (n = 10). *Statistically significant difference versus WT static and flow conditions ($p < 0.05$).

### 4.4.4. Syndecan-1 knockout inhibits RhoA activation by shear stress.

Activation of RhoA GTPases is a key step regulating endothelial cytoskeletal remodeling in response to shear stress[127-129]. To measure RhoA activity, we transduced WT and sdc-1 knockout cells with a retrovirus expressing a RhoA Biosensor[117]. The biosensor consists of a single peptide chain containing a Rho-binding domain (RBD), cyan fluorescent protein (CFP), a randomized linker, yellow fluorescent protein (YFP), and RhoA. When RhoA binds GTP and is activated, it binds to the RBD and increases the FRET efficiency between CFP and YFP. We exposed endothelial cells to flow and rapidly measured the RhoA activity using a fluorescence plate reader. A time course of RhoA activity in WT endothelial cells revealed an initial drop in activity followed by an increase to maximum activation after 15 minutes of flow (**Figure 4.5**). In sdc-1 knockout endothelial cells exposed to identical flow conditions, there was an initial drop in RhoA activity followed by a return to baseline levels of activity.

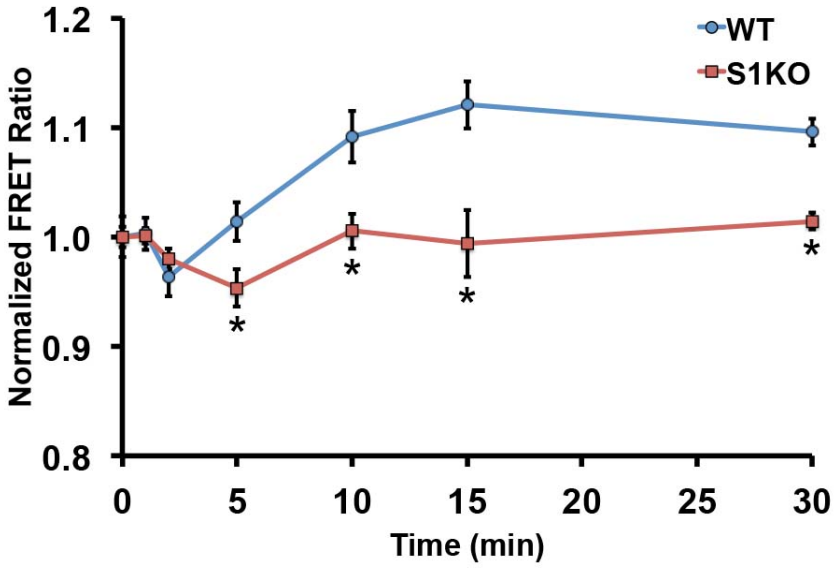


**Figure 4.5. Loss of sdc-1 alters shear stress-induced activation of RhoA.** Endothelial cells were transduced with a RhoA FRET biosensor construct and exposed to flow at 12 dynes/cm2. The WT cells exhibited a rapid drop in RhoA activity followed by an increase in activity. In contrast, S1KO cells had a rapid drop in activity without a following increase in activity (n = 6). *Statistically significant difference versus WT group at the same time point ($p < 0.05$).

### 4.4.5. Long-term exposure to flow produces a pro-atherosclerotic phenotype in syndecan-1 knockout cells.

The powerful atheroprotective effects of moderate levels of shear stress result from a broad regulation of genetic programs in endothelial cells that induces an athero-resistant phenotype. Members of the Krüppel-like factor (KLF) family of transcription factors are key regulators of shear stress-induced changes in endothelial phenotype and are involved in modulation of vasomotor tone, inflammation, and thrombosis[101-104]. KLF-2 and KLF-4 have been found to upregulate genes that are atheroprotective[101-103]. In contrast, KLF-5 activates pro-inflammatory gene expression in endothelial cells and injured arteries[104,130]. We applied 12 dynes/cm$^2$ of shear stress to endothelial cells for 24 hours and measured the gene expression of the KLF transcription factors, vasoregulatory factors, angiogenic factors, and inflammatory mediators. S1KO endothelial cells expressed reduced amounts of KLF-2 and KLF-4 in comparison to WT cells under static and flow conditions (**Figure 4.6A**). In addition, treatment with flow reduced expression of KLF-5 in WT cells but not in S1KO cells (**Figure 4.6A**). There was decreased expression of vasodilatory factors under atheroprotective flow in S1KO endothelial cells including the genes for endothelial nitric oxide synthase (eNOS), c-natrietic peptide (CNP), and argininosuccinate synthase (ASS) (**Figure 4.6B**). Angiogenesis related gene expression was increased in S1KO endothelial cells for Tie-2 under static conditions and angiopoietin-2 (Ang2) under both flow and static conditions (**Figure 4.6C**). In addition, gene expression for elastin was increased by over 100-fold in S1KO cells under static and flow conditions.

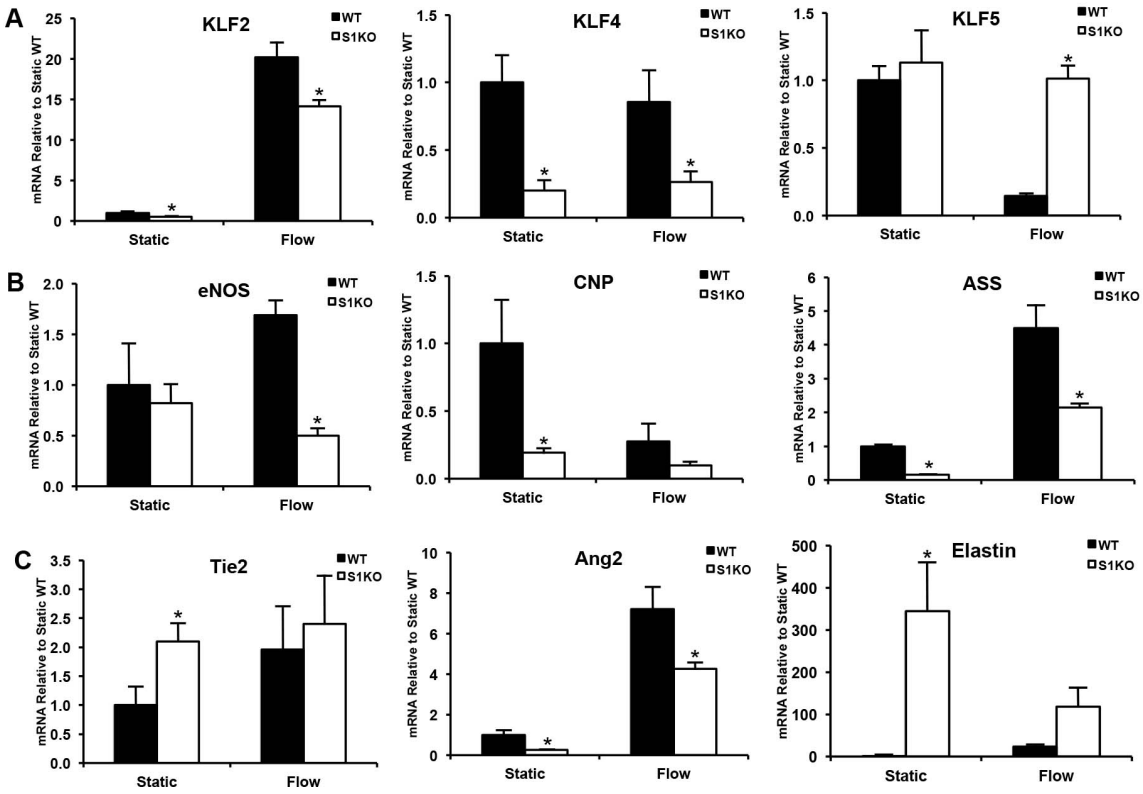


**Figure 4.6. Syndecan-1 alters gene expression for transcription factors, vasodilatory mediators, and angiogenesis factors induced by shear stress.** WT and S1KO endothelial cells were exposed to static conditions or flow at 12 dynes/cm$^2$ for 24 hours. (A) Gene expression for the flow-inducible transcription factors KLF-2 and KLF-4 was decreased for sdc-1 knockout endothelial cells while KLF-5 expression was increased. (B) Expression of vasodilatory factors was reduced in sdc-1 knockout cells under atheroprotective flow conditions. (C) Expression of angiogenesis mediators was increased in sdc-1 knockout cells. *$p < 0.05$ for S1KO versus WT group under same static/flow conditions. Abbreviations used are as follows: KLF, Krüppel-Like Factor; eNOS, endothelial nitric oxide synthase; CNP, c-natriuretic peptide; ASS, argininosuccinate synthetase; Tie2, angiopoietin-1 receptor; Ang2, angiopoietin-2.

### 4.4.6. Syndecan-1 knockout alters inflammatory cytokine expression.

We exposed WT and S1KO endothelial cells to 24 hours of laminar flow at 12 dynes/cm$^2$ and measured the expression of inflammatory cytokines using real time PCR and ELISA. For a subset of these factors including CXCL2, IL-1α, IL-6 and COX-2 we observed lower levels of cytokine expression under static condition but equal amounts of expression between WT and S1KO cells after exposure to flow (**Figure 4.7A**). We found

increased expression of CCL-5, IL-15, IP-10 and SDF-1 for S1KO cells under either static or flow conditions or both (**Figure 4.7B**). Following exposure to atheroprotective flow, we found increased gene expression for CXCL1, MCP-1 and MIP1-γ (**Figure 4.8A**). We performed an ELISA for these cytokines on the conditioned media after flow and found they were increased in S1KO cell condition media (**Figure 4.8B**).

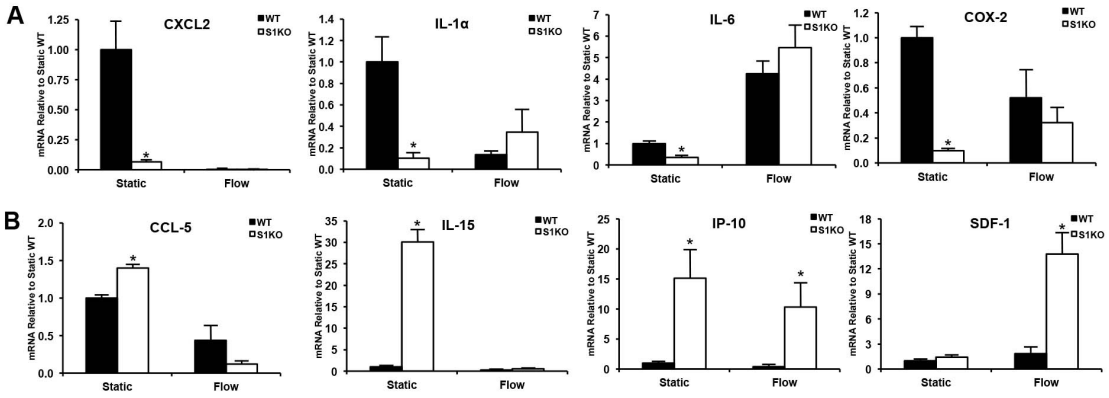


**Figure 4.7. Syndecan-1 knockout alters baseline and flow-induced cytokine expression.** WT and S1KO endothelial cells were exposed to steady flow at 12 dynes/cm$^2$ for 24 hours. Subsequently, mRNA was isolated and analyzed by real time PCR. (A) Under static conditions S1KO cells had low expression of some inflammatory cytokines including CXCL2, IL-1α, IL-6, and COX-2. These differences were abolished with exposure to flow. (B) Other inflammatory factors were increased under static and/or flow conditions for S1KO cells. *$p < 0.05$ for S1KO versus WT group under same static/flow conditions. Abbreviations used are as follows: CXCL, chemokine (C-X-C motif) ligand; IL, interleukin; COX-2, cyclooxygenase-2; CCL-5, chemokine (C-C motif) ligand 5; IP-10, interferon gamma-induced protein-10; SDF-1, stromal cell-derived factor-1.

### 4.4.7. Syndecan-1 knockout increases expression of cell adhesion receptors involved in leukocyte adhesion and increases adhesion of cultured monocytes under flow.

Having observed increased expression of inflammatory factors in sdc-1 knockout cells, we next examined whether there was regulation of cell adhesion receptors for leukocyte recruitment and a functional difference in the adhesion of monocytes to activated endothelial cells. Under static and atheroprotective flow conditions we found a

200-300 fold increase in ICAM-1 expression in S1KO cells in comparison to WT cells (**Figure 4.9A**). Under atheroprotective flow, S1KO cells had over four-fold more VCAM-1 gene expression. In addition, we created a lentiviral vector containing the sdc-1 gene and transduced the S1KO line with this construct (pSyn1). While ICAM-1 levels remained elevated, VCAM-1 and E-selectin expression levels were reduced in the pSyn1 model.

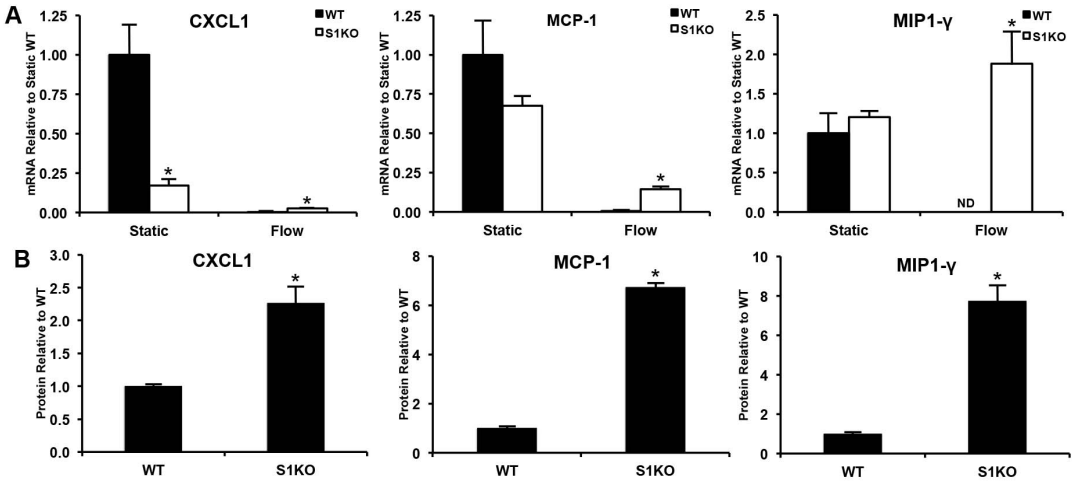


**Figure 4.8. Syndecan-1 knockout increases gene expression and protein levels of leukocyte recruiting inflammatory soluble factors.** WT and S1KO endothelial cells were exposed to steady flow at 12 dynes/cm$^2$ for 24 hours. Subsequently, mRNA was isolated and analyzed by real time PCR. (A) Gene expression for leukocyte recruiting inflammatory mediators was increased in sdc-1 knockout cells under flow. *$p < 0.05$ for S1KO versus WT group under same static/flow conditions. (B) Levels of the inflammatory factors were assessed in the culture media following 24 hours of flow using ELISA. *Statistically significant difference ($p < 0.05$) for S1KO versus WT cells. Abbreviations used are as follows: CXCL1, chemokine (C-X-C motif) ligand-1; MCP-1, monocyte chemotactic protein-1; MIP1-γ, macrophage inflammatory protein 1 gamma.

We next examined the functional consequences of sdc-1 knockout on monocyte adhesion in-vitro. We fluorescently-labeled cultured monocytes and measured their adhesion to a TNF-α stimulated endothelial monolayer under flow conditions (0.5 dynes/cm$^2$ for 5 min). About 50-fold more monocytes adhered to S1KO endothelial

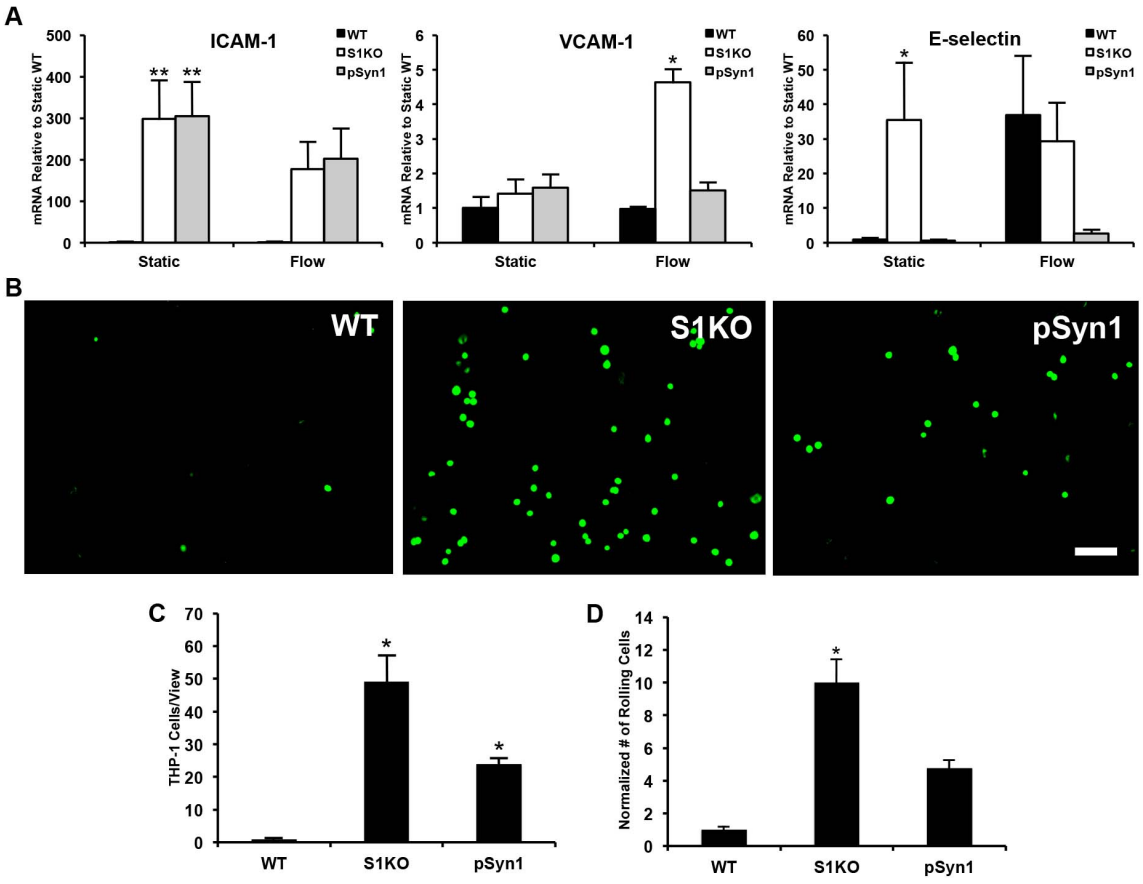


**Figure 4.9. Monocyte adhesion and macrophage recruitment are increased in sdc-1 knockout endothelial cells.** (A) WT and S1KO endothelial cells were exposed to 24 hours of flow at 12 dynes/cm$^2$. Gene expression for cell adhesion receptors was higher in the S1KO cells compared to WT cells following flow exposure. *$p < 0.05$ in comparison to all other groups in static or flow; **$p < 0.05$ in comparison to WT in static or flow. (B) Suspension cultured monocytes were fluorescently labeled and flowed over confluent endothelial monolayers of WT, S1KO, or S1KO cells transduced to overexpress sdc-1 (pSyn1) under flow creating 0.5 dynes/cm$^2$ of shear stress for 5 minutes. Prior to the flow adhesion assay the endothelial cells were stimulated with TNF-α for 4 hours. Size bar = 200 μm. (C) Leukocyte adhesion was increased in sdc-1 knockout cells and re-expression of sdc-1 in these cells decreased the number adhering leukocytes ($n = 8$). *$p < 0.05$ in comparison to all other groups. (D) The number of rolling monocytes over three 90-second intervals shows increased leukocyte rolling on sdc-1 knockout cells over both WT and pSyn1 cell line. *Statistically different from all other groups ($p < 0.05$).

monolayers than to WT monolayers under identical flow conditions (**Figure 4.9B and 4.9C**). More cells were also observed to roll on S1KO monolayers during the flow adhesion assay (**Figure 4.9D**). Overexpression of sdc-1 in the knockout cells using

lentiviral transduction reduced the number of adhered monocytes by about half in comparison to S1KO cells (**Figure 4.9C and 4.9D**).

### 4.4.8 Inhibiting syndecan-1 activation of integrins does not affect endothelial mechanotransduction response.

Finally, we took a mechanistic analysis of how syndecan-1 influences endothelial mechanotransduction. Using a synthetic peptide, synstatin, that blocks syndecan-1's ability to activate $\alpha_v\beta_3$ and $\alpha_v\beta_5$ integrins, we exposed HUVECs to 24 hours of shear stress and looked at gene expression levels of different inflammatory mediators and vasodilatory compounds (**Figure 4.10**). We found that blocking syndecan-1's ability to activate integrins was not responsible for the changes in shear stress behavior that we saw in our syndecan-1 knockout in vitro experiments.

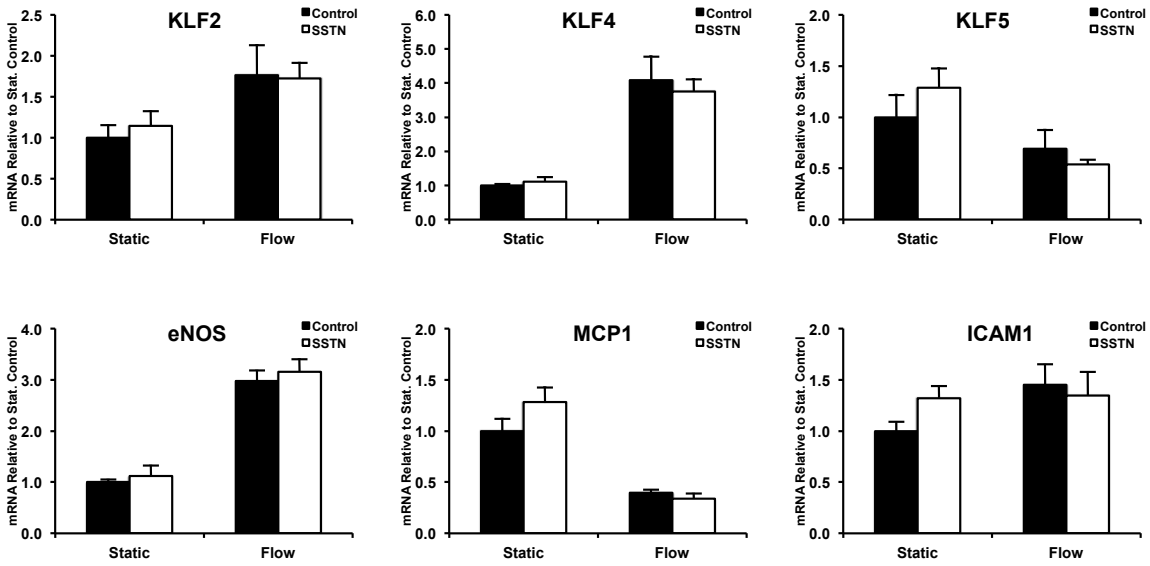


**Figure 4.10. Inhibition of syndecan-1 integrin activation does not alter endothelial mechanotransduction response.** HUVECs were exposed to 24 hours of flow at 12 dynes/cm$^2$ with 3 μM synstatin or control media. Gene expression in static or flow conditions did not significantly differ with synstatin treatment.

## 4.5. DISCUSSION

While the role of cell surface proteoglycans in shear stress sensing has been suspected for many years[28] there have been no studies, to our knowledge, that have examined their function in a mechanistic and detailed fashion. The primary experimental approach in studies to date has been to digest particular glycosaminoglycans of the glycocalyx using enzymes and to apply shear stress to interrogate whether the shear sensing of endothelial cells has changed from this treatment. Using this method, several studies have shown that shear stress-induced production of nitric oxide (NO) is reduced following enzymatic digestion of heparan sulfate or hyaluronic acid or treatment with neuraminidase[48,49]. In contrast, shear-induced increases in prostacyclin-2 (PGI2) were not affected by removal of heparan sulfate, sialic acid, chondroitin sulfate, or hyaluronan[131]. *In vivo* studies have also supported the involvement of proteoglycans in controlling shear stress-induced arterial vasodilation. Increases in blood flow cause arteries to dilate in an endothelium-dependent manner[50,51]. Several studies have supported the role of elements of the glycocalyx in the control of the shear-induced vasodilatory response of arteries. Another study examined the vasoconstriction of rabbit femoral arteries in *ex vivo* organ culture and found that incubation with neuraminidase, an enzyme that digests sialic acid moieties, reduced shear stress-induced NO release[52]. In addition, treatment with clinical levels of heparin led to a reduction in the duration of vasodilation in response to occlusion-induced reactive hyperemia in mice[132]. Our study adds to these results by defining several of the activities of sdc-1 in the initial steps of mechanosensing and in the regulation of endothelial phenotype.

We first examined the role of sdc-1 in the acute mechanosensing of shear stresses by endothelial cells. Interestingly, without sdc-1 endothelial cells were not able to activate Akt and RhoA nor develop a paxillin phosphorylation gradient in response to flow. These signaling events have been shown in previous studies to be key to flow-induced changes in endothelial alignment[123] and cytoskeletal remodeling[127-129] as well as

the regulation of oxidative stress[120], cell survival[121], and production of NO[122]. Our study also examined the longer-term effects of shear stress on endothelial cells in the absence of sdc-1 expression. Under atheroprotective flow, S1KO cells had decreased expression of atheroprotective transcription factors KLF-2 and KLF-4. These transcription factors regulate a set of genetic programs that profoundly alter the endothelial cell phenotype affecting pathways involved in inflammation, vasodilation, and thrombosis[101-103]. In contrast we found that KLF-5 expression was higher in S1KO endothelial cells after exposure to flow. This transcription factor has been linked to increased inflammation in endothelial cells[104,130]. Thus, the loss of sdc-1 alters the relative expression of KLF transcription factors and their regulation by atheroprotective flow. Consistent with these findings, S1KO cells had increased expression of pro-inflammatory genes, cytokines, and leukocyte adhesion receptors in comparison to WT cells. The functional result of these alterations in endothelial genetic programs was an increased leukocyte adhesion.

Taken together, our results suggest an atheroprotective role for sdc-1 with its expression supporting flow-mediated mechanosensing and the generation of the atheroprotective phenotype. Loss of sdc-1 also induced significant differences in baseline levels of many markers of endothelial phenotype. In the absence of flow, we found decreased levels of gene expression for KLF-4, CNP, ASS-1, Ang-2, and several of the inflammatory cytokines including CXCL1 and CXCL2. In contrast, under static conditions there was significantly increased gene expression for elastin, CCL-5, IL-15, IP-10 and ICAM-1. Thus, the effect of sdc-1 loss on flow-mediated signaling and phenotypic regulation should not be viewed as a simple effect of altered endothelial mechanotransduction but in the context of significant dysregulation of endothelial cell phenotype under baseline conditions. Interestingly, our experiments using synstatin suggest that this response is not due to integrin activation by syndecan-1. It should also be noted that the loss of sdc-1 leads to an increase in gene expression of the other glycocalyx components, specifically sdc-4 and gpc-1, as well as numerous

sulfotransferases involved in heparan sulfate synthesis. We believe this to be a compensatory mechanism; however, the mechanotransduction effects we observed despite this response further highlight the importance of sdc-1 in signal transduction.

Several recent studies have found results that are consistent and complementary to our findings here. Notably, a recent study identified that, among several proteoglycan core proteins, sdc-1 expression was specifically reduced in endothelial cells on exposure to atheroprone regimes of flow and increased under atheroprotective flow conditions[133]. Viewed from the context of our results these findings would suggest that regulation of sdc-1 by flow could contribute to atherosclerosis and the development of endothelial dysfunction. In addition, another study found that the glycocalyx in sdc-1 knockout mice was thinner than in WT mice using intravital microscopy[60]. They also observed an increased number of leukocytes adhered in the venules of the mice, consistent with our findings of increased leukocyte adhesion *in vitro*. In the context of these results, our studies support that loss of sdc-1 stimulated by exposure to atherogenic flow profiles would lead endothelial cells to adopt an atheroprone phenotype that is both pro-inflammatory and resistant to the anti-inflammatory stimulus of moderate shear stress.

Our findings also have several important implications for the understanding of vascular biology in the context of atherogenesis and inflammation. Sdc-1 and the other syndecan family members are highly sensitive to proteolytic degradation and shedding[134]. Thus, our findings imply that disease-induced increases in proteolytic activity leading to shedding of sdc-1 from the surface may alter endothelial inflammatory phenotype and shear sensitivity to atheroprotective flow. We have recently found that Ob/Ob mice given a high fat diet have lower levels of sdc-1 protein in their heart and skeletal muscle[135]. In addition, sdc-1 is a target for heparanase activity and leads to shedding from the cell surface[136]. Our group has recently identified a key role for the enzyme heparanase in restenosis and thrombosis in vascular injury[137,138]. We also found increased heparanase expression in severe atherosclerotic plaques and in arterial segments of the coronary

vessels with low shear stress in a diabetic, hyperlipidemic porcine model of atherosclerosis[118]. This finding has recently been corroborated in atherosclerotic plaques from human patients[139]. Another study has also identified heparanase to be key in controlling the inflammatory response in sepsis through degradation of the glycocalyx[140]. Thus, our findings suggest that heparanase/protease-induced shedding of sdc-1 could lead to modulation of endothelial phenotype and inflammatory properties potentially similar to our sdc-1 knockout cells in this study.

It should be noted that one potential limitation of our studies is the use of cultured cells to study the function of glycocalyx components. Cultured cells are known to have limited formation of glycocalyx in comparison to the extended structure found in *in vivo* vessels[141,142]. Thus, while our findings support a functional role for sdc-1 they do not rigorously substantiate it in the presence of the full glycocalyx structure that is present in *in vivo* conditions. Additionally, while the lentiviral overexpression of sdc-1 is highly effective in expressing the protein in knockout cells it also has some limitations. Namely, having high levels of sdc-1 may disrupt the normal function of the protein and overwhelm the heparan sulfate synthetic enzymes that perform the post-translational modification of the protein. In addition, sdc-1 is a ligand for the viral entry of the HIV lentivirus. Thus, there may be effects on this system from the cell response to lentiviral transduction. These mechanisms may, in part, explain why there is a partial, but not complete, reduction of leukocyte adhesion by sdc-1 overexpression.

### 4.6. CONCLUSIONS

In summary, our study demonstrates that sdc-1 is a key element in endothelial mechanosensing and suggests an atheroprotective role for sdc-1 in flow-mediated endothelial phenotypic regulation. Our work supports that loss of sdc-1 from the endothelial surface leads to the adoption of a pro-inflammatory phenotype that is

dysregulated in response to the atheroprotective effects of flow. Many disease states increase the expression of enzymes that could induce the shedding and degradation of sdc-1 causing its loss from the endothelial surface[135,143,144]. Thus, therapies that preserve or enhance sdc-1 on the endothelial surface, either through increased expression or inhibition of shedding, may have potential in preventing the early stages of atherogenesis and enhancing the atheroprotective effects of shear stress.

# Chapter 5: Role of Syndecan-1 In Vivo[3]

## 5.1 INTRODUCTION

To effectively investigate the effects of shear stress in a truly physiological framework, *in vivo* studies are required. While *in vitro* studies allow us to isolate particular elements of a complex system to test their effects, the complex nonlinear dynamics between endothelial cells and smooth muscle cells, blood components, and extracellular matrices must be tested in animal models to see if the *in vitro* findings might be able to translate to actual therapeutics. Since we used our wild-type and syndecan-1 knockout mice to isolate the cells for *in vitro* testing, we are able to use the same genetic systems to test in whole animals. By testing the effects of shear stress on our animal models we can examine some of these complex dynamics.

In our *in vivo* studies, we focused on three main areas of investigation. Firstly, we wanted to look at how regions of the vasculature that natively experience different levels of shear stress differ in their endothelial phenotype. The greater and lesser arches of the aorta have been shown to exhibit laminar and disturbed flow, respectively, and being next to each other in the same vessel are a very good target for examining differences that are most likely caused only by the shear stress itself. This works well for examining differences that chronically exist, but to examine short-term changes and differences that may arise from vessel occlusion we also conducted studies to look at differences in induced shear stress changes. Specifically, using a partial carotid ligation model we created disturbed flow along the left carotid artery and examined how that affected

[3] Some work contained in this chapter was previous published in the following journal article: Voyvodic, P. L., *et al*. Loss of syndecan-1 induces a pro-inflammatory phenotype in endothelial cells with a dysregulated response to atheroprotective flow. *Journal of Biological Chemistry* **289** (14), 9547-9559, doi: 10.1074/jbc.M113.541573 (2014). The individual contributions by the authors are as follows: Peter L Voyvodic- Principle author and conductor of the research; Daniel Min- Undergraduate research assistant to PL Voyvodic; Robert Liu- Undergraduate research assistant to PL Voyvodic; Evan Williams- Undergraduate research assistant to PL Voyvodic; Vipul Chitalia- No contribution to Chapter 5; Andrew K Dunn- Helped design laser speckle contrast imaging setup; Aaron B Baker- Supervisor to PL Voyvodic.

neointimal formation. Finally, we wanted to look at some broad changes in how syndecan-1 affects vessel structure and global inflammatory response. By looking at the aortic medial thickness and general response to transdermal inflammatory stimuli we showed that syndecan-1 knockout mice appear to have an elevated level of inflammation.

## 5.2. MATERIALS AND METHODS

### 5.2.1. Animal Experimentation

All animal procedures were conducted in accordance with protocols approved by the University of Texas at Austin's Institutional Animal Care and Use Committee. Syndecan-1 knockout ($Sdc1^{-/-}$) mice were used as previous described[145] and were a kind gift from Dr. Ram Sasisekharan (Massachusetts Institute of Technology).

### 5.2.2. Gene Expression in Aorta Regions with Different Native Shear Stress.

Wild-type and sdc-1 knockout mice were euthanized by $CO_2$ inhalation and sections of the greater and lesser aortic arch and the descending aorta were excised, rinsed in saline, and frozen in liquid nitrogen. The tissue segments were lysed by bead beating (Qialyser; Qiagen) and messenger RNA was isolated using an RNAeasy kit (Qiagen). The relative mRNA copy numbers were quantified using real time PCR as described previously[118,119]. Copy numbers were normalized to GAPDH gene expression.

### 5.2.3. Histological Analysis of Mouse Aortas.

Mice were euthanized via $CO_2$ inhalation and the chest cavity opened. The aorta was isolated from the surrounding connective tissue and a small incision was made in the descending aorta near the diaphragm. A small, approximately 8mm x 15mm piece of silicone membrane was placed under the aorta to separate it from the surrounding tissue. Using a 21G needle to puncture the left ventricle, the aorta was flushed with saline and then filled with optimal cutting temperature (OCT) compound. Liquid nitrogen-cooled isopentane was then poured onto the aorta to freeze it *in situ*, at which point it was

excised and frozen in liquid nitrogen. Later, the tissue was fixed for 48 hours in 10% formalin at 4°C with shaking and then stored in 70% ethanol at 4°C. Samples were paraffin embedded and sectioned along the coronal plane by the Histology and Immunohistochemistry Laboratory at The University of Texas Health Science Center at San Antonio and hematoxylin and eosin (H&E) staining was performed. Immunohistochemical staining with a Dako kit (Agilent) was performed with 1:250 primary antibody dilution against VCAM-1 (Cell Signaling) according to the manufacturer's directions.

Additionally, for the transverse sections of wild-type and sdc-1 knockout mice, aortae were flash frozen in liquid nitrogen-cooled isopentane and cryosectioned transversely along the descending aorta. Sections were then stained for a modified Verhoeff's Van Giesen stain as previously described[146].

### 5.2.4. Partial Carotid Ligation Surgery.

In order to examine the effects of induced changes in shear stress *in vivo*, we elected to use the partial carotid ligation surgery as previous developed by Nam *et al*[45]. Briefly, the mice were anesthetized with 3% isoflurane and an ~1cm vertical incision was made on the underside of the neck above the left carotid artery (LCA). Once the LCA is exposed, two ligations are made on the downstream branches with 5-0 silk sutures: one occludes the external carotid artery (ECA) and occipital artery (OA) and the other occludes the internal carotid artery (ICA). This forces all downstream blood flow through the superior thyroid artery (STA) and creates a large region of disturbed flow upstream in the LCA. After the ligations are tightened, the incision is sutured closed and the mouse is given an injection of 2 mg/kg of carprofen and monitored. We confirmed the effects of the partial carotid ligation surgery by monitoring blood flow velocity in the ligated and control carotid arteries using pulsed wave Doppler with a Vevo 2100, high frequency rodent ultrasound system (VisualSonics).

### 5.2.5. Histological Analysis of Mouse Carotid Arteries.

Thirty days after partial carotid ligation surgery, mice were euthanized via $CO_2$ inhalation and the control and ligated carotid arteries were frozen in liquid nitrogen-cooled isopentane. Later, the tissue was fixed with for 48 hours in 10% formalin at 4°C with shaking and then stored in 70% ethanol at 4°C. Samples were cut in half and sent to the Histology and Immunohistochemistry Laboratory at The University of Texas Health Science Center at San Antonio where they were paraffin embedded and sectioned transversely at either 2 mm or 7 mm downstream of the aorta. Hematoxylin and eosin (H&E) staining was performed according to standard protocols.

### 5.2.6. Measurement of Global Inflammatory Response using Laser Speckle Contrast Imaging.

To examine the inflammatory response of WT and S1KO mice, we anesthetized the mice and applied 5% allyl isothiocyanate, a potent inflammatory/permeability stimulus, to the hind feet of the mice. We subsequently imaged the feet of the mice over time using a laser speckle imager. Laser speckle imaging allows the real time measurement of tissue perfusion with tens of microns spatial and millisecond temporal resolution[147]. Briefly, a diode laser (785nm, 50mW; Thor Labs) was shown upon the footpad of a mouse hindlimb. A Basler 1920 x 1080 monochrome CCD with a zoom lens (Zoom7000; Navitar) mounted on a microscope boom stand was placed vertically over the foot and used to record speckle images of blood perfusion. The raw speckle images were converted into speckle contrast images using the following relation:

$$K = \frac{\sigma_S}{\langle I \rangle}$$

where $s_s$ is the standard deviation and $\langle I \rangle$ is the mean intensity over a 7 x 7 pixel region of the image. The speckle contrast images were quantified by assigning values of 0, 1, and 2 to the red, green, and blue channels and multiplying by the area to integrate the total signal. Each time point was then normalized to the pre-oil measurement.

### 5.2.7. Histological Analysis of Mouse Foot Pads.

The feet of mice from the mustard oil laser speckle experiment were fixed in 4% paraformaldehyde and stored at 4°C. The foot pads were then removed and stored in PBS/20% sucrose for 48 hours at 4°C with shaking before freezing in liquid nitrogen cooled isopentane. The frozen foot pads were cryosectioned and stained as described previously[119].

### 5.2.8. Statistical Analysis.

All results are shown as mean ± SEM. Comparisons were analyzed using a Student's t-test. A 2-tailed probability value $<0.05$ was considered statistically significant.

## 5.3 RESULTS

### 5.3.1. Lack of syndecan-1 causes elevated levels of E-selectin and VCAM-1 in atheroprone aorta regions.

In order to examine the effects of different levels of native shear stress on endothelial phenotype, we looked at the greater and lesser aortic arches. Previous experimental and computational data have shown that the greater arch experiences high levels of atheroprotective shear while the lesser arch experiences a disturbed, atheroprone shear profile[148]. To look at the gene expression differences present in these two environments, we lysed and performed real-time PCR on isolated sections of the greater and lesser arch from WT and S1KO mice. An excised ring from the descending aorta was used as a control (**Figure 5.1**). Although not statistically significant, the sdc-1 knockout mice exhibited higher levels of E-selectin and VCAM-1 expression in the lesser arch compared to the wild-type.

### 5.3.2. Syndecan-1 knockout mice have higher VCAM-1 expression in regions with atheroprotective flow.

We also looked at the differences in protein expression in the aortic regions of differing shear stress. Paraffin-embedded WT and S1KO aortae were coronally sectioned and stained for VCAM-1 using a Dako immunohistochemical staining kit (**Figure 5.2**). The reduction of VCAM-1 in the greater arch found in the WT was absent in the S1KO aorta.

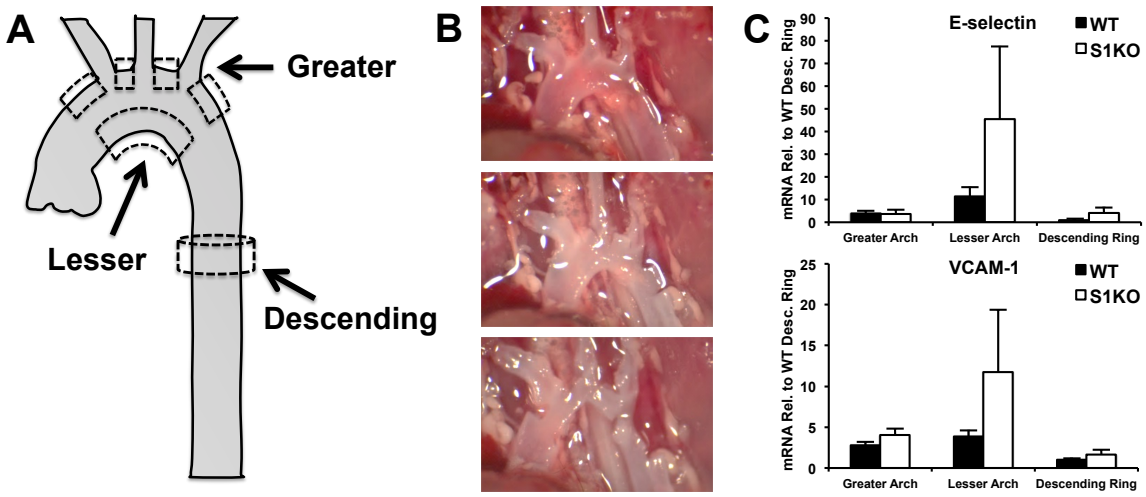


**Figure 5.1. Lack of syndecan-1 causes elevated levels of E-selectin and VCAM-1 in atheroprone aorta regions.** (A) Cartoon illustrating excised regions for gene expression analysis. (B) Pictures of aorta before, during, and after tissue removal. (C) S1KO mice appear to have higher gene expression levels of leukocyte-binding proteins E-selectin and VCAM-1.

### 5.3.3. Partial carotid ligation induces increased neointimal formation in Sdc-1 knockout mice.

To investigate the effects of a S1KO model in an induced disturbed flow environment, we used a partial ligation surgery technique previously developed by Nam *et al*[45]. To confirm the effects of the surgery and monitor the vessel remodeling, we used ultrasound imaging to measure vessel dimensions and blood flow. Post surgery, we

showed that the ligated carotid artery had a dramatic reduction in flow that included reverse flow at the end of each stroke (**Figure 5.3A and 5.3B**). Thirty days post-surgery we euthanized the mice and sectioned and stained the control and ligated carotid arteries with hematoxylin and eosin (H&E) to examine neointimal formation (**Figure 5.3C**). We measured the intimal, medial, and adventitial cross-sectional areas and found that the S1KO mice had a significantly increased neointimal formation (**Figure 5.3D**).

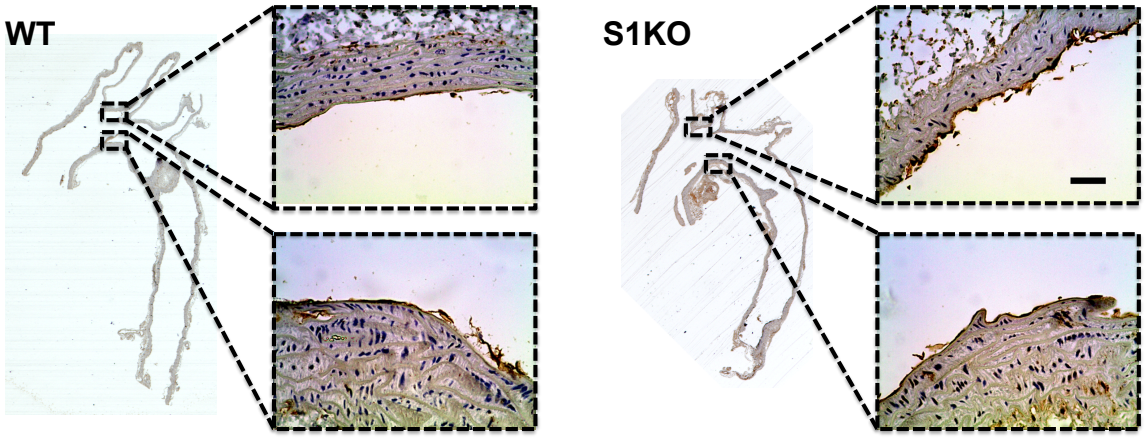


**Figure 5.2. Syndecan-1 knockout mice have higher VCAM-1 expression in regions with atheroprotective flow.** Immunohistochemical staining shows higher levels of VCAM-1 expression in the atheroprotective greater arch in syndecan-1 knockout mice.

### 5.3.4 Syndecan-1 knockout mice exhibit aortic medial thickening.

WT and S1KO mice aortas were cryosectioned and stained via a modified Verhoeff's Van Giesen stain to examine aorta medial thickness. Measurements were made using Metamorph by determining the average distance between the innermost and outmost elastic lamina. We observed that the S1KO aortae had an increased medial thickness (**Figure 5.4**).

### 5.3.5. Syndecan-1 knockout mice have increased global inflammatory response.

To examine the global inflammatory state we examined the functional response of WT and S1KO mice to a vasodilatory/inflammatory stimulus. We applied mustard oil to

the feet of anesthetized mice and measured the increase in blood flow over time using laser speckle imaging. We found that S1KO mice had a greater increase in perfusion in response to the same level of treatment with mustard oil (**Figure 5.5A and 5.5B**). Histological analysis revealed qualitatively greater edema in the feet of S1KO mice in comparison to WT mice (**Figure 5.5C**).

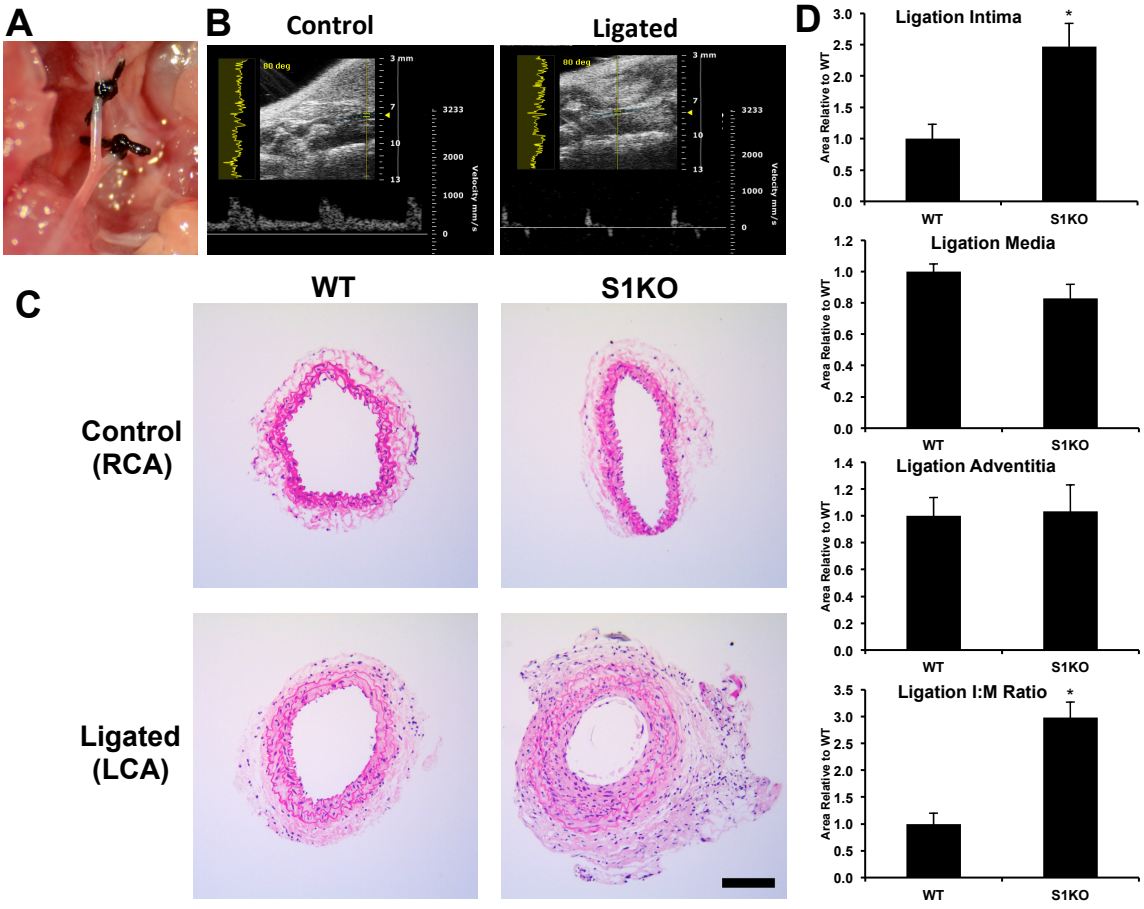


**Figure 5.3. Partial carotid ligation surgery induces increased neointimal formation in syndecan-1 knockout mice.** (A) Picture of ligation sites after left carotid artery bifurcation. (B) Ultrasound pulsed wave Doppler measurements confirmed post surgery that there was a dramatic reduction in flow with backflow in the ligated carotid. (C) H&E stains of control and ligated carotid artery sections thirty days after surgery. Scale bar = 200 μm. (D) S1KO mice exhibit higher levels of neointimal formation from intimal areas and intimal-to-medial ratios. *Statistically significant difference ($p<0.05$) between WT and S1KO.

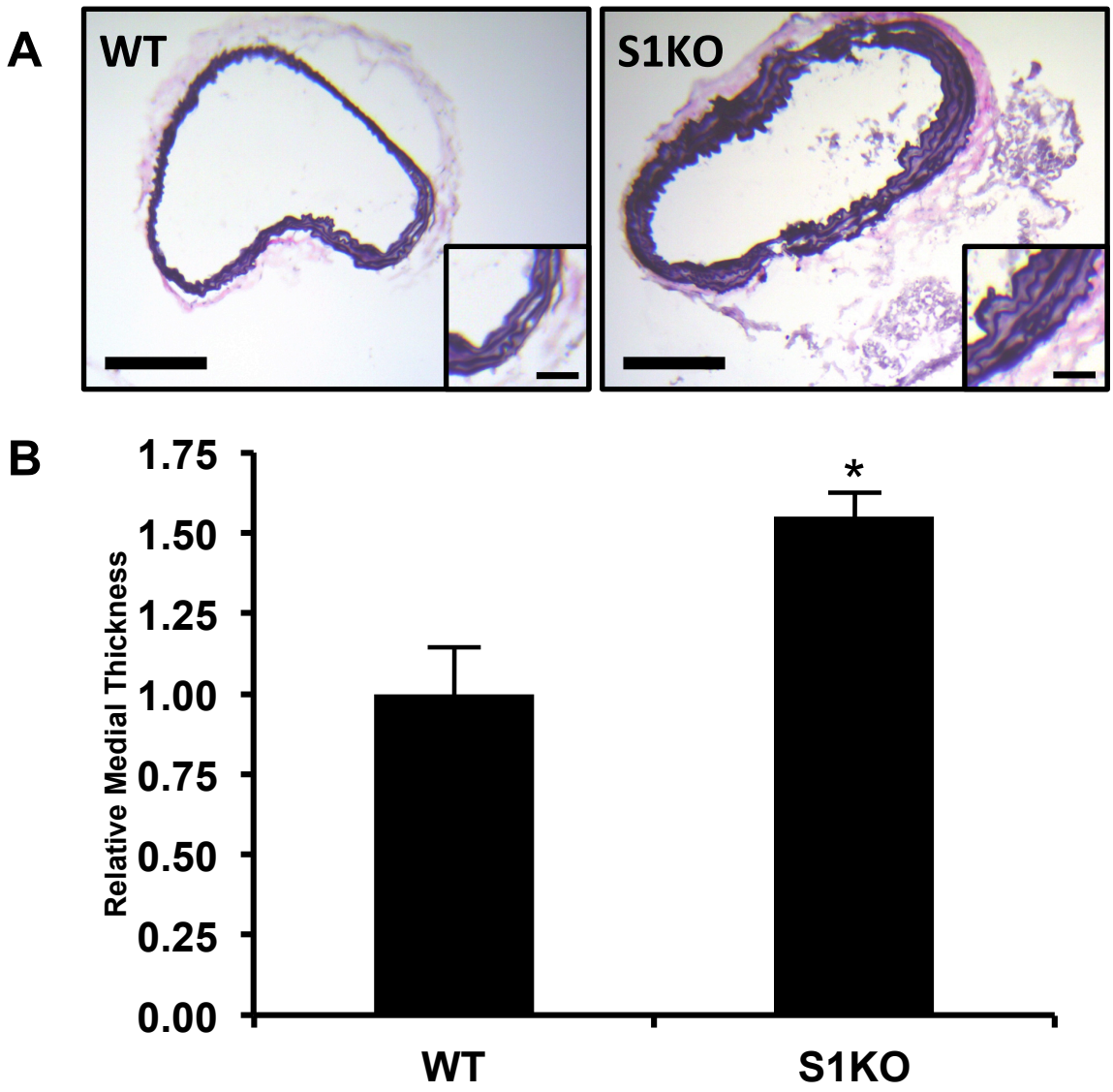


**Figure 5.4. Syndecan-1 knockout mice exhibit increased aortic medial thickness.** (A) WT and S1KO mouse aortae were sectioned and stained using a modified Verhoeff's Van Giesen stain. Scale bar = 200 μm (Mag = 50 μm). (B) Syndecan-1 knockout mice had thicker medial layers relative to the wild-type mice ($p<0.05$).

## 5.4 Discussion

While we can learn a lot about the mechanisms of mechanotransduction using *in vitro* studies, the complex dynamics between cell types and environmental niches necessitates *in vivo* validation to fully examine a physiologically relevant environment. In

order to investigate how syndecan-1 plays a role in endothelial mechanotransduction *in vivo*, we conducted animal studies using wild-type and syndecan-1 knockout mice. Having a mouse model in which our protein of interest is absent gives us a powerful toolset to study the effects of shear stress. We wanted to examine how the endothelium of syndecan-1 knockout mice might differ in both native and induced shear stress changes to see if our *in vitro* findings carry through to a larger order system.

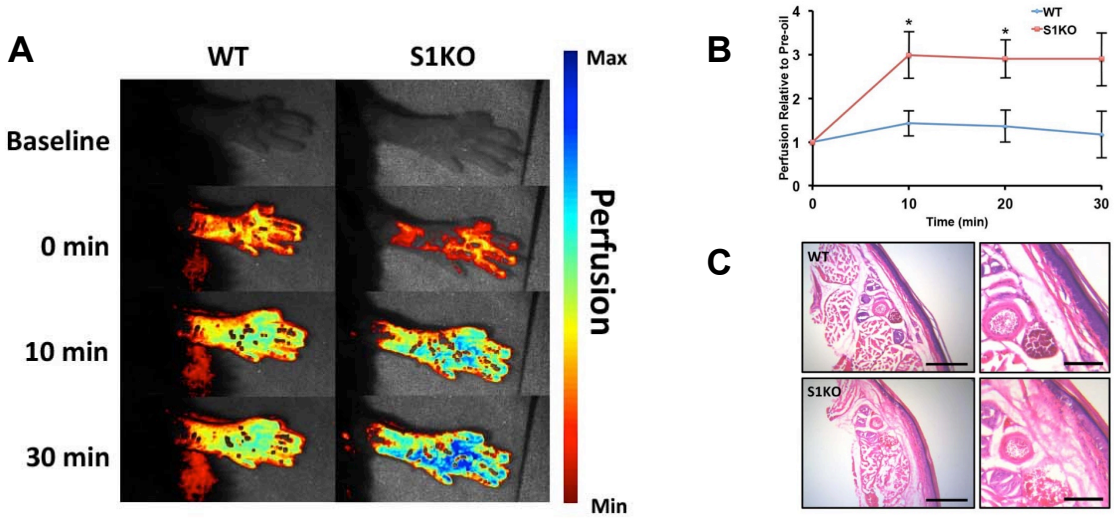


**Figure 5.5. Inflammatory responsiveness is increased in sdc-1 knockout mice.** (A) The foot pads of mice were treated with mustard oil (allyl isothiocyanate) and the response was measured by tracking tissue perfusion using laser speckle flow imaging. S1KO mice had an increased response to the mustard oil. (B) The S1KO mice showed an increase in relative blood perfusion relative to the WT mice. *$p < 0.05$ versus WT group at given time point. (C) Histological analysis of the foot pads of (WT) and S1KO mice after H&E staining. Scale bar = 400 μm (Mag = 150 μm).

Throughout the vasculature, the complex geometry that governs blood flow also leads to a complex range of wall shear stresses. In general, inside edges of high angle curvature and vessel expansions after bifurcations create regions of disturbed flow where development of atherosclerotic plaques is more common. We examined the aorta due to the differing shear stress levels present in close proximity to one another. These differences have been shown to contribute to a large number of phenotypic changes in the

respective endothelia, specifically higher VCAM-1 levels in atheroprone regions[149]. To examine these changes using our syndecan-1 knockout model, we examined both the gene and protein expression in these regions.

Using real-time PCR, we examined gene expression in the greater and lesser arches of WT and S1KO mice as well as in the descending aorta as a control. While the results are not quite statistically significant, they do suggest that the lesser arch of the syndecan-1 knockout aorta exhibits higher mRNA levels for both E-selectin and VCAM-1. The noise in the system is at least partially contributed to the method of the technique. When the tissue segments are excised and lysed, the endothelial cells only make up a fraction of the total cell number; most of the cells are smooth muscle cells. Thus some of the changes that might be clearer by looking only at endothelial cells are muted in our broad tissue lysis approach.

To examine the effects specifically on endothelial cells, we used histology and immunohistochemistry, which preserves the spatial geometry of the cells and can allow us to specifically examine the effects on the endothelium. By taking sections of aortae along the coronal plane, we were able to obtain sections that show the endothelium of both the greater and lesser arch of the aorta as well as the branches of the aortic birfurcations. We saw that similarly to our gene expression experiments, there was a higher expression of VCAM-1 in our S1KO model. Interestingly, while we didn't see a change in gene expression in the greater arch in mRNA, there appears to be higher protein levels of VCAM-1 in the S1KO greater arch. This is most likely due to the muting of the endothelial-specific expression signal when we lyse the entire vascular segment.

Native shear stress differences allow us to examine the effects of chronic differences in varying areas of the vasculature. However, these mice are healthy and do not experience much of the vessel occlusion that is present in later stages of atherosclerosis. To examine how the endothelium responds to changes in shear stress

levels we utilized surgical techniques to induce changes in shear. Several methods have been used previously to create these changes. The carotid cuff model was first used by Cheng *et al*. and involves placing a perivascular cuff around the carotid artery and tying it off to constrict blood flow[44]. While this is very effective at altering flow profiles within the artery, the cuff itself can cause an inflammatory response that is difficult to distinguish from changes due to the shear stress alone. We opted to use the partial carotid ligation surgery first developed by Nam *et al*[45]. This surgery involves tying off three of the four downstream bifurcations of the left carotid artery, which limits blood flow to the smaller superior thyroid artery. Nam *et al*. showed both computationally and experimentally that this creates a region of disturbed flow with oscillatory backflow along the length of the carotid artery without necessitating an implantation on the carotid itself. Using ultrasound imaging to confirm the success of our surgery, we found that after thirty days the S1KO mice developed a more pronounced neointimal formation than the WT mice. While the neointimal formation was not as profound as Nam *et al*. found in the more canonically atherosclerosis prone ApoE -/- mouse model, it does suggest that syndecan-1 may play a significant role in vessel stenosis.

Finally, we wanted to see how S1KO mice may differ in their aortic thickness and general inflammatory response. We found that the S1KO mice had pronounced aortic medial thickening when compared to the WT mice. This likely changes the mechanical properties of the aorta and may make them more prone to the development of aortic aneurysms. To test the mice for their general inflammatory response, we applied a 5% allyl isothiocyanate solution to the hind paws of anesthetized mice. This transdermal application has been shown to activate TRPA1 ion channels and induce an inflammatory response[150]. Using a custom laser speckle contrast imaging set up in our laboratory, we measured the increase in blood flow as the mouse responded to the inflammatory stimulus and saw that the S1KO mice had a more robust response. Additionally, histology of the footpads after the stimulus appears to show increased levels of edema in

the S1KO mice. These results are consistent with our findings that show that syndecan-1's absence induces a chronic inflammatory state and its translation to the hind foot paw may mean that syndecan-1 plays a specific role in peripheral vascular disease as well.

## 5.5 CONCLUSION

Determining the role of syndecan-1 in endothelial shear-mediated mechanotransduction necessitates using *in vivo* studies to validate *in vitro* findings. We showed that in native regions of different shear stress in the aorta an absence of syndecan-1 produces a pro-inflammatory environment, specifically through the upregulation of VCAM-1. Additionally, in response to an induced disturbed flow in the carotid artery via surgical techniques, S1KO mice exhibit a greater degree of neointimal formation. Finally, S1KO mice have thicker aortic medial layers and react more strongly to externally applied inflammatory stimuli. These findings help to validate the pro-inflammatory state we observed in S1KO endothelial cells *in vitro*. It is possible that delivery of syndecan-1 via proteolipisomal vectors could help regulate the endothelial mechanotransduction response and be involved in novel areas of cardiovascular therapeutics.

# Chapter 6: Conclusions

The main objective of this thesis was to investigate the initial sensory mechanisms that endothelial cells use in shear-mediated mechanotransduction to drive their overall expression to a healthy or diseased phenotype. We hypothesized that, based on previous research, the heparan sulfate proteoglycan, syndecan-1, was a good candidate for initiating the mechanosensing signaling cascade. While a growing body of research has investigated how endothelial cells change in response to shear stress, the initial sensing mechanisms responsible for driving these changes remained unclear. Recently, the thick layer of glycans and proteoglycans known as the glycocalyx has become an increasingly popular target of interest due to its pronounced protrusion into the lumen and direct interaction with blood flow. Previous studies demonstrated that the endothelial shear response is impaired by enzymatic degradation of the glycosaminoglycans found in the glycocalyx[48] and that levels of proteoglycan expression change in response to shear stress[19]. However, to date there had been no other comprehensive study of the involvement of specific proteoglycans in the mechanotransduction response. Thus we sought to investigate the role of syndecan-1 in this response.

To the best of our knowledge, the results of this dissertation are the first comprehensive study examining the endothelial shear-mediated mechanotransduction response of a glycocalyx proteoglycan using a global knockout model with both *in vitro* and *in vivo* studies. In order to conduct these experiments, we wanted to first improve upon existing *in vitro* shear stress application technology to facilitate cell culture experiments. We constructed three different shear stress application systems (Chapter 3): (1) an optimized, multithroughput parallel-plate system that allowed for unprecedented shear stress experiments in parallel while minimizing media volume requirements, (2) a modification of our first system to better accommodate downstream applications such as Western blotting and conditioned media assays, and (3) a modular cone-and-plate system

that enables the application of a wide range of physiologically dynamic shear waveforms. Using endothelial cells harvested from wild-type and syndecan-1 knockout mouse models, we showed that endothelial cells lacking syndecan-1 have a reduced response to shear stress and exhibit a persistent pro-inflammatory phenotype (Chapter 4). To validate these findings physiologically, we looked at the differences in wild-type and syndecan-1 knockout mice to both differing native and induced shear stress environments (Chapter 5). Syndecan-1 knockout mice exhibited higher levels of leukocyte-binding protein VCAM-1 in regions of known disturbed shear stress. Additionally, they exhibited increased neointimal formation in response to induced disturbed flow using a partial carotid ligation surgery. These findings demonstrate the syndecan-1 clearly has a role in the endothelial mechanotransduction pathways and further investigation of these pathways may lead to new targets for clinical therapeutics.

While we have uncovered many interesting findings regarding syndecan-1's role in shear stress, there remain several future work options to continue these studies. To examine the mechanisms by which syndecan-1 transmits a signaling cascade we have created several genetic mutations. Specifically, we have created a genetic version of syndecan-1 in which the five serine residues for glycosaminoglycan attachment have been mutated into alanines. This produces a syndecan-1 core protein that does not have any GAG component. Additionally, we've designed a mutant that contains a stop codon after the transmembrane segment and thus lacks the cytoplasmic tail. Using a lentiviral vector system, we will reintroduce either wild-type syndecan-1 or one of our mutations into sdc-1 knockout endothelial cells and examine how these mutated versions change the signaling response. This will give us a more detailed mechanistic understanding of these pathways and add to our new understanding of the role of syndecan-1 in flow-mediated endothelial mechanotransduction.

## References


1 Mozaffarian, D. *et al*. Heart disease and stroke statistics-2015 update: a report from the american heart association. *Circulation* **131**, e29 (2015).

2 Ng, M. *et al*. Global, regional, and national prevalence of overweight and obesity in children and adults during 1980–2013: a systematic analysis for the Global Burden of Disease Study 2013. *The Lancet* **384**, 766-781, doi:http://dx.doi.org/10.1016/S0140-6736(14)60460-8.

3 Lau, J. F., Weinberg, M. D. & Olin, J. W. Peripheral artery disease. Part 1: clinical evaluation and noninvasive diagnosis. *Nature reviews. Cardiology* **8**, 405-418, doi:10.1038/nrcardio.2011.66 (2011).

4 Pande, R. L., Perlstein, T. S., Beckman, J. A. & Creager, M. A. Secondary prevention and mortality in peripheral artery disease: National Health and Nutrition Examination Study, 1999 to 2004. *Circulation* **124**, 17-23, doi:10.1161/CIRCULATIONAHA.110.003954 (2011).

5 Nissen, S. E., Nicholls, S. J., Sipahi, I. & et al. Effect of very high-intensity statin therapy on regression of coronary atherosclerosis: The asteroid trial. *JAMA* **295**, 1556-1565, doi:10.1001/jama.295.13.jpc60002 (2006).

6 Davignon, J. Beneficial Cardiovascular Pleiotropic Effects of Statins. *Circulation* **109**, III-39-III-43, doi:10.1161/01.CIR.0000131517.20177.5a (2004).

7 Staels, B. *et al*. Mechanism of Action of Fibrates on Lipid and Lipoprotein Metabolism. *Circulation* **98**, 2088-2093, doi:10.1161/01.cir.98.19.2088 (1998).

8 Husain, S., Andrews, N. P., Mulcahy, D., Panza, J. A. & Quyyumi, A. A. Aspirin Improves Endothelial Dysfunction in Atherosclerosis. *Circulation* **97**, 716-720, doi:10.1161/01.cir.97.8.716 (1998).

9 Bradshaw, P. J., Jamrozik, K., Le, M., Gilfillan, I. & Thompson, P. L. Mortality and recurrent cardiac events after coronary artery bypass graft: long term outcomes in a population study. *Heart* **88**, 488-494 (2002).

10 Yusuf, S. *et al*. Effect of coronary artery bypass graft surgery on survival: overview of 10-year results from randomised trials by the Coronary Artery Bypass Graft Surgery Trialists Collaboration. *The Lancet* **344**, 563-570, doi:http://dx.doi.org/10.1016/S0140-6736(94)91963-1 (1994).

11 Davies, P. F., Remuzzi, A., Gordon, E. J., Dewey, C. F. & Gimbrone, M. A. Turbulent fluid shear stress induces vascular endothelial cell turnover in vitro. *Proceedings of the National Academy of Sciences* **83**, 2114-2117 (1986).

12 Chien, S. *Mechanotransduction and endothelial cell homeostasis: the wisdom of the cell*. Vol. 292 (2007).

13 Traub, O. & Berk, B. C. Laminar Shear Stress: Mechanisms by Which Endothelial Cells Transduce an Atheroprotective Force. *Arteriosclerosis, thrombosis, and vascular biology* **18**, 677-685, doi:10.1161/01.atv.18.5.677 (1998).

14 Li, Y.-S. J., Haga, J. H. & Chien, S. Molecular basis of the effects of shear stress on vascular endothelial cells. *Journal of Biomechanics* **38**, 1949-1971, doi:http://dx.doi.org/10.1016/j.jbiomech.2004.09.030 (2005).

15 Weinbaum, S., Zhang, X., Han, Y., Vink, H. & Cowin, S. C. Mechanotransduction and flow across the endothelial glycocalyx. *Proceedings of*

*the National Academy of Sciences* **100**, 7988-7995, doi:10.1073/pnas.1332808100 (2003).

16 Potter, D. R. & Damiano, E. R. The Hydrodynamically Relevant Endothelial Cell Glycocalyx Observed In Vivo Is Absent In Vitro. *Circulation research* **102**, 770-776, doi:10.1161/circresaha.107.160226 (2008).

17 Tarbell, J. M. & Pahakis, M. Mechanotransduction and the glycocalyx. *Journal of internal medicine* **259**, 339-350 (2006).

18 Pahakis, M. Y., Kosky, J. R., Dull, R. O. & Tarbell, J. M. The role of endothelial glycocalyx components in mechanotransduction of fluid shear stress. *Biochemical and Biophysical Research Communications* **355**, 228-233, doi:http://dx.doi.org/10.1016/j.bbrc.2007.01.137 (2007).

19 Koo, A., Dewey, C. F. & García-Cardeña, G. Hemodynamic shear stress characteristic of atherosclerosis-resistant regions promotes glycocalyx formation in cultured endothelial cells. *American Journal of Physiology-Cell Physiology* **304**, C137-C146 (2013).

20 Criqui, M. H. Peripheral arterial disease-epidemiological aspects. *Vascular medicine* **6**, 3-7 (2001).

21 Pfeffer, M. A. & Braunwald, E. Ventricular remodeling after myocardial infarction. Experimental observations and clinical implications. *Circulation* **81**, 1161-1172 (1990).

22 Tatemichi, T. *et al*. Cognitive impairment after stroke: frequency, patterns, and relationship to functional abilities. *Journal of Neurology, Neurosurgery & Psychiatry* **57**, 202-207 (1994).

23 Hahn, C. & Schwartz, M. A. Mechanotransduction in vascular physiology and atherogenesis. *Nature reviews. Molecular cell biology* **10**, 53-62, doi:10.1038/nrm2596 (2009).

24 O'Hare, A. M., Glidden, D. V., Fox, C. S. & Hsu, C. Y. High prevalence of peripheral arterial disease in persons with renal insufficiency: results from the National Health and Nutrition Examination Survey 1999-2000. *Circulation* **109**, 320-323, doi:10.1161/01.CIR.0000114519.75433.DD (2004).

25 Naghavi, M. *et al*. From Vulnerable Plaque to Vulnerable Patient: A Call for New Definitions and Risk Assessment Strategies: Part I. *Circulation* **108**, 1664-1672, doi:10.1161/01.cir.0000087480.94275.97 (2003).

26 Welt, F. G. P. & Rogers, C. Inflammation and Restenosis in the Stent Era. *Arteriosclerosis, thrombosis, and vascular biology* **22**, 1769-1776, doi:10.1161/01.atv.0000037100.44766.5b (2002).

27 Iakovou, I. *et al*. Incidence, predictors, and outcome of thrombosis after successful implantation of drug-eluting stents. *Jama* **293**, 2126-2130 (2005).

28 Davies, P. F. *et al*. Spatial relationships in early signaling events of flow-mediated endothelial mechanotransduction. *Annual review of physiology* **59**, 527-549, doi:10.1146/annurev.physiol.59.1.527 (1997).

29 Hoger, J. H., Ilyin, V. I., Forsyth, S. & Hoger, A. Shear stress regulates the endothelial Kir2.1 ion channel. *Proceedings of the National Academy of Sciences of the United States of America* **99**, 7780-7785, doi:10.1073/pnas.102184999 (2002).

30 Hutcheson, I. R. & Griffith, T. M. Mechanotransduction through the endothelial cytoskeleton: mediation of flow- but not agonist-induced EDRF release. *British journal of pharmacology* **118**, 720-726 (1996).
31 Iomini, C., Tejada, K., Mo, W., Vaananen, H. & Piperno, G. Primary cilia of human endothelial cells disassemble under laminar shear stress. *The Journal of cell biology* **164**, 811-817, doi:10.1083/jcb.200312133 (2004).
32 Malek, A. M., Zhang, J., Jiang, J., Alper, S. L. & Izumo, S. Endothelin-1 gene suppression by shear stress: pharmacological evaluation of the role of tyrosine kinase, intracellular calcium, cytoskeleton, and mechanosensitive channels. *Journal of molecular and cellular cardiology* **31**, 387-399, doi:10.1006/jmcc.1998.0873 (1999).
33 Schwartz, M. A. & DeSimone, D. W. Cell adhesion receptors in mechanotransduction. *Current opinion in cell biology* **20**, 551-556, doi:10.1016/j.ceb.2008.05.005 (2008).
34 Zarins, C. K. *et al*. Carotid bifurcation atherosclerosis. Quantitative correlation of plaque localization with flow velocity profiles and wall shear stress. *Circulation research* **53**, 502-514 (1983).
35 Levesque, M. & Nerem, R. The elongation and orientation of cultured endothelial cells in response to shear stress. *Journal of biomechanical engineering* **107**, 341-347 (1985).
36 Dimmeler, S. *et al*. Activation of nitric oxide synthase in endothelial cells by Akt-dependent phosphorylation. *Nature* **399**, 601-605 (1999).
37 Topper, J. N., Cai, J., Falb, D. & Gimbrone, M. A. Identification of vascular endothelial genes differentially responsive to fluid mechanical stimuli: cyclooxygenase-2, manganese superoxide dismutase, and endothelial cell nitric oxide synthase are selectively up-regulated by steady laminar shear stress. *Proceedings of the National Academy of Sciences* **93**, 10417-10422 (1996).
38 Dekker, R. J. *et al*. Prolonged fluid shear stress induces a distinct set of endothelial cell genes, most specifically lung Krüppel-like factor (KLF2). *Blood* **100**, 1689-1698 (2002).
39 SenBanerjee, S. *et al*. KLF2 Is a novel transcriptional regulator of endothelial proinflammatory activation. *The Journal of experimental medicine* **199**, 1305-1315 (2004).
40 Shyy, J. Y.-J. & Chien, S. Role of Integrins in Endothelial Mechanosensing of Shear Stress. *Circulation research* **91**, 769-775, doi:10.1161/01.res.0000038487.19924.18 (2002).
41 Tzima, E. *et al*. A mechanosensory complex that mediates the endothelial cell response to fluid shear stress. *Nature* **437**, 426-431, doi:http://www.nature.com/nature/journal/v437/n7057/suppinfo/nature03952_S1.html (2005).
42 Gelfand, B. D. *et al*. Hemodynamic activation of β-catenin and T-cell-specific transcription factor signaling in vascular endothelium regulates fibronectin expression. *Arteriosclerosis, thrombosis, and vascular biology* **31**, 1625-1633 (2011).

43 Cheng, C. *et al*. Atherosclerotic Lesion Size and Vulnerability Are Determined by Patterns of Fluid Shear Stress. *Circulation* **113**, 2744-2753, doi:10.1161/circulationaha.105.590018 (2006).
44 Cheng, C. *et al*. *Shear stress affects the intracellular distribution of eNOS: direct demonstration by a novel in vivo technique*. Vol. 106 (2005).
45 Nam, D. *et al*. *Partial carotid ligation is a model of acutely induced disturbed flow, leading to rapid endothelial dysfunction and atherosclerosis*. Vol. 297 (2009).
46 Couchman, J. R. & Pataki, C. A. An introduction to proteoglycans and their localization. *Journal of Histochemistry & Cytochemistry* **60**, 885-897 (2012).
47 Lekakis, J. *et al*. Methods for evaluating endothelial function: a position statement from the European Society of Cardiology Working Group on Peripheral Circulation. *European journal of cardiovascular prevention and rehabilitation : official journal of the European Society of Cardiology, Working Groups on Epidemiology & Prevention and Cardiac Rehabilitation and Exercise Physiology* **18**, 775-789, doi:10.1177/1741826711398179 (2011).
48 Florian, J. A. *et al*. Heparan sulfate proteoglycan is a mechanosensor on endothelial cells. *Circulation research* **93**, e136-142, doi:10.1161/01.RES.0000101744.47866.D5 (2003).
49 Kumagai, R., Lu, X. & Kassab, G. S. Role of glycocalyx in flow-induced production of nitric oxide and reactive oxygen species. *Free radical biology & medicine* **47**, 600-607, doi:10.1016/j.freeradbiomed.2009.05.034 (2009).
50 Pohl, U., Herlan, K., Huang, A. & Bassenge, E. EDRF-mediated shear-induced dilation opposes myogenic vasoconstriction in small rabbit arteries. *The American journal of physiology* **261**, H2016-2023 (1991).
51 Kamiya, A., Bukhari, R. & Togawa, T. Adaptive regulation of wall shear stress optimizing vascular tree function. *Bulletin of mathematical biology* **46**, 127-137 (1984).
52 Hecker, M., Mulsch, A., Bassenge, E. & Busse, R. Vasoconstriction and increased flow: two principal mechanisms of shear stress-dependent endothelial autacoid release. *The American journal of physiology* **265**, H828-833 (1993).
53 Mali, M., Jaakkola, P., Arvilommi, A.-M. & Jalkanen, M. Sequence of human syndecan indicates a novel gene family of integral membrane proteoglycans. *Journal of Biological Chemistry* **265**, 6884-6889 (1990).
54 Hayashida, K., Parks, W. C. & Park, P. W. Syndecan-1 shedding facilitates the resolution of neutrophilic inflammation by removing sequestered CXC chemokines. *Blood* **114**, 3033-3043 (2009).
55 Seidel, C. *et al*. Serum syndecan-1: a new independent prognostic marker in multiple myeloma. *Blood* **95**, 388-392 (2000).
56 Larraı´n, J., Carey, D. J. & Brandan, E. Syndecan-1 Expression Inhibits Myoblast Differentiation through a Basic Fibroblast Growth Factor-dependent Mechanism. *Journal of Biological Chemistry* **273**, 32288-32296, doi:10.1074/jbc.273.48.32288 (1998).
57 Beauvais, D. M., Ell, B. J., McWhorter, A. R. & Rapraeger, A. C. Syndecan-1 regulates αvβ3 and αvβ5 integrin activation during angiogenesis and is blocked

by synstatin, a novel peptide inhibitor. *The Journal of experimental medicine* **206**, 691-705 (2009).
58 Carey, D. J., Stahl, R. C., Cizmeci-Smith, G. & Asundi, V. K. Syndecan-1 expressed in Schwann cells causes morphological transformation and cytoskeletal reorganization and associates with actin during cell spreading. *The Journal of cell biology* **124**, 161-170 (1994).
59 Gotte, M. *et al*. Role of syndecan-1 in leukocyte-endothelial interactions in the ocular vasculature. *Investigative Ophthalmology and Visual Science* **43**, 1135-1141 (2002).
60 Savery, M. D., Jiang, J. X., Park, P. W. & Damiano, E. R. The endothelial glycocalyx in syndecan-1 deficient mice. *Microvasc. Res.* **87**, 83-91, doi:10.1016/j.mvr.2013.02.001 (2013).
61 Davies, P. F. Hemodynamic shear stress and the endothelium in cardiovascular pathophysiology. *Nature clinical practice. Cardiovascular medicine* **6**, 16-26, doi:10.1038/ncpcardio1397 (2009).
62 Chiu, J. J. & Chien, S. Effects of disturbed flow on vascular endothelium: pathophysiological basis and clinical perspectives. *Physiological reviews* **91**, 327-387, doi:10.1152/physrev.00047.2009 (2011).
63 Stroka, K. M. & Aranda-Espinoza, H. A biophysical view of the interplay between mechanical forces and signaling pathways during transendothelial cell migration. *The FEBS journal* **277**, 1145-1158, doi:10.1111/j.1742-4658.2009.07545.x (2010).
64 Deng, X., Marois, Y. & Guidoin, R. Fluid filtration across the arterial wall under flow conditions: is wall shear rate another factor affecting filtration rate? *Annals of the New York Academy of Sciences* **858**, 105-115 (1998).
65 Chien, S., Li, S. & Shyy, Y. J. Effects of mechanical forces on signal transduction and gene expression in endothelial cells. *Hypertension* **31**, 162-169 (1998).
66 Frangos, J. A., Eskin, S. G., McIntire, L. V. & Ives, C. L. Flow effects on prostacyclin production by cultured human endothelial cells. *Science* **227**, 1477-1479 (1985).
67 Geiger, R. V., Berk, B. C., Alexander, R. W. & Nerem, R. M. Flow-induced calcium transients in single endothelial cells: spatial and temporal analysis. *The American journal of physiology* **262**, C1411-1417 (1992).
68 Levitan, I., Helmke, B. P. & Davies, P. F. A chamber to permit invasive manipulation of adherent cells in laminar flow with minimal disturbance of the flow field. *Annals of biomedical engineering* **28**, 1184-1193 (2000).
69 Dewey, C. F., Jr., Bussolari, S. R., Gimbrone, M. A., Jr. & Davies, P. F. The dynamic response of vascular endothelial cells to fluid shear stress. *J Biomech Eng* **103**, 177-185 (1981).
70 Franke, R. P. *et al*. Induction of human vascular endothelial stress fibres by fluid shear stress. *Nature* **307**, 648-649 (1984).
71 Dai, G. *et al*. Distinct endothelial phenotypes evoked by arterial waveforms derived from atherosclerosis-susceptible and -resistant regions of human vasculature. *Proceedings of the National Academy of Sciences of the United States of America* **101**, 14871-14876, doi:10.1073/pnas.0406073101 (2004).

72 Young, E. W. & Simmons, C. A. Macro- and microscale fluid flow systems for endothelial cell biology. *Lab on a chip* **10**, 143-160, doi:10.1039/b913390a (2010).
73 Kim, J. *et al*. A programmable microfluidic cell array for combinatorial drug screening. *Lab on a chip*, doi:10.1039/c2lc21202a (2012).
74 Liu, L. *et al*. A microfluidic device for continuous cancer cell culture and passage with hydrodynamic forces. *Lab on a chip* **10**, 1807-1813, doi:10.1039/c003509b (2010).
75 Chau, L., Doran, M. & Cooper-White, J. A novel multishear microdevice for studying cell mechanics. *Lab on a chip* **9**, 1897-1902, doi:10.1039/b823180j (2009).
76 Lawson, C., Rose, M. & Wolf, S. Leucocyte adhesion under haemodynamic flow conditions. *Methods in molecular biology* **616**, 31-47, doi:10.1007/978-1-60761-461-6_3 (2010).
77 Liang, S., Slattery, M. J. & Dong, C. Shear stress and shear rate differentially affect the multi-step process of leukocyte-facilitated melanoma adhesion. *Experimental cell research* **310**, 282-292, doi:10.1016/j.yexcr.2005.07.028 (2005).
78 Kolandaivelu, K. *et al*. Stent thrombogenicity early in high-risk interventional settings is driven by stent design and deployment and protected by polymer-drug coatings. *Circulation* **123**, 1400-1409, doi:10.1161/CIRCULATIONAHA.110.003210 (2011).
79 Cornish, R. J. Flow in a Pipe of Rectangular Cross-Section. *Proc R Soc A* **12o**, 691-700 (1928).
80 Moscato, F., Colacino, F. M., Arabia, M. & Danieli, G. A. Pressure pulsation in roller pumps: a validated lumped parameter model. *Medical engineering & physics* **30**, 1149-1158, doi:10.1016/j.medengphy.2008.02.007 (2008).
81 van de Vosse, F. N. S., N. Pulse Wave Propagation in the Arterial Tree. *Ann Rev Fluid Mech* **43**, 467-499 (2011).
82 Glover, R. C. Liquid Pulsation Dampener. (1971).
83 Slattery, M. J., Liang, S. & Dong, C. Distinct role of hydrodynamic shear in leukocyte-facilitated tumor cell extravasation. *American journal of physiology. Cell physiology* **288**, C831-839, doi:10.1152/ajpcell.00439.2004 (2005).
84 Malek, A. & Izumo, S. Physiological fluid shear stress causes downregulation of endothelin-1 mRNA in bovine aortic endothelium. *The American journal of physiology* **263**, C389-396 (1992).
85 Kolandaivelu, K. & Edelman, E. R. Low background, pulsatile, in vitro flow circuit for modeling coronary implant thrombosis. *J Biomech Eng* **124**, 662-668 (2002).
86 Olesen, S. P., Clapham, D. E. & Davies, P. F. Haemodynamic shear stress activates a K+ current in vascular endothelial cells. *Nature* **331**, 168-170, doi:10.1038/331168a0 (1988).
87 Doebelin, E. *System Dynamics*. (CRC Pres, 1998).
88 Blackman, B. R., Garcia-Cardena, G. & Gimbrone, M. A., Jr. A new in vitro model to evaluate differential responses of endothelial cells to simulated arterial shear stress waveforms. *J Biomech Eng* **124**, 397-407 (2002).

89 Rubanyi, G. M., Romero, J. C. & Vanhoutte, P. M. Flow-induced release of endothelium-derived relaxing factor. *The American journal of physiology* **250**, H1145-1149 (1986).
90 Nishida, K. *et al*. Molecular cloning and characterization of the constitutive bovine aortic endothelial cell nitric oxide synthase. *The Journal of clinical investigation* **90**, 2092-2096, doi:10.1172/JCI116092 (1992).
91 Sessa, W. C., Pritchard, K., Seyedi, N., Wang, J. & Hintze, T. H. Chronic exercise in dogs increases coronary vascular nitric oxide production and endothelial cell nitric oxide synthase gene expression. *Circulation research* **74**, 349-353 (1994).
92 Davis, M. E., Cai, H., Drummond, G. R. & Harrison, D. G. Shear stress regulates endothelial nitric oxide synthase expression through c-Src by divergent signaling pathways. *Circulation research* **89**, 1073-1080 (2001).
93 Endemann, D. H. & Schiffrin, E. L. Endothelial dysfunction. *Journal of the American Society of Nephrology : JASN* **15**, 1983-1992, doi:10.1097/01.ASN.0000132474.50966.DA (2004).
94 Hsieh, H.-J., Liu, C.-A., Huang, B., Tseng, A. & Wang, D. L. Shear-induced endothelial mechanotransduction: the interplay between reactive oxygen species (ROS) and nitric oxide (NO) and the pathophysiological implications. *J Biomed Sci* **21** (2014).
95 Chappell, D. C., Varner, S. E., Nerem, R. M., Medford, R. M. & Alexander, R. W. Oscillatory shear stress stimulates adhesion molecule expression in cultured human endothelium. *Circulation research* **82**, 532-539 (1998).
96 Dai, G. *et al*. Distinct endothelial phenotypes evoked by arterial waveforms derived from atherosclerosis-susceptible and-resistant regions of human vasculature. *Proceedings of the National Academy of Sciences of the United States of America* **101**, 14871-14876 (2004).
97 Baker, A. B. *et al*. Endothelial cells provide feedback control for vascular remodeling through a mechanosensitive autocrine TGF-beta signaling pathway. *Circulation research* **103**, 289-297, doi:10.1161/CIRCRESAHA.108.179465 (2008).
98 Spruell, C. & Baker, A. B. Analysis of a high−throughput cone−and−plate apparatus for the application of defined spatiotemporal flow to cultured cells. *Biotechnology and bioengineering* **110**, 1782-1793 (2013).
99 Hoger, J. H., Ilyin, V. I., Forsyth, S. & Hoger, A. Shear stress regulates the endothelial Kir2.1 ion channel. *Proc. Natl. Acad. Sci. U. S. A.* **99**, 7780-7785, doi:10.1073/pnas.102184999 (2002).
100 Schwartz, M. A. & DeSimone, D. W. Cell adhesion receptors in mechanotransduction. *Curr. Opin. Cell Biol.* **20**, 551-556, doi:10.1016/j.ceb.2008.05.005 (2008).
101 Parmar, K. M. *et al*. Integration of flow-dependent endothelial phenotypes by Kruppel-like factor 2. *J. Clin. Invest.* **116**, 49-58, doi:10.1172/JCI24787 (2006).
102 Hamik, A. *et al*. Kruppel-like factor 4 regulates endothelial inflammation. *The Journal of biological chemistry* **282**, 13769-13779, doi:10.1074/jbc.M700078200 (2007).

103 Zhou, G. *et al*. Endothelial Kruppel-like factor 4 protects against atherothrombosis in mice. *J. Clin. Invest.* **122**, 4727-4731, doi:10.1172/JCI66056 (2012).
104 Kumekawa, M., Fukuda, G., Shimizu, S., Konno, K. & Odawara, M. Inhibition of monocyte chemoattractant protein-1 by Kruppel-like factor 5 small interfering RNA in the tumor necrosis factor- alpha-activated human umbilical vein endothelial cells. *Biological & pharmaceutical bulletin* **31**, 1609-1613 (2008).
105 Tzima, E. *et al*. A mechanosensory complex that mediates the endothelial cell response to fluid shear stress. *Nature* **437**, 426-431, doi:10.1038/nature03952 (2005).
106 Ebong, E. E., Macaluso, F. P., Spray, D. C. & Tarbell, J. M. Imaging the endothelial glycocalyx in vitro by rapid freezing/freeze substitution transmission electron microscopy. *Arteriosclerosis, thrombosis, and vascular biology* **31**, 1908-1915, doi:10.1161/ATVBAHA.111.225268 (2011).
107 Weinbaum, S., Zhang, X., Han, Y., Vink, H. & Cowin, S. C. Mechanotransduction and flow across the endothelial glycocalyx. *Proc. Natl. Acad. Sci. U. S. A.* **100**, 7988-7995, doi:10.1073/pnas.1332808100 (2003).
108 Bishop, J. R., Schuksz, M. & Esko, J. D. Heparan sulphate proteoglycans fine-tune mammalian physiology. *Nature* **446**, 1030-1037, doi:10.1038/nature05817 (2007).
109 Hsia, E., Richardson, T. P. & Nugent, M. A. Nuclear localization of basic fibroblast growth factor is mediated by heparan sulfate proteoglycans through protein kinase C signaling. *Journal of cellular biochemistry* **88**, 1214-1225, doi:10.1002/jcb.10470 (2003).
110 Tkachenko, E., Rhodes, J. M. & Simons, M. Syndecans: new kids on the signaling block. *Circul. Res.* **96**, 488-500, doi:10.1161/01.RES.0000159708.71142.c8 (2005).
111 Rapraeger, A. C. Synstatin: a selective inhibitor of the syndecan-1-coupled IGF1R-alphavbeta3 integrin complex in tumorigenesis and angiogenesis. *The FEBS journal* **280**, 2207-2215, doi:10.1111/febs.12160 (2013).
112 Okina, E., Manon-Jensen, T., Whiteford, J. R. & Couchman, J. R. Syndecan proteoglycan contributions to cytoskeletal organization and contractility. *Scandinavian journal of medicine & science in sports* **19**, 479-489, doi:10.1111/j.1600-0838.2009.00941.x (2009).
113 Roper, J. A., Williamson, R. C. & Bass, M. D. Syndecan and integrin interactomes: large complexes in small spaces. *Current opinion in structural biology* **22**, 583-590, doi:10.1016/j.sbi.2012.07.003 (2012).
114 Dong, Q. G. *et al*. A general strategy for isolation of endothelial cells from murine tissues. Characterization of two endothelial cell lines from the murine lung and subcutaneous sponge implants. *Arteriosclerosis, thrombosis, and vascular biology* **17**, 1599-1604 (1997).
115 Mostoslavsky, G. *et al*. Efficiency of transduction of highly purified murine hematopoietic stem cells by lentiviral and oncoretroviral vectors under conditions of minimal in vitro manipulation. *Mol. Ther.* **11**, 932-940, doi:10.1016/j.ymthe.2005.01.005 (2005).

116 Voyvodic, P. L., Min, D. & Baker, A. B. A multichannel dampened flow system for studies on shear stress-mediated mechanotransduction. *Lab on a chip* **12**, 3322-3330, doi:10.1039/c2lc40526a (2012).
117 Pertz, O., Hodgson, L., Klemke, R. L. & Hahn, K. M. Spatiotemporal dynamics of RhoA activity in migrating cells. *Nature* **440**, 1069-1072, doi:10.1038/nature04665 (2006).
118 Koskinas, K. C. *et al*. Natural history of experimental coronary atherosclerosis and vascular remodeling in relation to endothelial shear stress: a serial, in vivo intravascular ultrasound study. *Circulation* **121**, 2092-2101 (2010).
119 Chatzizisis, Y. S. *et al*. Augmented expression and activity of extracellular matrix-degrading enzymes in regions of low endothelial shear stress colocalize with coronary atheromata with thin fibrous caps in pigs. *Circulation* **123**, 621-630, doi:10.1161/CIRCULATIONAHA.110.970038 (2011).
120 Dai, G. *et al*. Biomechanical forces in atherosclerosis-resistant vascular regions regulate endothelial redox balance via phosphoinositol 3-kinase/Akt-dependent activation of Nrf2. *Circulation research* **101**, 723-733, doi:10.1161/CIRCRESAHA.107.152942 (2007).
121 Dimmeler, S., Assmus, B., Hermann, C., Haendeler, J. & Zeiher, A. M. Fluid shear stress stimulates phosphorylation of Akt in human endothelial cells: involvement in suppression of apoptosis. *Circulation research* **83**, 334-341 (1998).
122 Dimmeler, S. *et al*. Activation of nitric oxide synthase in endothelial cells by Akt-dependent phosphorylation. *Nature* **399**, 601-605, doi:10.1038/21224 (1999).
123 Zaidel-Bar, R., Kam, Z. & Geiger, B. Polarized downregulation of the paxillin-p130CAS-Rac1 pathway induced by shear flow. *J. Cell Sci.* **118**, 3997-4007, doi:10.1242/jcs.02523 (2005).
124 Orr, A. W., Ginsberg, M. H., Shattil, S. J., Deckmyn, H. & Schwartz, M. A. Matrix-specific suppression of integrin activation in shear stress signaling. *Mol. Biol. Cell* **17**, 4686-4697, doi:10.1091/mbc.E06-04-0289 (2006).
125 Hennig, T., Mogensen, C., Kirsch, J., Pohl, U. & Gloe, T. Shear stress induces the release of an endothelial elastase: role in integrin alpha(v)beta(3)-mediated FGF-2 release. *Journal of vascular research* **48**, 453-464, doi:10.1159/000327009 (2011).
126 Pampori, N. *et al*. Mechanisms and consequences of affinity modulation of integrin alpha(V)beta(3) detected with a novel patch-engineered monovalent ligand. *J. Biol. Chem.* **274**, 21609-21616 (1999).
127 Cicha, I. *et al*. Pharmacological inhibition of RhoA signaling prevents connective tissue growth factor induction in endothelial cells exposed to non-uniform shear stress. *Atherosclerosis* **196**, 136-145, doi:10.1016/j.atherosclerosis.2007.03.016 (2008).
128 Yang, B., Radel, C., Hughes, D., Kelemen, S. & Rizzo, V. p190 RhoGTPase-activating protein links the beta1 integrin/caveolin-1 mechanosignaling complex to RhoA and actin remodeling. *Arterioscler. Thromb. Vasc. Biol.* **31**, 376-383, doi:10.1161/ATVBAHA.110.217794 (2011).

129 Tzima, E. Role of small GTPases in endothelial cytoskeletal dynamics and the shear stress response. *Circul. Res.* **98**, 176-185, doi:10.1161/01.RES.0000200162.94463.d7 (2006).
130 Hoshino, Y. *et al*. Regulated expression of the BTEB2 transcription factor in vascular smooth muscle cells: analysis of developmental and pathological expression profiles shows implications as a predictive factor for restenosis. *Circulation* **102**, 2528-2534 (2000).
131 Pahakis, M. Y., Kosky, J. R., Dull, R. O. & Tarbell, J. M. The role of endothelial glycocalyx components in mechanotransduction of fluid shear stress. *Biochem Biophys Res Commun* **355**, 228-233 (2007).
132 Van Teeffelen, J. W., Brands, J., Stroes, E. S. & Vink, H. Endothelial glycocalyx: sweet shield of blood vessels. *Trends Cardiovasc Med* **17**, 101-105 (2007).
133 Koo, A., Dewey, C. F., Jr. & Garcia-Cardena, G. Hemodynamic shear stress characteristic of atherosclerosis-resistant regions promotes glycocalyx formation in cultured endothelial cells. *American journal of physiology. Cell physiology* **304**, C137-146, doi:10.1152/ajpcell.00187.2012 (2013).
134 Nam, E. J. & Park, P. W. Shedding of cell membrane-bound proteoglycans. *Methods Mol. Biol.* **836**, 291-305, doi:10.1007/978-1-61779-498-8_19 (2012).
135 Das, S., Singh, G. & Baker, A. B. Overcoming Disease-Induced Growth Factor Resistance in Therapeutic Angiogenesis Using Recombinant Co-Receptors Delivered by a Liposomal System. *Biomaterials* **(In Press)** (2013).
136 Ramani, V. C. *et al*. The heparanase/syndecan-1 axis in cancer: mechanisms and therapies. *FEBS J.* **280**, 2294-2306, doi:10.1111/febs.12168 (2013).
137 Baker, A. B. *et al*. Heparanase regulates thrombosis in vascular injury and stent-induced flow disturbance. *Journal of the American College of Cardiology* **59**, 1551-1560, doi:10.1016/j.jacc.2011.11.057 (2012).
138 Mobine, H. R. *et al*. Pheochromocytoma-induced cardiomyopathy is modulated by the synergistic effects of cell-secreted factors. *Circulation. Heart failure* **2**, 121-128, doi:10.1161/CIRCHEARTFAILURE.108.813261 (2009).
139 Blich, M. *et al*. Macrophage activation by heparanase is mediated by TLR-2 and TLR-4 and associates with plaque progression. *Arteriosclerosis, thrombosis, and vascular biology* **33**, e56-65, doi:10.1161/ATVBAHA.112.254961 (2013).
140 Schmidt, E. P. *et al*. The pulmonary endothelial glycocalyx regulates neutrophil adhesion and lung injury during experimental sepsis. *Nat. Med.* **18**, 1217-1223, doi:10.1038/nm.2843 (2012).
141 Potter, D. R. & Damiano, E. R. The hydrodynamically relevant endothelial cell glycocalyx observed in vivo is absent in vitro. *Circulation research* **102**, 770-776, doi:10.1161/CIRCRESAHA.107.160226 (2008).
142 Potter, D. R., Jiang, J. & Damiano, E. R. The recovery time course of the endothelial cell glycocalyx in vivo and its implications in vitro. *Circulation research* **104**, 1318-1325, doi:10.1161/CIRCRESAHA.108.191585 (2009).
143 Baker, A. B. *et al*. Regulation of heparanase expression in coronary artery disease in diabetic, hyperlipidemic swine. *Atherosclerosis* **213**, 436-442, doi:10.1016/j.atherosclerosis.2010.09.003 (2010).

144 Baker, A. B. *et al*. Heparanase alters arterial structure, mechanics, and repair following endovascular stenting in mice. *Circulation research* **104**, 380-387, doi:10.1161/CIRCRESAHA.108.180695 (2009).
145 Alexander, C. M. *et al*. Syndecan-1 is required for Wnt-1-induced mammary tumorigenesis in mice. *Nature genetics* **25**, 329-332, doi:10.1038/77108 (2000).
146 Garvey, W. e. a. A modified Verhoff Elastic Van Gieson Stain. *The Journal of Histotechnology* **14**, 113-114 (1991).
147 Dunn, A. K. Laser speckle contrast imaging of cerebral blood flow. *Annals of biomedical engineering* **40**, 367-377, doi:10.1007/s10439-011-0469-0 (2012).
148 Malek, A. M., Alper, S. L. & Izumo, S. Hemodynamic shear stress and its role in atherosclerosis. *Jama* **282**, 2035-2042 (1999).
149 Iiyama, K. *et al*. Patterns of Vascular Cell Adhesion Molecule-1 and Intercellular Adhesion Molecule-1 Expression in Rabbit and Mouse Atherosclerotic Lesions and at Sites Predisposed to Lesion Formation. *Circulation research* **85**, 199-207, doi:10.1161/01.res.85.2.199 (1999).
150 Bautista, D. M. *et al*. TRPA1 Mediates the Inflammatory Actions of Environmental Irritants and Proalgesic Agents. *Cell* **124**, 1269-1282, doi:http://dx.doi.org/10.1016/j.cell.2006.02.023 (2006).

# Vita

Peter Louis Voyvodic grew up in Aurora, Colorado. During the summer of 2002 he began his research career working under Dr. George Eisenbarth at the Barbara Davis Center for Childhood Diabetes at the University of Colorado at Denver, a position he continued in the summer of 2004. He graduated from Smoky Hill High School in 2003 having received both an International Baccalaureate Diploma and the National AP Scholar award. He was one of a handful of students out of several hundred offered a full ride scholarship to Boston University based upon performance on the College of Engineering Scholarship Examination, which tested competency in mathematics, biology, chemistry, and physics. During the summer of 2003, he worked on developing training materials for a course in Nonlinear Dynamics and Chaos Theory under Dean (later Provost) David Campbell as part of the Freshman Research Opportunity Program (FROP). While at Boston University, Peter engaged in a wide range of diverse and unique activities including a semester abroad in Dresden, Germany and pursuing a second bachelors degree in Film and Television production; the film "Fratelli Breaks" that he worked on during the spring of 2007 was later awarded 1st place at the Redstone Film Festival, the highest award for a Boston University short film. After completion of his senior design project looking to alter a genetic toggle switch to exhibit Boolean 'AND' characteristics in the laboratory of Prof. James Collins, he began a research technician position under Drs. Joseph and Lydia Bryan at the Pacific Northwest Diabetes Research Institute in Seattle, WA. Over three years, he sequenced samples from around the world from patients with neonatal diabetes or hyperinsulinemic hypoglycemia for new mutations in the Kir6.2 channel protein and later characterized these mutations to study how they altered protein kinetics. In 2010 he was accepted to the graduate school at The University of Texas at Austin to begin a Ph.D. program in the Department of Biomedical Engineering. He began in the laboratory of Dr. Aaron Baker at the inception of the Laboratory for Cardiovascular Bioengineering and Therapeutics and helped to build up the laboratory while formulating his dissertation topic investigating the role of syndecan-1 in endothelial shear-mediated mechanotransduction.

Permanent email: pvoyvodic@utexas.edu
This dissertation was typed by the author.